Charles University in Prague
Faculty of Mathematics and Physics

MASTER THESIS

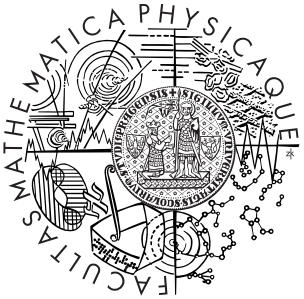

Zuzana Záhorová

Shape optimization of channels for incompressible flows

Department of Numerical Mathematics

Supervisor: Doc. Dr. Ing. Eduard Rohan
Study branch: Numerical and Computational Mathematics

2010

I would like to thank to all those who supported me in my master study and during the work on this thesis. I would like to express my gratitude to my supervisor Doc. Dr. Ing. Eduard Rohan for his help and guidance. I am grateful for numerous remarks, corrections and advices he gave me throughout my work. I very appreciate help and advices about the theoretical part of the thesis received from Prof. RNDr. Jaroslav Haslinger, DrSc. I would like to thank Ing. Robert Cimrman, Ph.D. for his many valuable information and help with the software SfePy and the code development.

Last but not least, I am in debt to my family and my close friends, whose support and patience made this work possible.

I confirm that I prepared the master thesis by my own, and that I listed all used sources of information in the bibliography. I agree with lending the master thesis.

In Prague, August 3, 2010 Zuzana Záhorová

Contents

Introduction **9**

1 The stationary Navier-Stokes equations **12**
1.1 Spaces of vector-valued functions 12
1.2 The Navier-Stokes equations with homogeneous boundary conditions . . . 13
1.2.1 Existence and uniqueness of the weak solution 16
1.3 The Navier-Stokes equations with nonhomogeneous boundary conditions 19
1.3.1 Existence of the weak solution 20
1.4 The Oseen problem 21
1.4.1 Existence and uniqueness of the weak solution of the Oseen problem 21
1.4.2 Oseen iteration process and the convergence 22

2 Stabilization of the Navier-Stokes equations **23**
2.1 Inf-sup condition 24
2.2 The discrete problem 25
2.3 Solvability of the discrete problem 26

3 Shape optimization problem **27**
3.1 Admissible domains 27
3.2 The state problem 28
3.3 Objective function 29
3.4 Existence of an optimal shape 30

4 Sensitivity analysis **34**
4.1 State problem of the stabilized Navier-Stokes equations 34
4.2 Objective function 35
4.3 Sensitivity analysis 36
4.3.1 Sensitivity formula 36
4.3.2 Partial shape derivatives 38
4.3.3 State problem without stabilization 43

5 Discretization of the state problems **45**
5.1 The state problem 45
5.2 Finite element discretization 46
5.3 The stabilized Navier-Stokes equations 46

5.4 The Navier-Stokes problem without stabilizations 47

6 Numerical methods **48**
6.1 SPBOX 48
6.1.1 Design variables and gradients 49
6.2 SfePy 50
6.2.1 Linear and nonlinear solvers 50
6.2.2 Optimization solver 50
6.2.3 Penalty function method 52
6.2.4 Input data 54

7 Numerical results **55**
7.1 State problem, objective functions and geometries 55
7.2 Stabilization parameters 56
7.2.1 Direct problem for different viscosity values 57
7.2.2 Optimization problem for both the stabilized and the unstabilized formulations 58
7.3 Influence of the geometry parametrization 61
7.4 Influence of the criterion domain 65
7.5 Influence of the penalty parameter value 68
7.6 Problem with three planar restrictions of the design 71

Conclusion **76**

Bibliography **78**

List of Figures

3.1 Computational domain 27
3.2 Criterion domain 29

6.1 Connection of spline boxes 48
6.2 Function g with respect to the plane p and the domain Ω 53

7.1 The unstabilized formulation, $\nu = 1.25 \cdot 10^{-3}\ m/s^2$ 57
7.2 The stabilized formulation, $\nu = 1.25 \cdot 10^{-3}\ m/s^2$, we choose $c_\gamma = 1$, $c_\tau = c_\kappa = 0.1$ 57
7.3 The stabilized formulation, $\nu = 1.25 \cdot 10^{-3}\ m/s^2$, we choose $c_\gamma = 10$, $c_\tau = c_\kappa = 1$ 57
7.4 The stabilized formulation, $\nu = 1.25 \cdot 10^{-5}\ m/s^2$, we choose $c_\gamma = 5.5$, $c_\tau = c_\kappa = 4$ 57
7.5 Initial design for the stabilized state problem 59
7.6 Optimized design for the stabilized state problem 59
7.7 Initial design for the unstabilized state problem 60
7.8 Optimized design for the unstabilized state problem 60
7.9 Convergence of the steepest descent optimization algorithm for the stabilized formulation 61
7.10 Convergence of the steepest descent optimization algorithm for the unstabilized formulation 61
7.11 Initial design for the first type of parametrization 62
7.12 Optimized design for the first type of parametrization 63
7.13 Initial design for the second type of parametrization 63
7.14 Optimized design for the second type of parametrization 64
7.15 Convergence of the steepest descent optimization algorithm for the first type of parametrization 64
7.16 Convergence of the steepest descent optimization algorithm for the second type of parametrization 64
7.17 Initial design for the objective function Ψ_1 66
7.18 Optimized design for the objective function Ψ_1 66
7.19 Initial design for the objective function Ψ_2 66
7.20 Optimized design for the objective function Ψ_2 66

7.21 Convergence of the steepest descent optimization algorithm for the objective function Ψ_1 . . . 67
7.22 Convergence of the steepest descent optimization algorithm for the objective function Ψ_2 . . . 67
7.23 Initial design for all penalty values . . . 68
7.24 Optimized design for the penalty value $\beta_0 = 0$ . . . 69
7.25 Optimized design for the penalty value $\beta_0 = 10$ . . . 69
7.26 Optimized design for the penalty value $\beta_0 = 100$ . . . 70
7.27 Convergence of the steepest descent optimization algorithm for the case without penalization, i.e. $\beta_0 = 0$ . . . 70
7.28 Convergence of the steepest descent optimization algorithm for the penalty value $\beta_0 = 10$ . . . 70
7.29 Convergence of the steepest descent optimization algorithm for the penalty value $\beta_0 = 100$ . . . 71
7.30 Initial design . . . 72
7.31 Optimized design without any restriction . . . 73
7.32 Optimized design considering three constraining planes . . . 73
7.33 Optimized design considering three constraining planes, second view . . . 74
7.34 Convergence of the steepest descent optimization algorithm without any restriction . . . 74
7.35 Convergence of the steepest descent optimization algorithm for three constraining planes . . . 74

List of Tables

6.1 Optimization solver settings 52

7.1 Description of geometries used for optimization 56
7.2 The stabilized and the unstabilized formulations - statistics 61
7.3 Comparison of two parametrization types - statistics 65
7.4 Comparison of two objective functions, Ψ_1 and Ψ_2 - statistics 67
7.5 Comparison of three penalty values $\beta_0 = 0, 10, 100$ - statistics 71
7.6 Comparison of the optimization process with and without linear geometry restrictions - statistics 75

Název práce: Optimalizace tvaru kanálu v úlohách nestlačitelného proudění
Autor: Zuzana Záhorová
Katedra: Katedra numerické matematiky
Vedoucí diplomové práce: Doc. Dr. Ing. Eduard Rohan
e-mail vedoucího: rohan@kme.zcu.cz

Abstrakt: V předložené práci studujeme problém tvarové optimalizace pro úlohy vnitřního proudění ve 3D. Uvažováno je laminární, nestlačitelné, stacionární proudění popsané Navier-Stokesovými rovnicemi. Jsou popsány stabilizace Navier-Stokesových rovnic potřebné pro řešení úloh s nízkou viskozitou. Předloženy jsou teoretické poznatky týkající se problému tvarové optimalizace včetně důkazu existence řešení. Je popsána adjungovaná metoda pro řešení optimalizační úlohy. Odvozena je analytická analýza citlivosti. Představujeme postupy využité při výpočtech a numerický software pro řešení optimalizačních úloh. Jsou prezentovány výsledky pro stabilizované i nestabilizované řešení Navier-Stokesových rovnic. Představíme výsledky zahrnující lineární omezení geometrie oblasti.

Klíčová slova: Nestlačitelné Navier-Stokesovy rovnice, SUPG/PSPG stabilizace, Adjungovaná metoda, Analýza citlivosti

Title: Shape optimization of channels for incompressible flows
Author: Zuzana Záhorová
Department: Department of Numerical Mathematics
Supervisor: Doc. Dr. Ing. Eduard Rohan
Supervisor's e-mail address: rohan@kme.zcu.cz

Abstract: In the present work we study the shape optimization problem for internal flows in 3D. We consider the laminar, incompressible, stationary flow described by the Navier-Stokes equations. Stabilization techniques which are necessary for solving low viscosity flows are described. Theoretical results concerning the optimization problem including the proof of the existence of solution are presented. We use the adjoint method for solving the optimization problem. The analytical sensitivity analysis is derived. Numerical software used for computations is presented. We introduce results for both the stabilized and unstabilized solution of the Navier-Stokes equations. We present results of problems including the linear geometry constraints.

Keywords: Incompressible Navier-Stokes equations, SUPG/PSPG stabilization techniques, Adjoint method, Sensitivity analysis

Introduction

The state of the art, survey of related studies

The shape optimization in fluid mechanics belongs to the most challenging areas of research in the structural optimization. It brings many difficulties in both the theory and the numerical implementation. But simultaneously, it is a very attractive topic due to broad engineering applications for example in the automotive industry or in the aerospace industry. Applications involve both the internal flows, such as the optimization of the shape of channels and obstacles placed in the stream, and the external flows, e.g. the optimization of the airplane design, blade profiles for turbines or the vehicle aerodynamics.

There are many books and articles concerning the shape optimization in fluids, for example [21]. Also two parts of articles, [33] and [34], bring both the theoretical background as well as practical examples for solving the shape optimization problems in aerodynamics.

In [3] the adjoint method is introduced and then used for the shape optimization problem in turbomachinery. The test case describes the usage of the method to determine the sensitivities of the outlet mass flow in a high-pressure turbine to the rotation of five-blade airfoils.

We can also find some doctoral thesis concerned with the shape optimization in fluid dynamics. In [20], the aerodynamic shape optimization procedure based on a discrete adjoint solver for the Navier-Stokes equations is developed and then applied to the problem of the shape optimization of transport aircraft wings. The discrete adjoint method is based on the approach where the adjoint equations are derived from the discretized problem. As opposed to the continuous adjoint method where the adjoint equations are derived from a continuous problem which is followed by discretizing the whole system. Comparison of these two approaches can be found in [22]. In this thesis, we shall use the continuous adjoint method.

Other doctoral thesis concerned with the shape optimization problem is [29]. It presents the shape optimization for the paper machine headbox which distributes a mixture of water and wood fibers in the paper making process. The state problem is represented by the generalized Navier-Stokes equations for the incompressible non-Newtonian fluid. There are results related to this doctoral thesis presented in [30, 31].

An example of the topology optimization in fluid dynamics can be found in [14]. The topology optimization with the material distribution technique for the steady-state viscous incompressible flow problem is presented.

Focus of the thesis

This thesis is concerned with 3D optimal shape problems. We focus entirely on the internal flows in closed channels. Shapes of channels or obstacles placed in the stream considerably influence the final flow. Its optimization plays an important role, e.g. in designing conduits for effective cooling or in biomechanical processes.

We deal with the incompressible, steady, viscous and laminar flow of the Newtonian liquid described by the Navier-Stokes equations. To be able to solve problems of low viscosity flows, there are stabilization techniques for the Navier-Stokes equations presented in the thesis. We employ the continuous adjoint method to deal with the analysis of the sensitivity to the fluid domain shape changes. The sensitivity analysis allows us to apply the gradient-based optimization method.

Another approach different from the adjoint method is described in [1]. The presented level-set method was investigated in [23]. This method enables us to handle certain kinds of topology changes, for example cancellation of holes.

Employed software

Softwares developed at the University of West Bohemia will be used for numerical simulations presented in the thesis. We shall use the software SPBOX to parametrize the computational domain. This parametrization is based on spline boxes and it was inspired by the free-form deformation technology, see [19, 27]. For the description of the software SPBOX see [26].

There are more approaches to the domain parametrization. In [35] the geometry parametrizations by the PARSEC method, the Hicks-Henne shape function method and the mesh-point method are described.

In [17] the parametrization is based on the usage of the Hicks-Henne bump functions. The article introduces the formulation and applications of the optimization technique for the aerodynamic shape design for both the inviscid and the viscous compressible flows.

Another approach is presented in [24]. The domain parametrization is based on a computation of the flow solution inside the domain and a suitable local criterion is applied to decide whether a fluid cell is "good" or "bad" for the flow in terms of the chosen cost function. Then the porosity distribution in a flow cell is considered to be a design variable.

In our simulations we use the software SfePy after the domain parametrization to deal with the shape optimization process. SfePy is a free software for computing problems using the finite element method. For information about the software SfePy see [5].

Aims of the thesis

In the thesis we shall focus on the following tasks.

- To study the theoretical background of approaches and methods of analyzing the shape optimization problems in fluid dynamics.
  This part is based on [11] for the theory of the Navier-Stokes equations and on [15] for the theory of the shape optimization problem.

  - We consider the incompressible, steady, viscous and laminar flow of the Newtonian liquid described by the Navier-Stokes equations.
  - We shall deal with the stabilization technique for the Navier-Stokes equations presented in [18]. This approach is necessary for solving low viscosity flows.
  - We shall explore the existence of solution of the shape optimization problem.

- To derive the sensitivity analysis for the stabilized formulation of the Navier-Stokes equations with the assistance of [8, 25].
  - We shall use the continuous adjoint method.
  - We shall employ the material derivative technique in the domain approach to derive the sensitivity formula.

- To get trained in using the numerical software and to use the software for solving selected model tasks.
  - We shall use the software SPBOX based on spline boxes for the domain parametrization. The description of software can be found in [25, 26].
  - We shall employ the software SfePy for solving the shape optimization problems. SfePy is being developed at the University of West Bohemia. For the documentation see [5, 6].

- To extend the problem for a linear inequality constraint of the domain shape and to cooperate with the development team from the University of West Bohemia to incorporate this feature to the software SfePy.

Overview of the thesis

The thesis is structured as follows. In Chapter 1 the theory of the Navier-Stokes equations is presented. We deal with the stationary Navier-Stokes equations completed by homogeneous as well as nonhomogeneous Dirichlet boundary conditions. The Oseen problem for solving the Navier-Stokes equations is described. Stabilization techniques are introduced in Chapter 2.

In Chapter 3 the theory of the shape optimization problem including the proof of the existence of solution is presented. In Chapter 4 the sensitivity analysis is derived. We present the analytical sensitivity formula in the thesis. The discretized problem is introduced in Chapter 5. We deal with two choices of finite element spaces for both the stabilized and the unstabilized formulation of the Navier-Stokes equations.

Some numerical techniques used in our test calculations are presented in Chapter 6. The last chapter summarizes results obtained for different geometries and for various problem configurations.

Chapter 1

The stationary Navier-Stokes equations

In this chapter we describe the basic theory of the Navier-Stokes equations. Results presented in this part are based on the book [11].

Because we shall work with N-component ($N = 2$, 3 in most cases) vector-valued functions, we have to introduce the notation for spaces of these functions in the following section.

1.1 Spaces of vector-valued functions

Definition 1.1 *Suppose that X is a space of scalar functions. Then we define the space of vector-valued functions as* $\boldsymbol{X} = \underbrace{X \times X \times \cdots \times X}_{\mathrm{N}\times}$.

That means $\quad \boldsymbol{v} = (v_1, \ldots, v_N) \in \boldsymbol{X} \quad \Leftrightarrow \quad v_i \in X \quad \forall\, i = 1, \ldots, N.$

We remind basic norms and scalar products on $\boldsymbol{L}^2(\Omega)$ and $\boldsymbol{H}^1(\Omega)$:

$$
\begin{aligned}
(u, v)_{L^2(\Omega)} &= \int_\Omega uv \, d\boldsymbol{x}, \\
(u, v)_{H^1(\Omega)} &= \int_\Omega (uv + \operatorname{grad} u \cdot \operatorname{grad} v) \, d\boldsymbol{x}, \\
(u, v)_{H^1_0(\Omega)} &= \int_\Omega \operatorname{grad} u \cdot \operatorname{grad} v \, d\boldsymbol{x}, \\
(\boldsymbol{u}, \boldsymbol{v})_{\boldsymbol{L}^2(\Omega)} &= \sum_{i=1}^{N} (u_i, v_i)_{L^2(\Omega)}, \qquad \boldsymbol{u}, \boldsymbol{v} \in \boldsymbol{L}^2(\Omega), \\
(\boldsymbol{u}, \boldsymbol{v})_{\boldsymbol{H}^1_0(\Omega)} &= \int_\Omega \sum_{i=1}^{N} \operatorname{grad} u_i \cdot \operatorname{grad} v_i \, d\boldsymbol{x} = \int_\Omega \sum_{i,j=1}^{N} \frac{\partial u_i}{\partial x_j} \frac{\partial v_i}{\partial x_j} \, d\boldsymbol{x} \\
&=: \int_\Omega \nabla \boldsymbol{u} : \nabla \boldsymbol{v} \, d\boldsymbol{x}, \\
(\boldsymbol{u}, \boldsymbol{v})_{\boldsymbol{H}^1(\Omega)} &= (\boldsymbol{u}, \boldsymbol{v})_{\boldsymbol{L}^2(\Omega)} + (\boldsymbol{u}, \boldsymbol{v})_{\boldsymbol{H}^1_0(\Omega)}.
\end{aligned}
$$

From the Friedrichs inequality yields that the following norms are equivalent in $\boldsymbol{H}_0^1(\Omega)$:

$$\|\boldsymbol{u}\|_{\boldsymbol{H}_0^1(\Omega)} = (\boldsymbol{u},\boldsymbol{u})^{\frac{1}{2}}_{\boldsymbol{H}_0^1(\Omega)},$$
$$\|\boldsymbol{u}\|_{\boldsymbol{H}^1(\Omega)} = (\boldsymbol{u},\boldsymbol{u})^{\frac{1}{2}}_{\boldsymbol{H}^1(\Omega)}.$$

I.e. there exists a constant $c_F > 0$ such that

$$\|\boldsymbol{u}\|_{\boldsymbol{H}_0^1(\Omega)} \le \|\boldsymbol{u}\|_{\boldsymbol{H}^1(\Omega)} \le c_F \|\boldsymbol{u}\|_{\boldsymbol{H}_0^1(\Omega)} \qquad \forall\, \boldsymbol{u} \in \boldsymbol{H}_0^1(\Omega). \tag{1.1}$$

We shall use a simplifying notations for the scalar product on $\boldsymbol{L}^2(\Omega)$:

$$(\boldsymbol{u},\boldsymbol{v})_{\boldsymbol{L}^2(\Omega)} = (\boldsymbol{u},\boldsymbol{v})_\Omega, \quad \boldsymbol{u},\boldsymbol{v} \in \boldsymbol{L}^2(\Omega).$$

1.2 The Navier-Stokes equations with homogeneous boundary conditions

Let us consider the boundary value problem for the stationary nonlinear Navier-Stokes equations with homogeneous Dirichlet boundary conditions: we seek $\boldsymbol{u}, p$ such that

$$\begin{aligned} -\nu\Delta\boldsymbol{u} + (\boldsymbol{u}\cdot\nabla)\boldsymbol{u} + \nabla p &= \boldsymbol{f} \qquad \text{in } \Omega, \\ \operatorname{div}\boldsymbol{u} &= 0 \qquad \text{in } \Omega, \\ \boldsymbol{u}|_{\partial\Omega} &= 0. \end{aligned} \tag{1.2}$$

The velocity vector is denoted by $\boldsymbol{u} = (u_1,\dots,u_N)$, p denotes the kinematic pressure. We assume that the kinematic viscosity $\nu = \text{const} > 0$ and the density of external volume force $\boldsymbol{f} : \Omega \to I\!R^N$ are given.

We can define the concept of a classical solution now.

Definition 1.2 *A couple $(\boldsymbol{u}, p)$ is called a classical solution of the Navier-Stokes problem with homogeneous boundary conditions, iff $\boldsymbol{u} \in \boldsymbol{C}^2(\overline{\Omega})$ and $p \in C^1(\overline{\Omega})$ satisfy equations (1.2).*

We need to define some special spaces for the velocity field which will be used in a weak formulation of the Navier-Stokes problem.

Definition 1.3 $\mathcal{V} = \{\boldsymbol{v} \in \boldsymbol{C}_0^\infty(\Omega); \operatorname{div}\boldsymbol{v} = 0 \text{ in } \Omega\}$; $\boldsymbol{V} = \overline{\mathcal{V}}^{\mathbf{H}_0^1(\Omega)} \subset \boldsymbol{H}_0^1(\Omega)$, *where $\overline{\mathcal{V}}^{\mathbf{H}_0^1(\Omega)}$ means the closure of the space $\mathcal{V}$ in $\mathbf{H}_0^1(\Omega)$.*

Lemma 1.4 $\boldsymbol{V} = \{\boldsymbol{u} \in \boldsymbol{H}_0^1(\Omega); \operatorname{div}\boldsymbol{u} = 0$ *in* $\Omega\}$.

Proof can be found in [11].

We can now formulate the Navier-Stokes problem in a weak sense.

Let $(\boldsymbol{u}, p)$ be the classical solution of (1.2). Multiplying $(1.2)_1$ by an arbitrary vector function $\boldsymbol{v} = (v_1,\dots,v_N) \in \mathcal{V}$ and integrating over Ω, we obtain

$$-\nu\int_\Omega \Delta\boldsymbol{u}\cdot\boldsymbol{v}\,d\boldsymbol{x} + \int_\Omega (\boldsymbol{u}\cdot\nabla)\boldsymbol{u}\cdot\boldsymbol{v}\,d\boldsymbol{x} + \int_\Omega \boldsymbol{v}\cdot\nabla p\,d\boldsymbol{x} = \int_\Omega \boldsymbol{f}\cdot\boldsymbol{v}\,d\boldsymbol{x} \qquad \forall\,\boldsymbol{v} \in \mathcal{V}.$$

The integrals on the left side can be transformed with the use of the Green's theorem:

$$\begin{aligned} -\nu \int_\Omega \Delta \boldsymbol{u} \cdot \boldsymbol{v}\, d\boldsymbol{x} &= -\nu \int_{\partial\Omega} \frac{\partial \boldsymbol{u}}{\partial n} \boldsymbol{v}\, dS + \nu \int_\Omega \nabla \boldsymbol{u} : \nabla \boldsymbol{v}\, d\boldsymbol{x}, \\ \int_\Omega \boldsymbol{v} \cdot \nabla p\, d\boldsymbol{x} &= \int_{\partial\Omega} p \boldsymbol{v} \cdot \boldsymbol{n}\, dS - \int_\Omega p\, (\nabla \cdot \boldsymbol{v})\, d\boldsymbol{x}, \end{aligned}$$

where $\boldsymbol{n}$ denotes the unit outer normal to $\partial\Omega$ and $\frac{\partial}{\partial n}$ is the derivative with respect to the direction $\boldsymbol{n}$.
All integrals along $\partial\Omega$ vanish because $\boldsymbol{v}|_{\partial\Omega} = 0$. Next we have

$$\int_\Omega p\, (\nabla \cdot \boldsymbol{v})\, d\boldsymbol{x} = 0,$$

as $\operatorname{div} \boldsymbol{v} = 0$ for $\boldsymbol{v} \in \mathcal{V}$.

Using the notation (summation convection is employed)

$$\begin{aligned} a_\Omega(\boldsymbol{u}, \boldsymbol{v}) &= \nu(\nabla \boldsymbol{u}, \nabla \boldsymbol{v})_\Omega = \nu \int_\Omega \frac{\partial u_i}{\partial x_j} \frac{\partial v_i}{\partial x_j}\, d\boldsymbol{x}, \\ b_\Omega(\boldsymbol{u}, \boldsymbol{v}, \boldsymbol{w}) &= ((\boldsymbol{u} \cdot \nabla)\boldsymbol{v}, \boldsymbol{w})_\Omega = \int_\Omega u_j \frac{\partial v_i}{\partial x_j} w_i\, d\boldsymbol{x}, \end{aligned}$$

we get the identity

$$a_\Omega(\boldsymbol{u}, \boldsymbol{v}) + b_\Omega(\boldsymbol{u}, \boldsymbol{u}, \boldsymbol{v}) = (\boldsymbol{f}, \boldsymbol{v})_\Omega \qquad \forall\, \boldsymbol{v} \in \mathcal{V},$$

for $\boldsymbol{u} = (u_1, \ldots, u_N), \boldsymbol{v} = (v_1, \ldots, v_n), \boldsymbol{w} = (w_1, \ldots, w_n)$ "sufficiently smooth" in $\overline{\Omega}$.

Due to this result and the density of $\mathcal{V}$ in the space $\boldsymbol{V}$, we can introduce a generalized concept of solution of the Navier-Stokes problem.

Definition 1.5 *Let $\nu > 0$ and $\boldsymbol{f} \in \boldsymbol{L}^2(\Omega)$ be given. We say that a vector function $\boldsymbol{u} : \Omega \to \mathbb{R}^N$ is a weak solution of the Navier-Stokes problem with homogeneous boundary condition, iff*

$$\boldsymbol{u} \in \boldsymbol{V} \quad \text{and} \quad a_\Omega(\boldsymbol{u}, \boldsymbol{v}) + b_\Omega(\boldsymbol{u}, \boldsymbol{u}, \boldsymbol{v}) = (\boldsymbol{f}, \boldsymbol{v})_\Omega \quad \forall\, \boldsymbol{v} \in \boldsymbol{V}. \tag{1.3}$$

Conditions $(1.2)_2$ and $(1.2)_3$ are already included in the assumption $\boldsymbol{u} \in \boldsymbol{V}$. Conditions (1.3) form the *weak formulation* of the Navier-Stokes problem.

Lemma 1.6 *The mapping '$\boldsymbol{u}, \boldsymbol{v}, \boldsymbol{w} \to b_\Omega(\boldsymbol{u}, \boldsymbol{v}, \boldsymbol{w})$' is a continuous trilinear form on $\boldsymbol{H}^1(\Omega) \times \boldsymbol{H}^1(\Omega) \times \boldsymbol{H}^1(\Omega)$ (and thus on $\boldsymbol{V} \times \boldsymbol{V} \times \boldsymbol{V}$).*
I.e, there exists a constant $\tilde{c} > 0$ such that

$$|b_\Omega(\boldsymbol{u}, \boldsymbol{v}, \boldsymbol{w})| \le \tilde{c} \|\boldsymbol{u}\|_{\boldsymbol{H}^1_0(\Omega)} \|\boldsymbol{v}\|_{\boldsymbol{H}^1_0(\Omega)} \|\boldsymbol{w}\|_{\boldsymbol{H}^1_0(\Omega)} \qquad \forall\, \boldsymbol{u}, \boldsymbol{v}, \boldsymbol{w} \in \boldsymbol{V}. \tag{1.4}$$

Proof: Let $\boldsymbol{u}, \boldsymbol{v}, \boldsymbol{w} \in \boldsymbol{H}^1(\Omega), \boldsymbol{u} = (u_1, \ldots, u_N), \boldsymbol{v} = (v_1, \ldots, v_N), \boldsymbol{w} = (w_1, \ldots, w_N)$. Then $u_i, v_i, w_i \in H^1(\Omega)$. Hence, $\frac{\partial v_i}{\partial x_j} \in L^2(\Omega)$.
In virtue of the continuous embedding of $H^1(\Omega)$ into $L^4(\Omega)$ (take into account that $N = 2$ or $N = 3$), we have $u_j, w_i \in L^4(\Omega)$. This implies $u_j w_i \frac{\partial v_i}{\partial x_j} \in L^1(\Omega)$. It means that the integral in the definition of b_Ω exists and is finite. The form b_Ω is thus defined on

$\boldsymbol{H}^1(\Omega) \times \boldsymbol{H}^1(\Omega) \times \boldsymbol{H}^1(\Omega)$. Its linearity with respect to arguments $\boldsymbol{u}, \boldsymbol{v}, \boldsymbol{w}$ is obvious. Let us prove the continuity of b_Ω. Due to the continuous embedding of $H^1(\Omega)$ into $L^4(\Omega)$, there exists a constant c_4 such that

$$\|u\|_{L^4(\Omega)} \le c_4 \|u\|_{H^1(\Omega)} \qquad \forall u \in H^1(\Omega). \tag{1.5}$$

Let $\boldsymbol{u}, \boldsymbol{v}, \boldsymbol{w} \in \boldsymbol{H}^1(\Omega)$. The generalized Hölder inequality and (1.5) yield

$$\begin{aligned}
\left| \int_\Omega u_j \frac{\partial v_i}{\partial x_j} w_i \, d\boldsymbol{x} \right| &\le \int_\Omega \left| u_j \frac{\partial v_i}{\partial x_j} w_i \right| d\boldsymbol{x} \le \\
&\le \left(\int_\Omega u_j^4 \, d\boldsymbol{x} \right)^{\frac{1}{4}} \left(\int_\Omega w_i^4 \, d\boldsymbol{x} \right)^{\frac{1}{4}} \left(\int_\Omega \left(\frac{\partial v_i}{\partial x_j} \right)^2 d\boldsymbol{x} \right)^{\frac{1}{2}} = \\
&= \|u_j\|_{L^4(\Omega)} \|w_i\|_{L^4(\Omega)} \|\nabla v_i\|_{L^2(\Omega)} \le \\
&\le c_4^2 \|u_j\|_{H^1(\Omega)} \|w_i\|_{H^1(\Omega)} \|v_i\|_{H^1(\Omega)}.
\end{aligned}$$

Summing these inequalities for $i, j = 1, \dots, N$, we obtain

$$|b_\Omega(\boldsymbol{u}, \boldsymbol{v}, \boldsymbol{w})| \le \bar{c} \|\boldsymbol{u}\|_{\boldsymbol{H}^1(\Omega)} \|\boldsymbol{v}\|_{\boldsymbol{H}^1(\Omega)} \|\boldsymbol{w}\|_{\boldsymbol{H}^1(\Omega)} \qquad \forall\, \boldsymbol{u}, \boldsymbol{v}, \boldsymbol{w} \in \boldsymbol{H}^1(\Omega).$$

Using (1.1) we get

$$|b_\Omega(\boldsymbol{u}, \boldsymbol{v}, \boldsymbol{w})| \le \tilde{c} \|\boldsymbol{u}\|_{\boldsymbol{H}^1_0(\Omega)} \|\boldsymbol{v}\|_{\boldsymbol{H}^1_0(\Omega)} \|\boldsymbol{w}\|_{\boldsymbol{H}^1_0(\Omega)} \qquad \forall\, \boldsymbol{u}, \boldsymbol{v}, \boldsymbol{w} \in \boldsymbol{V}.$$

⊠

Lemma 1.7 *Let $\boldsymbol{u} \in \boldsymbol{H}^1(\Omega), \operatorname{div} \boldsymbol{u} = 0$ and $\boldsymbol{v}, \boldsymbol{w} \in \boldsymbol{H}^1_0(\Omega)$. Then*

$$\text{(i)} \quad b_\Omega(\boldsymbol{u}, \boldsymbol{v}, \boldsymbol{v}) = 0, \qquad \text{(ii)} \quad b_\Omega(\boldsymbol{u}, \boldsymbol{v}, \boldsymbol{w}) = -b_\Omega(\boldsymbol{u}, \boldsymbol{w}, \boldsymbol{v}).$$

Proof: Since b is a continuous trilinear form and $\boldsymbol{C}_0^\infty(\Omega)$ is dense in $\boldsymbol{H}^1_0(\Omega)$, it is sufficient to prove assertion (i) for $\boldsymbol{v} \in \boldsymbol{C}_0^\infty(\Omega)$. By the Green's theorem

$$\begin{aligned}
b_\Omega(\boldsymbol{u}, \boldsymbol{v}, \boldsymbol{v}) &= \sum_{i,j=1}^N \int_\Omega u_j \frac{\partial v_i}{\partial x_j} v_i \, d\boldsymbol{x} = \sum_{i,j=1}^N \int_\Omega u_j \frac{1}{2} \frac{\partial}{\partial x_j} (v_i^2) \, d\boldsymbol{x} \\
&= -\sum_{i,j=1}^N \frac{1}{2} \int_\Omega \frac{\partial u_j}{\partial x_j} v_i^2 \, d\boldsymbol{x} = -\sum_{i=1}^N \frac{1}{2} \int_\Omega v_i^2 (\nabla \cdot \boldsymbol{u}) \, d\boldsymbol{x} = 0.
\end{aligned}$$

Assertion (ii) is obtained from (i) by substituting $\boldsymbol{v} + \boldsymbol{w}$ for $\boldsymbol{v}$:

$$\begin{aligned}
0 &= b_\Omega(\boldsymbol{u}, \boldsymbol{v} + \boldsymbol{w}, \boldsymbol{v} + \boldsymbol{w}) \\
&= b_\Omega(\boldsymbol{u}, \boldsymbol{v}, \boldsymbol{v}) + b_\Omega(\boldsymbol{u}, \boldsymbol{v}, \boldsymbol{w}) + b_\Omega(\boldsymbol{u}, \boldsymbol{w}, \boldsymbol{v}) + b_\Omega(\boldsymbol{u}, \boldsymbol{w}, \boldsymbol{w}) \\
&= b_\Omega(\boldsymbol{u}, \boldsymbol{v}, \boldsymbol{w}) + b_\Omega(\boldsymbol{u}, \boldsymbol{w}, \boldsymbol{v}).
\end{aligned} \tag{1.6}$$

⊠

1.2.1 Existence and uniqueness of the weak solution

We shall deal with the existence and the uniqueness of the weak solution of the Navier-Stokes equations in this section.

Lemma 1.8 *Let* $\boldsymbol{u}^\alpha, \boldsymbol{u} \in \boldsymbol{V}, \alpha = 1, 2, \ldots,$ *and* $\boldsymbol{u}^\alpha \to \boldsymbol{u}$ *in* $\boldsymbol{L}^2(\Omega)$ *as* $\alpha \to \infty$. *Then* $b_\Omega(\boldsymbol{u}^\alpha, \boldsymbol{u}^\alpha, \boldsymbol{v}) \to b_\Omega(\boldsymbol{u}, \boldsymbol{u}, \boldsymbol{v})$ *for each* $\boldsymbol{v} \in \mathcal{V}$.

Proof can be found in [11].

The following auxiliary lemma is necessary in the proof of the existence theorem.

Lemma 1.9 *Let* $\boldsymbol{X}$ *be a finite dimensional Hilbert space with the scalar product* $(\cdot,\cdot)_{\boldsymbol{X}}$ *which induces the norm* $\|\cdot\|_{\boldsymbol{X}}$ *in* $\boldsymbol{X}$. *Let* $P : \boldsymbol{X} \to \boldsymbol{X}$ *be a continuous mapping and*

$$\exists\, K > 0 : \quad (P(\xi), \xi)_{\boldsymbol{X}} \geq 0 \quad \forall\, \xi \in \boldsymbol{X}, \|\xi\|_{\boldsymbol{X}} \leq K.$$

Then there exists $\xi_1 \in \boldsymbol{X}, \|\xi_1\|_{\boldsymbol{X}} = K : \quad P(\xi_1) = 0.$

Proof: The proof is based on the Brower fixed-point theorem.
We consider $P(\xi) \neq 0\ \forall \xi \in B_K(0)$, where $B_K(0) = \{\xi \in \boldsymbol{X}; \|\xi\|_{\boldsymbol{X}} \leq K\}$.
We define a continuous mapping $S : B_K(0) \to B_K(0)$ as $S(\xi) = -K\frac{P(\xi)}{\|P(\xi)\|_{\boldsymbol{X}}},\ \xi \in B_K(0)$.
Because $B_K(0) \neq \emptyset$ is a closed, bounded and convex set, we employ the Brower theorem and we get: $\exists \xi \in B_K(0) : \xi = S(\xi)$.
It leads to a contradiction:
$0 < \|\xi\|^2_{\boldsymbol{X}} = \|S(\xi)\|^2_{\boldsymbol{X}} = K^2 = (\xi,\xi)_{\boldsymbol{X}} = (S(\xi),\xi)_{\boldsymbol{X}} = -K\frac{1}{\|P(\xi)\|_{\boldsymbol{X}}}(P(\xi),\xi)_{\boldsymbol{X}} \leq 0.$

⊠

Theorem 1.10 *There exists at least one weak solution of the Navier-Stokes problem with homogeneous boundary conditions.*

Proof: We shall use the Galerkin method in this proof.

1. Since $\boldsymbol{V}$ is a separable Hilbert space, there exists a sequence $\{\tilde{\boldsymbol{w}}^\alpha\}_{\alpha=1}^\infty$ dense in $\boldsymbol{V}$. By the definition of $\boldsymbol{V}$ ($\boldsymbol{V} = \overline{\mathcal{V}}^{\mathbf{H}^1_0(\Omega)}$), there exists a sequence $\{\boldsymbol{w}^{\alpha_j}\}_{j=1}^\infty \subset \mathcal{V}$ for each α such that $\boldsymbol{w}^{\alpha_j} \to \tilde{\boldsymbol{w}}^\alpha$ in $\boldsymbol{H}^1(\Omega)$ as $j \to \infty$.
If we order all elements $\boldsymbol{w}^{\alpha_j}, j = 1, 2, \ldots, \alpha = 1, 2, \ldots$ into a sequence (and omit, if they occur, elements which can be written as linear combinations of the preceding ones), we obtain a sequence $\{\boldsymbol{w}^\alpha\}_{\alpha=1}^\infty \subset \mathcal{V}$ of linearly independent elements such that

$$\boldsymbol{V} = \overline{\bigcup_{k=1}^{\infty} \boldsymbol{X}_k}^{\boldsymbol{H}^1_0(\Omega)}, \tag{1.7}$$

where

$$\boldsymbol{X}_k = [\boldsymbol{w}^1, \ldots, \boldsymbol{w}^k]$$

is the linear space spanned over the set $\{\boldsymbol{w}^1, \ldots, \boldsymbol{w}^k\}$. $\boldsymbol{X}_k$ is a finite-dimensional Hilbert space equipped with the scalar product $(\cdot,\cdot)_{\boldsymbol{H}^1_0(\Omega)}$.

2. In the second step of this proof we want to show the existence of approximative solutions.
For any $k = 1, 2, \ldots$ let $\boldsymbol{u}^k \in \boldsymbol{X}_k$ satisfy

$$a_\Omega(\boldsymbol{u}^k, \boldsymbol{w}^i) + b_\Omega(\boldsymbol{u}^k, \boldsymbol{u}^k, \boldsymbol{w}^i) = (\boldsymbol{f}, \boldsymbol{w}^i)_\Omega \qquad \forall\, i = 1, \ldots, k. \tag{1.8}$$

We call $\boldsymbol{u}^k$ the Galerkin's approximation on the finite dimensional space $\boldsymbol{X}_k$.
Since

$$\boldsymbol{u}^k = \sum_{j=1}^{k} \xi_j^k \boldsymbol{w}^j, \quad \xi_j^k \in I\!R^1,$$

the condition (1.8) represents a system of k nonlinear algebraic equations with respect to k unknowns $\xi_1^k, \ldots, \xi_k^k$.
Let us prove the existence of the solution $\boldsymbol{u}^k$. Let $\boldsymbol{\omega} \in \boldsymbol{X}_k, \boldsymbol{v} \in \boldsymbol{X}_k$. By Lemma 1.6, the mapping '$\boldsymbol{v} \in \boldsymbol{X}_k \to a_\Omega(\boldsymbol{\omega}, \boldsymbol{v}) + b_\Omega(\boldsymbol{\omega}, \boldsymbol{\omega}, \boldsymbol{v}) - (\boldsymbol{f}, \boldsymbol{v})_\Omega \in I\!R$' is a continuous linear functional on $\boldsymbol{X}_k$ for any $\boldsymbol{\omega} \in \boldsymbol{X}_k$. In virtue of the Riesz theorem, there exists $P_k(\boldsymbol{\omega}) \in \boldsymbol{X}_k$ such that

$$(P_k(\boldsymbol{\omega}), \boldsymbol{v})_{\boldsymbol{H}_0^1(\Omega)} = a_\Omega(\boldsymbol{\omega}, \boldsymbol{v}) + b_\Omega(\boldsymbol{\omega}, \boldsymbol{\omega}, \boldsymbol{v}) - (\boldsymbol{f}, \boldsymbol{v})_\Omega \qquad \forall\, \boldsymbol{\omega}, \boldsymbol{v} \in \boldsymbol{X}_k.$$

Hence, $P_k : \boldsymbol{X}_k \to \boldsymbol{X}_k$ and the existence of solution of (1.8) is equivalent with the condition $P_k(\boldsymbol{u}_k) = 0$. To employ Lemma 1.9 we need to verify its conditions .
Since spaces $\boldsymbol{X}_k$ and $I\!R^k$ are isomorphic and the quadratic functions '$(\xi_1, \ldots, \xi_k) \in I\!R^k \to a_\Omega(\boldsymbol{\omega}, \boldsymbol{w}^i) + b_\Omega(\boldsymbol{\omega}, \boldsymbol{\omega}, \boldsymbol{w}^i) - (\boldsymbol{f}, \boldsymbol{w}^i)_\Omega$, where $\boldsymbol{\omega} = \sum_{j=1}^k \xi_j \boldsymbol{w}^j$', are obviously continuous for all $i = 1, \ldots, k$, the mapping P_k is also continuous. That means, we need to verify the last condition from Lemma 1.9. Using (1.1) and Lemma 1.7,

$$\begin{aligned}
(P_k(\boldsymbol{\omega}), \boldsymbol{\omega})_{\boldsymbol{H}_0^1(\Omega)} &= a_\Omega(\boldsymbol{\omega}, \boldsymbol{\omega}) + b_\Omega(\boldsymbol{\omega}, \boldsymbol{\omega}, \boldsymbol{\omega}) - (\boldsymbol{f}, \boldsymbol{\omega})_\Omega \\
&= \nu \|\boldsymbol{\omega}\|^2_{\boldsymbol{H}_0^1(\Omega)} - (\boldsymbol{f}, \boldsymbol{\omega})_\Omega \\
&\geq \nu \|\boldsymbol{\omega}\|^2_{\boldsymbol{H}_0^1(\Omega)} - c_F \|\boldsymbol{f}\|_{\boldsymbol{L}^2(\Omega)} \|\boldsymbol{\omega}\|_{\boldsymbol{H}_0^1(\Omega)}
\end{aligned}$$

for any $\boldsymbol{\omega} \in \boldsymbol{X}_k$. That means $(P(\boldsymbol{\omega}), \boldsymbol{\omega})_{\boldsymbol{H}_0^1(\Omega)} \to \infty$ for $\|\boldsymbol{\omega}\|_{\boldsymbol{H}_0^1(\Omega)} \to \infty$ and therefore there exists $K > 0$ such that $(P(\boldsymbol{\omega}), \boldsymbol{\omega})_{\boldsymbol{H}_0^1(\Omega)} \geq 0\ \forall\, \boldsymbol{\omega} \in \boldsymbol{X}_k, \|\boldsymbol{\omega}\|_{\boldsymbol{H}_0^1(\Omega)} = K$.
We verified all presumptions and we could use Lemma 1.9 now. It implies that for each $k = 1, 2, \ldots$ there exists at least one solution $\boldsymbol{u}^k$ of the equation $P_k(\boldsymbol{u}^k) = 0$.

3. In the next step of this proof we need to show that the sequence $\{\boldsymbol{u}^k\}_{k=1}^\infty$ is bounded in $\boldsymbol{V}$.
By (1.8),

$$a_\Omega(\boldsymbol{u}^k, \boldsymbol{v}) + b_\Omega(\boldsymbol{u}^k, \boldsymbol{u}^k, \boldsymbol{v}) = (\boldsymbol{f}, \boldsymbol{v})_\Omega \qquad \forall\, \boldsymbol{v} \in \boldsymbol{X}_k.$$

Substituting $\boldsymbol{v} := \boldsymbol{u}^k$, we obtain from (1.1)

$$\nu \|\boldsymbol{u}^k\|^2_{\boldsymbol{H}_0^1(\Omega)} = (\boldsymbol{f}, \boldsymbol{u}^k)_\Omega \leq \|\boldsymbol{f}\|_{\boldsymbol{L}^2(\Omega)} \|\boldsymbol{u}^k\|_{\boldsymbol{L}^2(\Omega)} \leq c_F \|\boldsymbol{f}\|_{\boldsymbol{L}^2(\Omega)} \|\boldsymbol{u}^k\|_{\boldsymbol{H}_0^1(\Omega)},$$

which immediately implies

$$\|\boldsymbol{u}^k\|_{\boldsymbol{H}_0^1(\Omega)} \leq \frac{c_F \|\boldsymbol{f}\|_{\boldsymbol{L}^2(\Omega)}}{\nu} \qquad \forall\, k = 1, 2, \ldots$$

4. In the final step we need to make a limit for $k \to \infty$.
Because $\boldsymbol{V}$ is a reflexive Banach's space and the sequence $\left\{\boldsymbol{u}^k\right\}_{k=1}^\infty$ is bounded in $\boldsymbol{V}$, a weakly convergent subsequence can be subtracted: $\exists\, \boldsymbol{u} \in \boldsymbol{V}, \left\{\boldsymbol{u}^{k_\alpha}\right\}_{\alpha=1}^\infty$ such that

$$\boldsymbol{u}^{k_\alpha} \to \boldsymbol{u} \quad \text{weakly in } \boldsymbol{V} \text{ as } \alpha \to \infty. \tag{1.9}$$

In virtue of the inclusion $\boldsymbol{V} \subset \boldsymbol{H}_0^1(\Omega)$ and the compact embedding $\boldsymbol{H}_0^1(\Omega) \subset \boldsymbol{L}^2(\Omega)$,

$$\boldsymbol{u}^{k_\alpha} \to \boldsymbol{u} \quad \text{strongly in } \boldsymbol{L}^2(\Omega).$$

From (1.9) we obtain

$$(\boldsymbol{u}^{k_\alpha}, \boldsymbol{w}^i)_{\boldsymbol{H}^1_0(\Omega)} \to (\boldsymbol{u}, \boldsymbol{w}^i)_{\boldsymbol{H}^1_0(\Omega)} \quad \text{as } \alpha \to \infty \quad \forall\, i = 1, 2, \ldots$$

Further, by Lemma 1.8, we have

$$b_\Omega(\boldsymbol{u}^{k_\alpha}, \boldsymbol{u}^{k_\alpha}, \boldsymbol{w}^i) \to b_\Omega(\boldsymbol{u}, \boldsymbol{u}, \boldsymbol{w}^i) \quad \text{as } \alpha \to \infty \quad \forall\, i = 1, 2, \ldots$$

In view of (1.8),

$$a_\Omega(\boldsymbol{u}^{k_\alpha}, \boldsymbol{w}^i) + b_\Omega(\boldsymbol{u}^{k_\alpha}, \boldsymbol{u}^{k_\alpha}, \boldsymbol{w}^i) = (\boldsymbol{f}, \boldsymbol{w}^i)_\Omega \qquad \forall\, i = 1, \ldots, k_\alpha,\ \forall\, \alpha = 1, 2, \ldots.$$

Passing to the limit as $\alpha \to \infty$, we find from the above relations that

$$a_\Omega(\boldsymbol{u}, \boldsymbol{w}^i) + b_\Omega(\boldsymbol{u}, \boldsymbol{u}, \boldsymbol{w}^i) = (\boldsymbol{f}, \boldsymbol{w}^i)_\Omega \qquad \forall\, i = 1, 2, \ldots$$

Hence, by (1.7), we have

$$a_\Omega(\boldsymbol{u}, \boldsymbol{v}) + b_\Omega(\boldsymbol{u}, \boldsymbol{u}, \boldsymbol{v}) = (\boldsymbol{f}, \boldsymbol{v})_\Omega \qquad \forall\, \boldsymbol{v} \in \boldsymbol{V},$$

which means that $\boldsymbol{u}$ is a weak solution of the Navier-Stokes problem.

⊠

Theorem 1.11 *Let the condition*

$$\nu^2 > \tilde{c} c_F \|\boldsymbol{f}\|_{\boldsymbol{L}^2(\Omega)} \tag{1.10}$$

be fulfilled with the constants $\tilde{c}$ and c_F from (1.4) and (1.1), respectively. Then there exists exactly one weak solution of the Navier-Stokes problem with homogeneous boundary conditions.

Proof: Let $\boldsymbol{u}_1, \boldsymbol{u}_2$ be two solutions of (1.3). It means that for $i = 1, 2$

$$\boldsymbol{u}_i \in \boldsymbol{V}, \quad a_\Omega(\boldsymbol{u}_i, \boldsymbol{v}) + b_\Omega(\boldsymbol{u}_i, \boldsymbol{u}_i, \boldsymbol{v}) = (\boldsymbol{f}, \boldsymbol{v})_\Omega \qquad \forall\, \boldsymbol{v} \in \boldsymbol{V}. \tag{1.11}$$

Substituting $\boldsymbol{v} := \boldsymbol{u}_i$ we easily obtain

$$\nu \|\boldsymbol{u}_i\|^2_{\boldsymbol{H}^1_0(\Omega)} = (\boldsymbol{f}, \boldsymbol{u}_i)_\Omega \le \|\boldsymbol{f}\|_{\boldsymbol{L}^2(\Omega)} \|\boldsymbol{u}_i\|_{\boldsymbol{L}^2(\Omega)} \le c_F \|\boldsymbol{f}\|_{\boldsymbol{L}^2(\Omega)} \|\boldsymbol{u}_i\|_{\boldsymbol{H}^1_0(\Omega)}$$

and, hence,

$$\|\boldsymbol{u}_i\|_{\boldsymbol{H}^1_0(\Omega)} \le \frac{c_F \|\boldsymbol{f}\|_{\boldsymbol{L}^2(\Omega)}}{\nu}. \tag{1.12}$$

Let us set $\boldsymbol{u} = \boldsymbol{u}_1 - \boldsymbol{u}_2$. Subtracting equations (1.11), $i = 1, 2$, and using the properties of the form b, we obtain

$$\begin{aligned} 0 &= a_\Omega(\boldsymbol{u}_1, \boldsymbol{v}) + b_\Omega(\boldsymbol{u}_1, \boldsymbol{u}_1, \boldsymbol{v}) - a_\Omega(\boldsymbol{u}_2, \boldsymbol{v}) - b_\Omega(\boldsymbol{u}_2, \boldsymbol{u}_2, \boldsymbol{v}) \\ &= a_\Omega(\boldsymbol{u}, \boldsymbol{v}) + b_\Omega(\boldsymbol{u}_1, \boldsymbol{u}, \boldsymbol{v}) + b_\Omega(\boldsymbol{u}, \boldsymbol{u}_2, \boldsymbol{v}) \end{aligned}$$

for each $\boldsymbol{v} \in \boldsymbol{V}$. If we choose $\boldsymbol{v} = \boldsymbol{u}$, then, in view of Lemma 1.7,

$$a_\Omega(\boldsymbol{u}, \boldsymbol{u}) = -b_\Omega(\boldsymbol{u}, \boldsymbol{u}_2, \boldsymbol{u}),$$

from which, due to inequalities (1.4) and (1.12), we derive the estimate

$$\nu \|\boldsymbol{u}\|^2_{\boldsymbol{H}^1_0(\Omega)} \le \tilde{c} \|\boldsymbol{u}\|^2_{\boldsymbol{H}^1_0(\Omega)} \|\boldsymbol{u}_2\|_{\boldsymbol{H}^1_0(\Omega)} \le c_F \tilde{c} \nu^{-1} \|\boldsymbol{f}\|_{\boldsymbol{L}^2(\Omega)} \|\boldsymbol{u}\|^2_{\boldsymbol{H}^1_0(\Omega)}.$$

Thus,

$$\|\boldsymbol{u}\|^2_{\boldsymbol{H}^1_0(\Omega)} \left(\nu - c_F \tilde{c} \nu^{-1} \|\boldsymbol{f}\|_{\boldsymbol{L}^2(\Omega)}\right) \le 0.$$

This inequality and (1.10) immediately imply that $\|\boldsymbol{u}\|_{\boldsymbol{H}^1_0(\Omega)} = 0$, i.e. $\boldsymbol{u}_1 = \boldsymbol{u}_2$.

⊠

1.3 The Navier-Stokes equations with nonhomogeneous boundary conditions

We seek $\boldsymbol{u}$ and p satisfying

$$\begin{aligned} -\nu\Delta\boldsymbol{u} + (\boldsymbol{u}\cdot\nabla)\boldsymbol{u} + \nabla p &= \boldsymbol{f} \qquad \text{in } \Omega, \\ \operatorname{div}\boldsymbol{u} &= 0 \qquad \text{in } \Omega, \\ \boldsymbol{u}|_{\partial\Omega} &= \boldsymbol{\varphi}. \end{aligned} \tag{1.13}$$

The constant $\nu > 0$ and functions $\boldsymbol{f}$ and $\boldsymbol{\varphi}$ are given.

The classical solution of this problem is defined analogously as in Definition 1.2.

We introduce the space of traces on $\partial\Omega$:

$$\boldsymbol{H}^{\frac{1}{2}}(\partial\Omega) = \{\boldsymbol{v} \in \boldsymbol{L}^2(\partial\Omega); \exists\, \boldsymbol{w} \in \boldsymbol{H}^1(\Omega), \boldsymbol{w}|_{\partial\Omega} = \boldsymbol{v}\}.$$

Let us assume $\boldsymbol{f} \in \boldsymbol{L}^2(\Omega), \boldsymbol{\varphi} \in \boldsymbol{H}^{\frac{1}{2}}(\partial\Omega)$ and

$$\int_{\partial\Omega} \boldsymbol{\varphi}\cdot\boldsymbol{n}\, dS = 0. \tag{1.14}$$

It could be shown that provided $\boldsymbol{u} \in \boldsymbol{H}^1(\Omega)$ satisfies conditions $(1.13)_2$ and $(1.13)_3$ (in the sense of traces), the relation (1.14) is fulfilled. It means that (1.14) is a *necessary condition* for the solvability of the problem (1.13).

Lemma 1.12 *Let the function $\boldsymbol{\varphi} \in \boldsymbol{H}^{\frac{1}{2}}(\partial\Omega)$ satisfies (1.14). Then there exists $\boldsymbol{g} \in \boldsymbol{H}^1(\Omega)$ such that*

$$\begin{aligned} &\operatorname{div}\boldsymbol{g} = 0 \qquad \textit{in } \Omega, \\ &\boldsymbol{g}|_{\partial\Omega} = \boldsymbol{\varphi} \qquad \textit{(in the sense of traces).} \end{aligned} \tag{1.15}$$

For the proof see [11].

Definition 1.13 *Let $\boldsymbol{f} \in \boldsymbol{L}^2(\Omega), \boldsymbol{\varphi} \in \boldsymbol{H}^{\frac{1}{2}}(\partial\Omega)$ and let (1.14) holds. Supposing that $\boldsymbol{g}$ is a function from Lemma 1.12, we call $\boldsymbol{u}$ a weak solution of the Navier-Stokes problem (1.13), iff*

$$\begin{aligned} &\boldsymbol{u} \in \boldsymbol{H}^1(\Omega), \\ &\boldsymbol{u} - \boldsymbol{g} \in \boldsymbol{V}, \\ &a_\Omega(\boldsymbol{u}, \boldsymbol{v}) + b_\Omega(\boldsymbol{u}, \boldsymbol{u}, \boldsymbol{v}) = (\boldsymbol{f}, \boldsymbol{v})_\Omega \quad \forall\, \boldsymbol{v} \in \boldsymbol{V}. \end{aligned} \tag{1.16}$$

Condition $(1.16)_3$ is a weak version of equation $(1.13)_1$, while conditions $(1.16)_1$ and $(1.16)_2$ ensure that the condition $(1.13)_3$ is fulfilled in the sense of traces.

1.3.1 Existence of the weak solution

Theorem 1.14 *Let $\boldsymbol{f} \in \boldsymbol{L}^2(\Omega)$, $\boldsymbol{g}$ be from Lemma 1.12 and $\boldsymbol{\varphi} \in \boldsymbol{H}^{\frac{1}{2}}(\partial\Omega)$ satisfies*

$$\int_\Gamma \boldsymbol{\varphi} \cdot \boldsymbol{n}\, dS = 0 \qquad \text{for each component } \Gamma \text{ of } \partial\Omega. \tag{1.17}$$

Then the problem (1.16) has at least one solution.

Proof: The solution will be sought in the form $\boldsymbol{u} = \hat{\boldsymbol{u}} + \boldsymbol{g}$, where $\hat{\boldsymbol{u}} \in \boldsymbol{V}$ and $\boldsymbol{g}$ is a suitable function with properties (1.15). Substituting this representation into (1.16), we see that the unknown $\hat{\boldsymbol{u}}$ is a solution of the problem

$$\begin{aligned} &\hat{\boldsymbol{u}} \in \boldsymbol{V}, \\ &a_\Omega(\hat{\boldsymbol{u}}, \boldsymbol{v}) + b_\Omega(\hat{\boldsymbol{u}}, \hat{\boldsymbol{u}}, \boldsymbol{v}) + b_\Omega(\hat{\boldsymbol{u}}, \boldsymbol{g}, \boldsymbol{v}) + b_\Omega(\boldsymbol{g}, \hat{\boldsymbol{u}}, \boldsymbol{v}) = \langle \hat{\boldsymbol{f}}, \boldsymbol{v} \rangle \qquad \forall\, \boldsymbol{v} \in \boldsymbol{V}, \end{aligned} \tag{1.18}$$

where $\hat{\boldsymbol{f}}$ is a continuous linear functional on $\boldsymbol{V}$ defined by the relation

$$\langle \hat{\boldsymbol{f}}, \boldsymbol{v} \rangle = (\boldsymbol{f}, \boldsymbol{v})_\Omega - a_\Omega(\boldsymbol{g}, \boldsymbol{v}) - b_\Omega(\boldsymbol{g}, \boldsymbol{g}, \boldsymbol{v}) \qquad \forall\, \boldsymbol{v} \in \boldsymbol{V}.$$

Existence of the solution $\hat{\boldsymbol{u}}$ of the problem (1.18) will be proved in a similar way as in the case of the problem with homogeneous boundary conditions. Only main steps of the proof will be written on this place. For more information see [11].

The procedure of the proof is as follows:

1. Consider such a sequence $\{\boldsymbol{w}^k\}_{k=1}^\infty \subset \mathcal{V}$ that

   $$\boldsymbol{V} = \overline{\bigcup_{k=1}^{\infty} \boldsymbol{X}_k}^{\boldsymbol{H}_0^1(\Omega)},$$

   where $\boldsymbol{X}_k = [\boldsymbol{w}^1, \ldots, \boldsymbol{w}^k]$.

2. Prove the existence of solution $\hat{\boldsymbol{u}}^k \in \boldsymbol{X}_k$ of the problem

   $$a_\Omega(\hat{\boldsymbol{u}}^k, \boldsymbol{w}^j) + b_\Omega(\hat{\boldsymbol{u}}^k, \hat{\boldsymbol{u}}^k, \boldsymbol{w}^j) + b_\Omega(\hat{\boldsymbol{u}}^k, \boldsymbol{g}, \boldsymbol{w}^j) + b_\Omega(\boldsymbol{g}, \hat{\boldsymbol{u}}^k, \boldsymbol{w}^j) = \langle \hat{\boldsymbol{f}}, \boldsymbol{w}^j \rangle \qquad j = 1, \ldots, k.$$

3. On the basis of Lemma 1.7 we derive from the previous equality the following estimate:

   $$\|\hat{\boldsymbol{u}}^k\|_{\boldsymbol{H}_0^1(\Omega)} \le \tilde{c} \|\hat{\boldsymbol{f}}\|_{\boldsymbol{V}^*} \qquad \forall\, k = 1, 2, \ldots$$

4. We subtract a subsequence $\{\hat{\boldsymbol{u}}^{k_j}\}$ from $\{\hat{\boldsymbol{u}}^k\}$ converging to some $\hat{\boldsymbol{u}} \in \boldsymbol{V}$ weakly in $\boldsymbol{V}$ and strongly in $\boldsymbol{L}^2(\Omega)$.

5. Use the obvious limit passages (where the third one follows from Lemma 1.8)

   $$\begin{aligned} &b_\Omega(\hat{\boldsymbol{u}}^{k_j}, \boldsymbol{g}, \boldsymbol{v}) \to b_\Omega(\hat{\boldsymbol{u}}, \boldsymbol{g}, \boldsymbol{v}) \qquad \forall\, \boldsymbol{v} \in \boldsymbol{V}, \\ &b_\Omega(\boldsymbol{g}, \hat{\boldsymbol{u}}^{k_j}, \boldsymbol{v}) \to b_\Omega(\boldsymbol{g}, \hat{\boldsymbol{u}}, \boldsymbol{v}) \qquad \forall\, \boldsymbol{v} \in \boldsymbol{V} \\ &b_\Omega(\hat{\boldsymbol{u}}^{k_j}, \hat{\boldsymbol{u}}^{k_j}, \boldsymbol{v}) \to b_\Omega(\hat{\boldsymbol{u}}, \hat{\boldsymbol{u}}, \boldsymbol{v}) \qquad \forall\, \boldsymbol{v} \in \boldsymbol{V} \end{aligned}$$

   to find that $\hat{\boldsymbol{u}}$ is a solution of $(1.16)_1$-$(1.16)_3$.

⊠

Remark In the case that the condition (1.17) is not satisfied (only the weaker condition (1.14) holds), the existence of a weak solution can be established only for "small data", i.e. for small $\|\boldsymbol{f}\|_{\boldsymbol{L}^2(\Omega)}, \|\varphi\|_{\boldsymbol{H}^{\frac{1}{2}}(\partial\Omega)}$ and large ν.

1.4 The Oseen problem

One possible approach to the linearization of the Navier-Stokes equations is to use the so-called Oseen problem. This method is based on replacing of the unknown velocity field in the convective term by some other, known convective velocity. Then the problem is linear with respect to the velocity field. Results presented in this section are based on [11].

We can formulate the Oseen problem in the following way:

Definition 1.15 *Let* $\boldsymbol{b} \in \boldsymbol{C}^1(\overline{\Omega}), \operatorname{div} \boldsymbol{b} = 0$ *in* Ω, $\boldsymbol{f} : \overline{\Omega} \to I\!R^N$ *and let* $\boldsymbol{\varphi} : \partial\Omega \to I\!R^N$ *fulfills (1.14). Then a classical solution of the Oseen problem is defined as a couple* $(\boldsymbol{u}, p) \in \boldsymbol{C}^2(\overline{\Omega}) \times C^1(\overline{\Omega})$ *satisfying*

$$\begin{aligned} -\nu\Delta\boldsymbol{u} + (\boldsymbol{b}\cdot\nabla)\boldsymbol{u} + \nabla p &= \boldsymbol{f} \qquad \text{in } \Omega, \\ \operatorname{div}\boldsymbol{u} &= 0 \qquad \text{in } \Omega, \\ \boldsymbol{u}|_{\partial\Omega} &= \boldsymbol{\varphi}. \end{aligned} \tag{1.19}$$

Definition 1.16 *Let* $\boldsymbol{b} \in \boldsymbol{H}^1(\Omega), \operatorname{div}\boldsymbol{b} = 0, \boldsymbol{f} \in \boldsymbol{L}^2(\Omega)$ *and let* $\boldsymbol{g}$ *be a function from Lemma 1.12. We call* $\boldsymbol{u}$ *a weak solution of the Oseen problem (1.19), iff*

$$\begin{aligned} &\boldsymbol{u} \in \boldsymbol{H}^1(\Omega), \\ &\boldsymbol{u} - \boldsymbol{g} \in \boldsymbol{V}, \\ &a_\Omega(\boldsymbol{u}, \boldsymbol{v}) + b_\Omega(\boldsymbol{b}, \boldsymbol{u}, \boldsymbol{v}) = (\boldsymbol{f}, \boldsymbol{v}) \qquad \forall\, \boldsymbol{v} \in \boldsymbol{V}. \end{aligned} \tag{1.20}$$

Remark We denote

$$L_0^2(\Omega) = \left\{ q \in L^2(\Omega); \int_\Omega q\, d\boldsymbol{x} = 0 \right\},$$
$$c_\Omega(\boldsymbol{v}, p) = \int_\Omega q \operatorname{div}\boldsymbol{v}\, d\boldsymbol{x}.$$

Let $\boldsymbol{u}$ be a weak solution of the Oseen problem defined by (1.20). Then there exists a pressure function $p \in L_0^2(\Omega)$ associated with $\boldsymbol{u}$ such that

$$a_\Omega(\boldsymbol{u}, \boldsymbol{v}) + b_\Omega(\boldsymbol{b}, \boldsymbol{u}, \boldsymbol{v}) - c_\Omega(\boldsymbol{v}, p) = (\boldsymbol{f}, \boldsymbol{v})_\Omega \qquad \forall\, \boldsymbol{v} \in \boldsymbol{H}_0^1(\Omega).$$

Proof of this statement can be found in [11].

1.4.1 Existence and uniqueness of the weak solution of the Oseen problem

The solvability of the Oseen problem can be established on the basis of the Lax-Milgram lemma:

Theorem 1.17 *Problem (1.20) has a unique solution.*

Proof: Put

$$a_{\boldsymbol{b}}(\hat{\boldsymbol{u}}, \boldsymbol{v}) = a_\Omega(\hat{\boldsymbol{u}}, \boldsymbol{v}) + b_\Omega(\boldsymbol{b}, \hat{\boldsymbol{u}}, \boldsymbol{v})$$

defined for all $\hat{\boldsymbol{u}}, \boldsymbol{v} \in \boldsymbol{V}$. The properties of b_Ω imply that $a_{\boldsymbol{b}}$ is a continuous bilinear form defined on $\boldsymbol{V} \times \boldsymbol{V}$. Using Lemma 1.7 we can find that $a_{\boldsymbol{b}}$ is $\boldsymbol{V}$-elliptic:

$$\begin{aligned} a_{\boldsymbol{b}}(\hat{\boldsymbol{u}}, \hat{\boldsymbol{u}}) &= a_\Omega(\hat{\boldsymbol{u}}, \hat{\boldsymbol{u}}) + b_\Omega(\boldsymbol{b}, \hat{\boldsymbol{u}}, \hat{\boldsymbol{u}}) \\ &= a_\Omega(\hat{\boldsymbol{u}}, \hat{\boldsymbol{u}}) = \nu \|\hat{\boldsymbol{u}}\|^2_{\boldsymbol{H}^1_0(\Omega)} \qquad \forall\, \hat{\boldsymbol{u}} \in \boldsymbol{V}. \end{aligned}$$

Let us seek a solution of the problem (1.20) in the form $\boldsymbol{u} = \hat{\boldsymbol{u}} + \boldsymbol{g}$ where $\hat{\boldsymbol{u}} \in \boldsymbol{V}$ is unknown. Then $(1.20)_3$ is equivalent to the problem

$$\hat{\boldsymbol{u}} \in \boldsymbol{V}, \quad a_{\boldsymbol{b}}(\hat{\boldsymbol{u}}, \boldsymbol{b}) = \langle \underline{l}, \boldsymbol{v} \rangle \quad \forall\, \boldsymbol{v} \in \boldsymbol{V}, \tag{1.21}$$

where $\underline{l} \in \boldsymbol{V}^*$ is given by

$$\langle \underline{l}, \boldsymbol{v} \rangle = (\boldsymbol{f}, \boldsymbol{v})_\Omega - a_\Omega(\boldsymbol{g}, \boldsymbol{v}) - b_\Omega(\boldsymbol{b}, \boldsymbol{g}, \boldsymbol{v}), \quad \boldsymbol{v} \in \boldsymbol{V}.$$

From the Lax-Milgram lemma we immediately obtain the unique solvability of the problem (1.21) with respect to $\hat{\boldsymbol{u}} \in \boldsymbol{V}$ and, thus, the unique solvability of (1.20).

⊠

1.4.2 Oseen iteration process and the convergence

The Oseen problem offers the following iterative process for the approximate solution of the Navier-Stokes equations:
Let us suppose to have $\boldsymbol{u}^* \in \boldsymbol{H}^1(\Omega), \boldsymbol{u}^*|_{\partial\Omega} = \boldsymbol{\varphi}$.

1. Choose $\boldsymbol{u}^0 \in \boldsymbol{H}^1(\Omega) : \boldsymbol{u}^0 - \boldsymbol{u}^* \in \boldsymbol{H}^1_0(\Omega)$.

2. Let us suppose that we already have $\boldsymbol{u}^k \in \boldsymbol{H}^1(\Omega) : \boldsymbol{u}^k - \boldsymbol{u}^* \in \boldsymbol{H}^1_0(\Omega)$.
   We seek for $\boldsymbol{u}^{k+1} \in \boldsymbol{H}^1(\Omega), \boldsymbol{u}^{k+1} - \boldsymbol{u}^* \in \boldsymbol{H}^1_0(\Omega)$ and $p^{k+1} \in L^2_0(\Omega)$ such that

   $$\begin{aligned} a_\Omega(\boldsymbol{u}^{k+1}, \boldsymbol{v}) + b_\Omega(\boldsymbol{u}^k, \boldsymbol{u}^{k+1}, \boldsymbol{v}) - c_\Omega(\boldsymbol{v}, p^{k+1}) &= (\boldsymbol{f}, \boldsymbol{v})_\Omega, \\ c_\Omega(\boldsymbol{u}^{k+1}, q) &= 0, \end{aligned} \tag{1.22}$$

   for all $(\boldsymbol{v}, p) \in \boldsymbol{H}^1_0(\Omega) \times L^2_0(\Omega)$.

Theorem 1.18 *If the condition*

$$\nu^2 > \tilde{c} c_F \|\boldsymbol{f}\|_{\boldsymbol{L}^2(\Omega)},$$

with the constants $\tilde{c}$ and c_F from (1.4) and (1.1) is satisfied, then the sequence of solutions $(\boldsymbol{u}^k, p^k)$ of the problem (1.22) converges in $\boldsymbol{H}^1(\Omega) \times L^2_0(\Omega)$ to the unique solution $(\boldsymbol{u}, p)$ of the following problem:
Find $\boldsymbol{u} \in \boldsymbol{H}^1(\Omega), \boldsymbol{u} - \boldsymbol{u}^* \in \boldsymbol{H}^1_0(\Omega)$ and $p \in L^2_0(\Omega)$:

$$\begin{aligned} a_\Omega(\boldsymbol{u}, \boldsymbol{v}) + b_\Omega(\boldsymbol{u}, \boldsymbol{u}, \boldsymbol{v}) - c_\Omega(\boldsymbol{v}, p) &= (\boldsymbol{f}, \boldsymbol{v})_\Omega, \\ c_\Omega(\boldsymbol{u}, q) &= 0, \end{aligned}$$

for all $(\boldsymbol{v}, p) \in \boldsymbol{H}^1_0(\Omega) \times L^2_0(\Omega)$ as $k \to \infty$.

Proof can be found in [12].

Chapter 2

Stabilization of the Navier-Stokes equations

Motivation for the stabilization of the Navier-Stokes equations arises from the finite element simulation of the incompressible Navier-Stokes equations. The main problem occurs when the convective term dominates over the dissipative term, i.e. for fluids with a low viscosity value. Then spurious oscillations could arise in the solution. Second problem is that pairs of equal-order finite element spaces violate the discrete inf-sup condition. We can treat both problems together by using the approach introduced below. Chapter is based on [18].

We consider the nonstationary, incompressible Navier-Stokes problem

$$\begin{aligned} \frac{\partial \boldsymbol{u}}{\partial t} - \nu\Delta\boldsymbol{u} + (\boldsymbol{u}\cdot\nabla)\boldsymbol{u} + \nabla p &= \boldsymbol{f} \qquad \text{in } \Omega, \\ \operatorname{div}\boldsymbol{u} &= 0 \qquad \text{in } \Omega, \\ \boldsymbol{u} &= 0 \qquad \text{on } \partial\Omega, \end{aligned} \tag{2.1}$$

for the velocity field $\boldsymbol{u}$ and the pressure p in a polyhedral domain $\Omega \subset I\!R^d, d = 2, 3$, with a source term $\boldsymbol{f}$. This general problem could be easily adapted for special cases of flow - like a stationary flow for example.

One possible method for solving the problem (2.1) is to semidiscretize it in time and then to apply the fixed-point iteration within each step with updating the convective velocity. This approach leads to an auxiliary problem of the Oseen type in each iteration step:

$$\begin{aligned} L_O(\boldsymbol{b};\boldsymbol{u},p) := -\nu\Delta\boldsymbol{u} + (\boldsymbol{b}\cdot\nabla)\boldsymbol{u} + \sigma\boldsymbol{u} + \nabla p &= \boldsymbol{f} \qquad \text{in } \Omega, \\ \operatorname{div}\boldsymbol{u} &= 0 \qquad \text{in } \Omega, \\ \boldsymbol{u} &= 0 \qquad \text{on } \partial\Omega. \end{aligned} \tag{2.2}$$

Also an iterative solution of the steady-state Navier-Stokes equations leads to a problem of type (2.2) with $\sigma = 0$.

By discretization the basic Galerkin finite element method (FEM) may suffer from two problems: the dominating advection in the case of $0 < \nu << \|\boldsymbol{b}\|_{\boldsymbol{L}^\infty(\Omega)}$ and (or) the violation of the discrete inf-sup stability condition for the velocity and pressure approximations.

The *streamline-upwind/Petrov-Galerkin method (SUPG)* and the *pressure-stabilization/ Petrov-Galerkin method (PSPG)* opened the possibility to treat both problems in a unique framework using arbitrary FE approximations of velocity and pressure, including equal-order pairs.

An additional stabilization of the divergence constraint $(2.2)_2$, called *grad-div stabilization*, is important for the robustness if $0 < \nu << \|\boldsymbol{b}\|_{\boldsymbol{L}^\infty(\Omega)}$.

We shall start with the inf-sup condition. The discretization of the Oseen problem with stabilizations and the fundamental lemma about solvability of the discrete problem will follow.

2.1 Inf-sup condition

Lemma 2.1 *The operator* div *is a mapping of* $\boldsymbol{H}_0^1(\Omega)$ *onto* $L_0^2(\Omega)$. *More precisely, the operator* div *is an isomorphism of the orthogonal complement*

$$\boldsymbol{V}^\perp = \{\boldsymbol{u} \in \boldsymbol{H}_0^1(\Omega); (\boldsymbol{u}, \boldsymbol{v})_{\boldsymbol{H}_0^1(\Omega)} = 0 \ \forall\, \boldsymbol{v} \in \boldsymbol{V}\}$$

of the subspace $\boldsymbol{V} \subset \boldsymbol{H}_0^1(\Omega)$ *onto* $L_0^2(\Omega)$.

Proof can be found in [13].

By this lemma, there exists a unique function $\boldsymbol{v} \in \boldsymbol{V}^\perp$ for each $q \in L_0^2(\Omega)$ such that

$$\operatorname{div} \boldsymbol{v} = q, \qquad \|\boldsymbol{v}\|_{\boldsymbol{H}_0^1(\Omega)} \le c\|q\|_{L^2(\Omega)},$$

where $c > 0$ is a constant independent of q. Hence, taking $q \neq 0$, we have $\boldsymbol{v} \neq 0$ and

$$\frac{(q, \operatorname{div} \boldsymbol{v})_\Omega}{\|\boldsymbol{v}\|_{\boldsymbol{H}_0^1(\Omega)}} = \frac{\|q\|^2_{L^2(\Omega)}}{\|\boldsymbol{v}\|_{\boldsymbol{H}_0^1(\Omega)}} \ge \frac{\|q\|_{L^2(\Omega)}}{c}.$$

This leads to the inequality

$$\sup_{\boldsymbol{v} \in \boldsymbol{H}_0^1(\Omega),\, \boldsymbol{v} \neq 0} \frac{(q, \operatorname{div} \boldsymbol{v})_\Omega}{\|q\|_{L^2(\Omega)} \|\boldsymbol{v}\|_{\boldsymbol{H}_0^1(\Omega)}} \ge \gamma, \qquad q \in L_0^2(\Omega),$$

where $\gamma = 1/c > 0$. This condition can be written in the equivalent form

$$\inf_{q \in L_0^2(\Omega),\, q \neq 0} \sup_{\boldsymbol{v} \in \boldsymbol{H}_0^1(\Omega),\, \boldsymbol{v} \neq 0} \frac{(q, \operatorname{div} \boldsymbol{v})_\Omega}{\|q\|_{L^2(\Omega)} \|\boldsymbol{v}\|_{\boldsymbol{H}_0^1(\Omega)}} \ge \gamma, \qquad q \in L_0^2(\Omega), \tag{2.3}$$

which represents the so-called *inf-sup (or Babuška-Brezzi) condition*. This condition guarantees that the problem is well posed. Its discrete version plays an important role in the analysis of numerical methods for the Navier-Stokes problem - it provides sufficient conditions for a stable mixed formulation.

2.2 The discrete problem

Let $\Omega \subset I\!R^d, d = 2, 3$ be a bounded polygonal or polyhedral domain.

The generalized Oseen equations with homogeneous Dirichlet boundary conditions reads

$$\begin{aligned} -\nu\Delta \boldsymbol{u} + (\boldsymbol{b}\cdot\nabla)\boldsymbol{u} + \sigma\boldsymbol{u} + \nabla p &= \boldsymbol{f} \quad \text{in } \Omega, \\ \operatorname{div} \boldsymbol{u} &= 0 \quad \text{in } \Omega, \\ \boldsymbol{u} &= 0 \quad \text{on } \partial\Omega, \end{aligned} \tag{2.4}$$

where $\boldsymbol{b} \in \boldsymbol{H}_0^1(\Omega), \nu, \sigma \in L^\infty(\Omega)$ are given and

$$\operatorname{div} \boldsymbol{b} = 0, \qquad 0 < \sigma < \infty, \qquad \nu = \text{const} > 0.$$

We define for $\boldsymbol{u}, \boldsymbol{v} \in \boldsymbol{H}_0^1(\Omega)$ and $p, q \in L_0^2(\Omega)$ the bilinear form A and the linear form L by

$$\begin{aligned} A((\boldsymbol{u}, p), (\boldsymbol{v}, q)) &:= a_\Omega(\boldsymbol{u}, \boldsymbol{v}) + b_\Omega(\boldsymbol{b}, \boldsymbol{u}, \boldsymbol{v}) + \sigma(\boldsymbol{u}, \boldsymbol{v})_\Omega - c_\Omega(\boldsymbol{v}, p) + c_\Omega(\boldsymbol{u}, q), \\ L((\boldsymbol{v}, q)) &:= (\boldsymbol{f}, \boldsymbol{v})_\Omega. \end{aligned}$$

A weak formulation of the Oseen equations (2.4) reads: find $(\boldsymbol{u}, p) \in \boldsymbol{H}_0^1(\Omega) \times L_0^2(\Omega)$ such that

$$A((\boldsymbol{u}, p), (\boldsymbol{v}, q)) = L((\boldsymbol{v}, q)) \qquad \forall\, (\boldsymbol{v}, q) \in \boldsymbol{H}_0^1(\Omega) \times L_0^2(\Omega). \tag{2.5}$$

Let $\{\mathcal{T}_h\}$ be a family of shape-regular triangulations of the domain Ω such that

$$\overline{\Omega} = \bigcup_{K \in \mathcal{T}_h} \overline{K}$$

holds true for all triangulations $\mathcal{T}_h$.

Let $\boldsymbol{X}_h$ be a conforming finite element space based on $\mathcal{T}_h$ for approximation of the velocity. The space M_h is a discretized space for the pressure. We are interested in an inf-sup stable discretization, i.e. the condition

$$\inf_{q_h \in M_h} \sup_{\boldsymbol{v}_h \in \boldsymbol{X}_h} \frac{(\operatorname{div} \boldsymbol{v}_h, q_h)_\Omega}{\|\boldsymbol{v}_h\|_{\boldsymbol{H}_0^1(\Omega)} \|q_h\|_{L^2(\Omega)}} \geq \beta$$

is valid for all $\mathcal{T}_h$ with a constant β which is independent of the mesh parameter h.

We assume that for all cells $K \in \mathcal{T}_h$ the following inverse inequalities

$$\|\operatorname{div} \boldsymbol{v}_h\|_{\boldsymbol{L}^2(K)} \leq \begin{array}{ll} \|\Delta \boldsymbol{v}_h\|_{\boldsymbol{L}^2(K)} \leq \mu\, h_K^{-1} \|\nabla \boldsymbol{v}_h\|_{\boldsymbol{L}^2(K)} & \forall\, \boldsymbol{v}_h \in \boldsymbol{X}_h, \\ \|\nabla \boldsymbol{v}_h\|_{\boldsymbol{L}^2(K)} \leq \mu\, h_K^{-1} \|\boldsymbol{v}_h\|_{\boldsymbol{L}^2(K)} & \forall\, \boldsymbol{v}_h \in \boldsymbol{X}_h, \\ \|\nabla q_h\|_{\boldsymbol{L}^2(K)} \leq \mu\, h_K^{-1} \|q_h\|_{\boldsymbol{L}^2(K)} & \forall\, q_h \in M_h, \end{array} \tag{2.6}$$

hold with a constant μ which depends only on the shape-regularity parameter of the family of triangulations.

Using the finite element spaces $\boldsymbol{X}_h$ and M_h, we can formulate the discretization of (2.5) which reads: find $(\boldsymbol{u}_h, p_h) \in \boldsymbol{X}_h \times M_h$ such that

$$A((\boldsymbol{u}_h, p_h), (\boldsymbol{v}_h, q_h)) = L((\boldsymbol{v}_h, q_h)) \qquad \forall\, (\boldsymbol{v}_h, q_h) \in \boldsymbol{X}_h \times M_h. \tag{2.7}$$

In the case of a locally dominating convection, we may get solution of (2.7) with spurious oscillations which are generally not localized to regions with a dominating convection. In order to stabilize the discrete problem, we introduce a modified bilinear form and a modified linear form by

$$\begin{aligned} A_S((\boldsymbol{u},p),(\boldsymbol{v},q)) &:= A((\boldsymbol{u},p),(\boldsymbol{v},q)) + \gamma(\nabla\cdot\boldsymbol{u},\nabla\cdot\boldsymbol{v})_\Omega \\ &\quad + \sum_{K\in\mathcal{T}_h} (-\nu\Delta\boldsymbol{u} + (\boldsymbol{b}\cdot\nabla)\boldsymbol{u} + \sigma\boldsymbol{u} + \nabla p, \kappa_K(\boldsymbol{b}\cdot\nabla)\boldsymbol{v} + \tau_K\nabla q)_K, \\ L_S((\boldsymbol{v},q)) &:= L((\boldsymbol{v},q)) + \sum_{K\in\mathcal{T}_h} (\boldsymbol{f}, \kappa_K(\boldsymbol{b}\cdot\nabla)\boldsymbol{v} + \tau_K\nabla q)_K, \end{aligned}$$

where τ_K (PSPG stabilization) and κ_K (SUPG stabilization) are user-defined and cell-dependent parameters while γ (grad-div stabilization) is a global user-defined parameter.

The stabilized discrete problem reads: find $(\boldsymbol{u}_h, p_h) \in \boldsymbol{X}_h \times M_h$ such that

$$A_S((\boldsymbol{u}_h,p_h),(\boldsymbol{v}_h,q_h)) = L_S((\boldsymbol{v}_h,q_h)) \qquad \forall\,(\boldsymbol{v}_h,q_h) \in \boldsymbol{X}_h \times M_h. \tag{2.8}$$

2.3 Solvability of the discrete problem

To show that the stabilized discrete problem (2.8) is uniquely solvable, we need to prove the inf-sup condition on $\boldsymbol{X}_h \times M_h$ for the bilinear form A_S, where the inf-sup constant is independent of the mesh size h and the parameter ν.

We define

$$\varphi := \sqrt{\nu + \sigma c_F^2} + 2\|\boldsymbol{b}\|_{\boldsymbol{L}^\infty(\Omega)} \min\left(\frac{1}{\sqrt{\sigma}}, \frac{c_F}{\sqrt{\nu}}\right) + \sqrt{\gamma},$$

where c_F is the Friedrichs constant for Ω. Let the constant δ satisfy

$$0 \le \delta \le \min\left(\frac{\mu^2 c_F^2}{12}, \frac{\mu}{2}\sqrt{\frac{2}{21}} \min\left(\frac{1}{\sigma}, \frac{c_F^2}{\nu}\right), \frac{17}{105\,840}\beta^2\right), \tag{2.9}$$

where μ is the constant from the inverse inequalities (2.6) and β is the inf-sup constant for the pair $(\boldsymbol{X}_h, M_h)$. We assume that the stabilization parameters fulfill

$$0 \le \gamma, \quad \kappa_K := \delta\frac{\beta^2}{\mu^2\varphi^2}h_K^2, \quad 0 \le \tau_K \le \kappa_K. \tag{2.10}$$

We introduce the norm

$$\begin{aligned} |\!|\!|(\boldsymbol{v},q)|\!|\!|^2 &:= \nu\|\boldsymbol{v}\|^2_{\boldsymbol{H}^1_0(\Omega)} + \sigma\|\boldsymbol{v}\|^2_{\boldsymbol{L}^2(\Omega)} + \gamma\|\operatorname{div}\boldsymbol{v}\|^2_{\boldsymbol{L}^2(\Omega)} + \sum_{K\in\mathcal{T}_h} \kappa_K\|(\boldsymbol{b}\cdot\nabla)\boldsymbol{v}\|^2_{L^2(K)} \\ &\quad + \alpha\|q\|^2_{L^2(\Omega)} + \sum_{K\in\mathcal{T}_h} \tau_K\|\nabla q\|^2_{L^2(\Omega)}, \end{aligned}$$

where the parameter $\alpha > 0$ is determined in the proof of the next lemma.

Lemma 2.2 *Let the stabilization parameters fulfill (2.9) and (2.10). Then there exists a positive constant β_S independent of the mesh size h and parameter ν such that*

$$\inf_{(\boldsymbol{v}_h,q_h)} \sup_{(\boldsymbol{w}_h,r_h)} \frac{A_S((\boldsymbol{v}_h,q_h),(\boldsymbol{w}_h,r_h))}{|\!|\!|(\boldsymbol{v}_h,q_h)|\!|\!|\,|\!|\!|(\boldsymbol{w}_h,r_h)|\!|\!|} \ge \beta_S \ge 0$$

holds true where the infimum and supremum are taken over $\boldsymbol{X}_h \times M_h$.

For the proof see [18].

Chapter 3

Shape optimization problem

Aim of this part is to formulate the shape optimization problem and to prove the existence of its solution. For simplicity, we consider the Navier-Stokes equations with homogeneous Dirichlet boundary conditions as a state problem. The approach presented in this chapter is motivated e.g. by [15, 21].

3.1 Admissible domains

In the shape optimization problems, the domains in which the state problems are solved are objects of the optimization, i.e. they are changing during the optimization process.

We consider here the model of the flow in a channel $\Omega \subset I\!R^3$ which can be modified by changing the shape of a boundary part $\Gamma_D \subsetneq \partial\Omega$. We denote by Ω_D the design domain and by Ω_F the fixed part of domain,

$$\overline{\Omega} = \overline{\Omega_D \cup \Omega_F}.$$

We denote by Γ_{in} the inlet and by Γ_{out} the outlet boundary parts, $\Gamma_F = \partial\Omega_D \cap \partial\Omega_F$. For the domain description see Figure 3.1. The shape of Ω can be changed by moving the boundary parts Γ_D while the subdomain Ω_F and boundary parts $\Gamma_{in}, \Gamma_{out}$ stay unchanged.

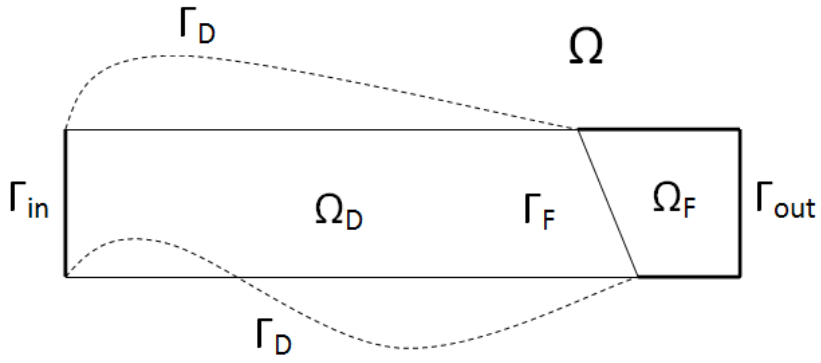

Figure 3.1: Computational domain

Now we need to define the cone property of the domain. We introduce the cone in $\mathbb{R}^3$ (the concept could be analogously generalized for $\mathbb{R}^n$): let $h > 0, \theta \in (0, \frac{\pi}{2})$ and $\xi \in \mathbb{R}^3, \|\xi\| = 1$, be given. The set

$$C(\xi, \theta, h) = \{\boldsymbol{x} \in \mathbb{R}^3; (\boldsymbol{x}, \xi) \geq \|\boldsymbol{x}\| \cos\theta, \|\boldsymbol{x}\| \leq h\}$$

is called the cone of angle θ, height h and axis ξ.

Definition 3.1 *A domain $\Omega \subset \mathbb{R}^3$ is said to satisfy the cone property, iff there exist numbers $\theta \in (0, \frac{\pi}{2}), h > 0, r \in (0, \frac{h}{2})$ with the property that $\forall\, \boldsymbol{x} \in \partial\Omega\ \exists\, C_{\boldsymbol{x}} := C_{\boldsymbol{x}}(\xi, \theta, h)$ such that $\forall\, \boldsymbol{y} \in B_r(\boldsymbol{x}) \cap \Omega$ the set $\boldsymbol{y} + C_{\boldsymbol{x}} \subset \Omega$.*

It could be shown that the domain Ω possesses the cone property, iff $\Omega \in C^{0,1}$. Proof can be found in [4].

Next definition establishes the idea of the uniform cone property.

Definition 3.2 *Let $\hat{\Omega} \subset \mathbb{R}^3$ be a bounded domain and $\overline{\theta} \in (0, \frac{\pi}{2}), \overline{h} > 0, \overline{r} \in (0, \frac{h}{2})$ be given. The set of all domains contained in $\hat{\Omega}$ and satisfying the cone property with the numbers $\overline{\theta}, \overline{h}, \overline{r}$ will be denoted by $\mathcal{M}(\overline{\theta}, \overline{h}, \overline{r})$. We say that the system $\mathcal{M}(\overline{\theta}, \overline{h}, \overline{r})$ contains domains satisfying the uniform cone property.*

Now we need to define the set of *admissible domains* $\mathcal{O}$. We shall consider domains with the uniform cone property for a fixed $\hat{\Omega} \subset \mathbb{R}^3, \overline{\theta} \in (0, \frac{\pi}{2}), \overline{h} > 0$ and $\overline{r} \in (0, \frac{h}{2})$. Next we consider a domain Ω_{min} which restricts the shape of admissible domains:

$$\mathcal{O} = \{\Omega; \Omega \in \mathcal{M}(\overline{\theta}, \overline{h}, \overline{r}), \Omega_{min} \subseteq \Omega \subseteq \hat{\Omega}\}. \tag{3.1}$$

Definition 3.3 *Let $\{\Omega_n\} \subset \mathcal{O}$ be a sequence of domains, $(\Gamma_D)_n \subset \partial\Omega_n, \Gamma_D \subset \partial\Omega$. We say that $\{\Omega_n\}$ converges to Ω, iff $(\Gamma_D)_n \rightrightarrows \Gamma_D$, where the symbol '$\rightrightarrows$' means the uniform convergence. We denote it $\Omega_n \rightsquigarrow \Omega$.*

3.2 The state problem

We deal with a continuous formulation of the Navier-Stokes problem in this chapter (we do not consider a stabilized formulation). We consider homogeneous Dirichlet boundary conditions. We shall derive some basic results for this problem.

The state problem reads: find $\boldsymbol{u}, p$ such that

$$\begin{aligned} -\nu\Delta\boldsymbol{u} + (\boldsymbol{u}\cdot\nabla)\boldsymbol{u} + \nabla p &= \boldsymbol{f} \qquad \text{in } \Omega, \\ \operatorname{div}\boldsymbol{u} &= 0 \qquad \text{in } \Omega, \\ \boldsymbol{u}|_{\partial\Omega} &= 0. \end{aligned}$$

We can reformulate it in a weak sense: find $\boldsymbol{u} \in \boldsymbol{V}(\Omega) = \{\boldsymbol{v} \in \boldsymbol{H}_0^1(\Omega); \operatorname{div}\boldsymbol{v} = 0 \text{ in } \Omega\}$ such that

$$a_\Omega(\boldsymbol{u}, \boldsymbol{v}) + b_\Omega(\boldsymbol{u}, \boldsymbol{u}, \boldsymbol{v}) = (\boldsymbol{f}, \boldsymbol{v})_\Omega \qquad \forall\, \boldsymbol{v} \in \boldsymbol{V}(\Omega). \tag{3.2}$$

We studied this problem in the first chapter. We know from Theorem 1.10 that there exists at least one solution of the problem (3.2). But we do not have the uniqueness of the weak solution of the Navier-Stokes problem in general.

We shall define the graph of the multiple valued mapping $\Omega \mapsto \boldsymbol{u}$ restricted to $\mathcal{O}$:

$$\mathcal{G} := \{(\Omega, \boldsymbol{u}); \Omega \in \mathcal{O}, \boldsymbol{u} \text{ is a solution of (3.2) in } \Omega\}.$$

3.3 Objective function

A typical problem in the shape optimization is to find a shape of domain which is optimal in such a way that it minimizes a certain *objective function* while satisfying given constraints. The objective function could depend on the solution of a given partial differential equations defined in a variable domain. The final objective function could be also a combination of more than one functionals.

If we denote a general objective function by $\mathcal{J}(\Omega, \boldsymbol{u})$, the shape optimization problem reads:

$$\begin{aligned} &\text{Find } (\Omega^*, \boldsymbol{u}^*) \in \mathcal{G} \\ &\mathcal{J}(\Omega^*, \boldsymbol{u}^*) \leq \mathcal{J}(\Omega, \boldsymbol{u}) \quad \forall\, (\Omega, \boldsymbol{u}) \in \mathcal{G}. \end{aligned}$$

In our case, the shape optimization is performed by changing the boundary part $\Gamma_D \subset \partial\Omega$. We introduce a criterion domain $\Omega_C \subseteq \Omega$ where the objective function will be computed, see Figure 3.2.

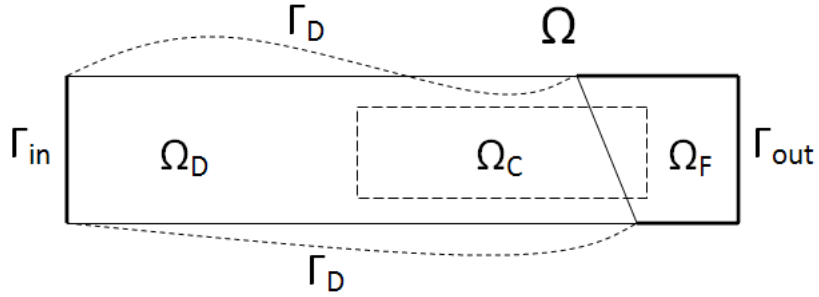

Figure 3.2: Criterion domain

Our goal is to reduce gradients of the flow velocity in Ω_C and thereby to achieve the flow uniformity in this part of geometry. This intention is equivalent with the problem of minimization of the specific objective function

$$\Psi(\Omega, \boldsymbol{u}) = \frac{\nu}{2} \int_{\Omega_C} |\nabla \boldsymbol{u}|^2 \, d\boldsymbol{x} = \frac{1}{2} a_{\Omega_C}(\boldsymbol{u}, \boldsymbol{u}). \tag{3.3}$$

We solve the following optimization problem:

$$\begin{aligned} &\text{Find } (\Omega^*, \boldsymbol{u}^*) \in \mathcal{G} : \\ &\Psi(\Omega^*, \boldsymbol{u}^*) \leq \Psi(\Omega, \boldsymbol{u}) \quad \forall\, (\Omega, \boldsymbol{u}) \in \mathcal{G}. \end{aligned} \tag{3.4}$$

The condition $(\Omega, \boldsymbol{u}) \in \mathcal{G}$ constraints values of Ψ for such pairs $(\Omega, \boldsymbol{u})$ that $\boldsymbol{u}$ solves the state problem in Ω.

3.4 Existence of an optimal shape

In this section we present results concerning the existence of an optimal shape.

One of the main difficulty in a shape optimization problem is that functions are defined in variable domains whose shapes are the objects of optimization. One possible way how to solve this difficulty is to extend functions from domains where are they defined to a larger fixed domain containing all admissible domains. We shall present this approach for a homogeneous Dirichlet boundary value problem. Extension of this method for other boundary conditions can be found in [15].

Because we have

$$\Omega \subseteq \hat{\Omega} \quad \forall\, \Omega \in \mathcal{O},$$

we can introduce the extension of functions defined in Ω to the domain $\hat{\Omega}$. We prolongate them by zero outside domains $\Omega \in \mathcal{O}$, preserving their norms:

$$\tilde{\boldsymbol{u}} = \begin{cases} \boldsymbol{u} & \text{in } \Omega \\ 0 & \text{in } \hat{\Omega} \setminus \Omega. \end{cases}$$

Lemma 3.4 *System $\mathcal{O}$ is compact with respect to convergence introduced in Definition 3.3.*

For the proof see [21].

Now we shall prove a basic theorem which we need for the proof of the existence of solution of the shape optimization problem. The following proof is a modification of a proof presented in [15].

Theorem 3.5 *Let $\{\Omega_n\} \subset \mathcal{O}$ and $\Omega \in \mathcal{O}$ be such that $\Omega_n \rightsquigarrow \Omega$ and let $\boldsymbol{u}_n$ be the solution of (3.2) for Ω_n, $n \to \infty$. Then there exists a subsequence $\{\tilde{\boldsymbol{u}}_{n_k}\} \subset \{\tilde{\boldsymbol{u}}_n\}$:*

$$\tilde{\boldsymbol{u}}_{n_k} \to \boldsymbol{u} \qquad \text{in } \boldsymbol{V}(\hat{\Omega}), \quad k \to \infty,$$

and $\boldsymbol{u}_\Omega := \boldsymbol{u}|_\Omega$ solves (3.2) for Ω.

Proof: Because $\boldsymbol{u}_n \in \boldsymbol{V}(\Omega_n)$ is the solution of (3.2), we know

$$\nu \int_{\Omega_n} \nabla \boldsymbol{u}_n : \nabla \boldsymbol{v}\, d\boldsymbol{x} + \int_{\Omega_n} (\boldsymbol{u}_n \cdot \nabla \boldsymbol{u}_n) \cdot \boldsymbol{v}\, d\boldsymbol{x} = \int_{\Omega_n} \boldsymbol{f} \cdot \boldsymbol{v}\, d\boldsymbol{x} \qquad \forall\, \boldsymbol{v} \in \boldsymbol{V}(\Omega_n).$$

By setting $\boldsymbol{v} := \boldsymbol{u}_n$ we get

$$\nu \int_{\Omega_n} |\nabla \boldsymbol{u}_n|^2\, d\boldsymbol{x} + \int_{\Omega} (\boldsymbol{u}_n \cdot \nabla \boldsymbol{u}_n) \cdot \boldsymbol{u}_n\, d\boldsymbol{x} = \int_{\Omega_n} \boldsymbol{f} \cdot \boldsymbol{u}_n\, d\boldsymbol{x}.$$

Now we employ the extension of functions $\boldsymbol{u}_n$ and we obtain relations:

$$\bullet \int_{\Omega_n} |\nabla \boldsymbol{u}_n|^2\, d\boldsymbol{x} = \int_{\hat{\Omega}} |\nabla \tilde{\boldsymbol{u}}_n|^2\, d\boldsymbol{x} \geq \frac{1}{c_F} \|\tilde{\boldsymbol{u}_n}\|^2_{\boldsymbol{H}^1(\hat{\Omega})}, \tag{3.5}$$

$$\bullet \int_{\Omega_n} \boldsymbol{f} \cdot \boldsymbol{u}_n\, d\boldsymbol{x} = \int_{\hat{\Omega}} \boldsymbol{f} \cdot \tilde{\boldsymbol{u}}_n\, d\boldsymbol{x} \leq \|\boldsymbol{f}\|_{\boldsymbol{L}^2(\hat{\Omega})} \|\tilde{\boldsymbol{u}}_n\|_{\boldsymbol{H}^1(\hat{\Omega})},$$

$$\bullet \int_{\Omega_n} (\boldsymbol{u}_n \cdot \nabla \boldsymbol{u}_n) \cdot \boldsymbol{u}_n\, d\boldsymbol{x} = \int_{\hat{\Omega}} (\tilde{\boldsymbol{u}}_n \cdot \nabla \tilde{\boldsymbol{u}}_n) \cdot \tilde{\boldsymbol{u}}_n\, d\boldsymbol{x} = 0,$$

where the last equality stems from Lemma 1.7.
That means: $\exists c > 0 : \|\tilde{\boldsymbol{u}}_n\|_{\boldsymbol{H}^1(\hat{\Omega})} \leq c$ and therefore,

$$\exists \tilde{\boldsymbol{u}}_{n_k} \subset \tilde{\boldsymbol{u}}_n, \boldsymbol{u} \in \boldsymbol{H}_0^1(\hat{\Omega}) : \tilde{\boldsymbol{u}}_{n_k} \rightharpoonup \boldsymbol{u} \quad \text{in } \boldsymbol{H}_0^1(\hat{\Omega}),$$

where '$\rightharpoonup$' means the weak convergence.
It holds that the space $\boldsymbol{W}(\Omega) = \{\boldsymbol{v} \in \boldsymbol{C}_0^\infty(\Omega); \operatorname{div} \boldsymbol{v} = 0 \text{ in } \Omega\}$ is dense in $\boldsymbol{V}(\Omega)$. For the proof see [32]. Then considering $\Omega_{n_k} \rightsquigarrow \Omega$ we know that for all $\boldsymbol{v} \in \boldsymbol{H}_0^1(\Omega)$ it holds

$$\tilde{\boldsymbol{v}}|_{\Omega_{n_k}} \in \boldsymbol{V}(\Omega_{n_k}) \quad \forall\, k \geq k_0, \text{ where } k_0 \text{ is great enough.} \tag{3.6}$$

Now let us denote $\boldsymbol{u}_\Omega := \boldsymbol{u}|_\Omega$ and we want to know if this function solves the problem (3.2) in Ω.

1. We need to show $\boldsymbol{u}_\Omega \in \boldsymbol{V}(\Omega)$.
   At first we want to know $\boldsymbol{u}_\Omega \in \boldsymbol{H}_0^1(\Omega)$. This problem is equivalent with $\boldsymbol{u}_\Omega \equiv 0$ in $\hat{\Omega} \setminus \Omega$. This fact could be proved by considering $\Omega_{n_k} \rightsquigarrow \Omega$.

   Next we must prove that $\operatorname{div} \boldsymbol{u}_\Omega = 0$ in Ω.
   This condition could be rewritten in the form

   $$\int_\Omega \operatorname{div} \boldsymbol{u}_\Omega \, \varphi \, d\boldsymbol{x} = 0 \qquad \forall\, \varphi \in C_0^\infty(\Omega),$$

   and using the Green's theorem and $\boldsymbol{u}_\Omega \in \boldsymbol{H}_0^1(\Omega)$,

   $$\int_\Omega \boldsymbol{u}_\Omega \cdot \nabla \varphi \, d\boldsymbol{x} = 0 \qquad \forall\, \varphi \in C_0^\infty(\Omega).$$

   Let us consider a fixed $\varphi \in C_0^\infty(\Omega)$. Then $\tilde{\varphi}|_{\Omega_{n_k}} \in C_0^\infty(\Omega_{n_k})$ for k great enough ($k \geq k_0$) and we can use $\tilde{\varphi}$ as a test function in Ω_{n_k}. Since $\boldsymbol{u}_{n_k} \in \boldsymbol{V}(\Omega_{n_k})$, we have

   $$\int_{\Omega_{n_k}} \boldsymbol{u}_{n_k} \cdot \nabla \tilde{\varphi} \, d\boldsymbol{x} = 0 \qquad \forall\, k \geq k_0.$$

   We employ the characteristic functions χ_{n_k} of domains Ω_{n_k}:

   $$\int_{\hat{\Omega}} \chi_{n_k} \tilde{\boldsymbol{u}}_{n_k} \cdot \nabla \tilde{\varphi} \, d\boldsymbol{x} = 0 \qquad \forall\, k \geq k_0,$$

   and considering $\chi_{n_k} \to \chi$ in $\boldsymbol{L}^{p_1}(\hat{\Omega}), 1 \leq p_1 < \infty$, where χ is the characteristic function of Ω, and passing limit with $k \to \infty$ we arrive at

   $$\int_\Omega \boldsymbol{u}_\Omega \cdot \nabla \varphi \, d\boldsymbol{x} = 0 \qquad \forall\, \varphi \in C_0^\infty(\Omega).$$

2. We know $\boldsymbol{u}_\Omega \in \boldsymbol{V}(\Omega)$ and we must prove that $\boldsymbol{u}_\Omega$ solves the problem (3.2) in Ω. We again employ the characteristic functions χ_{n_k} in this step:

   $$\nu \int_{\Omega_{n_k}} \nabla \boldsymbol{u}_{n_k} : \nabla \boldsymbol{v} \, d\boldsymbol{x} + \int_{\Omega_{n_k}} (\boldsymbol{u}_{n_k} \cdot \nabla \boldsymbol{u}_{n_k}) \cdot \boldsymbol{v} \, d\boldsymbol{x} = \int_{\Omega_{n_k}} \boldsymbol{f} \cdot \boldsymbol{v} \, d\boldsymbol{x} \tag{3.7}$$
   $$\forall\, \boldsymbol{v} \in \boldsymbol{V}(\Omega_{n_k}) \quad \Leftrightarrow$$
   $$\nu \int_{\hat{\Omega}} \chi_{n_k} (\nabla \tilde{\boldsymbol{u}}_{n_k} : \nabla \tilde{\boldsymbol{v}}) \, d\boldsymbol{x} + \int_{\hat{\Omega}} \chi_{n_k} (\tilde{\boldsymbol{u}}_{n_k} \cdot \nabla \tilde{\boldsymbol{u}}_{n_k}) \cdot \tilde{\boldsymbol{v}} \, d\boldsymbol{x} = \int_{\hat{\Omega}} \chi_{n_k} (\boldsymbol{f} \cdot \tilde{\boldsymbol{v}}) \, d\boldsymbol{x}$$
   $$\forall\, \boldsymbol{v} \in \boldsymbol{V}(\Omega_{n_k}).$$

Because of (3.6) we could use an arbitrary function from $\boldsymbol{V}(\Omega)$ as a test function in (3.7). Using the convergences

$$\begin{array}{ll} \bullet\ \chi_{n_k} \to \chi & \text{in } \boldsymbol{L}^{p_1}(\hat{\Omega}),\ \ 1 \le p_1 < \infty, \\ \bullet\ \boldsymbol{u}_{n_k} \to \boldsymbol{u} & \text{in } \boldsymbol{L}^{p_2}(\hat{\Omega}),\ \ 1 \le p_2 < 6, \\ \bullet\ \nabla \boldsymbol{u}_{n_k} \rightharpoonup \nabla \boldsymbol{u} & \text{in } \boldsymbol{L}^{p_3}(\hat{\Omega}),\ \ p_3 = 2 \end{array}$$

and the Hölder's inequality, we obtain the convergence of (3.7) to

$$\nu \int_\Omega (\nabla \boldsymbol{u} : \nabla \boldsymbol{v})\, d\boldsymbol{x} + \int_\Omega \chi(\boldsymbol{u} \cdot \nabla \boldsymbol{u}) \cdot \boldsymbol{v}\, d\boldsymbol{x} = \int_\Omega \chi(\boldsymbol{f} \cdot \boldsymbol{v})\, d\boldsymbol{x} \qquad \forall\, \boldsymbol{v} \in \boldsymbol{V}(\Omega). \tag{3.8}$$

As the last step of the proof we need to show the strong convergence, $\tilde{\boldsymbol{u}}_{n_k} \to \boldsymbol{u}$ in $\boldsymbol{H}^1_0(\hat{\Omega})$. We employ $(3.5)_3$:

$$\begin{aligned} &\nu \|\tilde{\boldsymbol{u}}_{n_k}\|_{\boldsymbol{H}^1_0(\hat{\Omega})} = \nu \int_{\hat{\Omega}} \chi_{n_k} |\nabla \tilde{\boldsymbol{u}}_{n_k}|^2\, d\boldsymbol{x} = \nu \int_{\hat{\Omega}} \chi_{n_k} |\nabla \tilde{\boldsymbol{u}}_{n_k}|^2\, d\boldsymbol{x} \\ &+ \int_{\hat{\Omega}} \chi_{n_k} (\tilde{\boldsymbol{u}}_{n_k} \cdot \nabla \tilde{\boldsymbol{u}}_{n_k}) \cdot \tilde{\boldsymbol{u}}_{n_k}\, d\boldsymbol{x} = \int_{\hat{\Omega}} \chi_{n_k} (\boldsymbol{f} \cdot \tilde{\boldsymbol{u}}_{n_k})\, d\boldsymbol{x} \longrightarrow \int_{\hat{\Omega}} \chi(\boldsymbol{f} \cdot \boldsymbol{u})\, d\boldsymbol{x} \\ &= \nu \int_{\hat{\Omega}} \chi |\nabla \boldsymbol{u}|^2\, d\boldsymbol{x} + \int_{\hat{\Omega}} \chi(\boldsymbol{u} \cdot \nabla \boldsymbol{u}) \cdot \boldsymbol{u}\, d\boldsymbol{x} = \nu \|\boldsymbol{u}\|_{\boldsymbol{H}^1_0(\hat{\Omega})}. \end{aligned}$$

⊠

Remark Under the assumption from Theorem 1.11,

$$\nu^2 > \tilde{c} c_F \|\boldsymbol{f}\|_{\boldsymbol{L}^2(\Omega)},$$

there exists exactly one solution of the Navier-Stokes equations. Constant c_F is from (1.1) and $\tilde{c}$ is the continuity constant of b_Ω from (1.4). Both constants are independent of the domain Ω:

1. In (1.1) the norm is preserved for $\tilde{\boldsymbol{u}}$ defined in $\hat{\Omega}$, $\|\tilde{\boldsymbol{u}}\|_{\boldsymbol{H}^1_0(\hat{\Omega})} = \|\boldsymbol{u}\|_{\boldsymbol{H}^1_0(\Omega)}$, and therefore we get
$$\|\tilde{\boldsymbol{u}}\|_{\boldsymbol{H}^1(\hat{\Omega})} \le c_F \|\tilde{\boldsymbol{u}}\|_{\boldsymbol{H}^1_0(\hat{\Omega})} \qquad \forall\, \boldsymbol{u} \in \boldsymbol{H}^1_0(\Omega),\ \forall\, \Omega \in \mathcal{O}.$$

2. For the trilinear form b_Ω, it holds $b_\Omega(\boldsymbol{u}, \boldsymbol{v}, \boldsymbol{w}) = b_{\hat{\Omega}}(\tilde{\boldsymbol{u}}, \tilde{\boldsymbol{v}}, \tilde{\boldsymbol{w}})\ \forall\, \boldsymbol{u}, \boldsymbol{v}, \boldsymbol{w} \in \boldsymbol{H}^1_0(\Omega)$ and
$$\begin{gathered} |b_{\hat{\Omega}}(\tilde{\boldsymbol{u}}, \tilde{\boldsymbol{v}}, \tilde{\boldsymbol{w}})| \le \tilde{c} \|\tilde{\boldsymbol{u}}\|_{\boldsymbol{H}^1_0(\hat{\Omega})} \|\tilde{\boldsymbol{v}}\|_{\boldsymbol{H}^1_0(\hat{\Omega})} \|\tilde{\boldsymbol{w}}\|_{\boldsymbol{H}^1_0(\hat{\Omega})} \\ \forall\, \boldsymbol{u}, \boldsymbol{v}, \boldsymbol{w} \in \boldsymbol{H}^1_0(\Omega),\ \forall\, \Omega \in \mathcal{O}. \end{gathered}$$

Now we prove the existence of solution of the optimization problem (3.4).

Theorem 3.6 *Problem (3.4) has a solution.*

Proof: Denote

$$q := \inf_{(\Omega,\boldsymbol{u})\in\mathcal{G}} \Psi(\Omega,\boldsymbol{u}) = \lim_{n\to\infty} \Psi(\Omega_n,\boldsymbol{u}_n),$$

where $\{(\Omega_n,\boldsymbol{u}_n)\},(\Omega_n,\boldsymbol{u}_n)\in\mathcal{G}$ is a minimizing sequence. Since the system $\mathcal{O}$ is compact, we can pass to a subsequence such that $\Omega_{n_k}\rightsquigarrow\Omega^*,\Omega^*\in\mathcal{O}$. Then from Theorem 3.5 we have

$$\tilde{\boldsymbol{u}}_{n_k}\to\boldsymbol{u}^* \qquad \text{in } \boldsymbol{V}(\hat{\Omega}),\quad k\to\infty,$$

and $\boldsymbol{u}^*|_{\Omega^*}$ solves (3.2) in Ω^*.
From this and the continuity of Ψ we have

$$q = \lim_{k\to\infty} \Psi(\Omega_{n_k},\boldsymbol{u}_{n_k}) = \Psi(\Omega^*,\boldsymbol{u}^*|_{\Omega^*}) \geq q,$$

i.e. $(\Omega^*,\boldsymbol{u}^*|_{\Omega^*})$ is an optimal pair for (3.4).

⊠

Remark We consider one particular objective function Ψ given by (3.3). To ensure the existence of solution to (3.4) with an arbitrary objective function $\mathcal{J}$, we need $\mathcal{J}$ to have a property of the lower semicontinuity:

$$\left.\begin{array}{l}\Omega_n\rightsquigarrow\Omega,\ \Omega_n,\Omega\in\mathcal{O}\\ \boldsymbol{u}_n\to\boldsymbol{u},\ \boldsymbol{u}_n\in\boldsymbol{V}(\Omega_n),\boldsymbol{u}\in\boldsymbol{V}(\Omega)\end{array}\right\}\Rightarrow \liminf_{n\to\infty}\mathcal{J}(\Omega_n,\boldsymbol{u}_n)\geq\mathcal{J}(\Omega,\boldsymbol{u}).$$

In our case, Ψ is continuous.

Chapter 4

Sensitivity analysis

In this section we explain the sensitivity analysis for the optimal shape problem. The presented approach is based on articles [8, 25].

4.1 State problem of the stabilized Navier-Stokes equations

In this section we shall consider the nonlinear Navier-Stokes problem solved by the Oseen iterations and with SUPG/PSPG and grad-div stabilizations.

We consider the same admissible domains as in the previous chapter, see Figure 3.2. We denote by $(\boldsymbol{u}, p)$ the solution in the domain Ω.

We employ the Navier-Stokes problem with homogeneous Dirichlet boundary conditions and without a source term:

$$\begin{aligned} -\nu\Delta\boldsymbol{u} + (\boldsymbol{u}\cdot\nabla)\boldsymbol{u} + \nabla p &= 0 \qquad \text{in } \Omega, \\ \operatorname{div}\boldsymbol{u} &= 0 \qquad \text{in } \Omega, \\ \boldsymbol{u}|_{\partial\Omega} &= 0. \end{aligned} \tag{4.1}$$

The nonlinear Navier-Stokes equations are solved with aid of the Oseen problem, where the convective term $\boldsymbol{u}\cdot\nabla\boldsymbol{u}$ is replaced by $\boldsymbol{b}\cdot\nabla\boldsymbol{u}$ with the known convective velocity $\boldsymbol{b}$:

$$\begin{aligned} -\nu\Delta\boldsymbol{u} + (\boldsymbol{b}\cdot\nabla)\boldsymbol{u} + \nabla p &= 0 \qquad \text{in } \Omega, \\ \operatorname{div}\boldsymbol{u} &= 0 \qquad \text{in } \Omega, \\ \boldsymbol{u}|_{\partial\Omega} &= 0. \end{aligned} \tag{4.2}$$

The weak formulation of the Oseen problem reads: find $\boldsymbol{u} \in \boldsymbol{H}^1_0(\Omega)$ and $p \in L^2_0(\Omega)$ such that

$$\begin{aligned} a_\Omega(\boldsymbol{u},\boldsymbol{v}) + b_\Omega(\boldsymbol{b},\boldsymbol{u},\boldsymbol{v}) - c_\Omega(\boldsymbol{v},p) &= 0 \qquad \forall\, \boldsymbol{v} \in \boldsymbol{H}^1_0(\Omega), \\ c_\Omega(\boldsymbol{u},q) &= 0 \qquad \forall\, q \in L^2_0(\Omega). \end{aligned}$$

Let us consider a decomposition $\mathcal{T}$ of the domain Ω into $K \in \mathcal{T}$ such that

- $K \in \mathcal{T}$ are closed convex regions,
- $\bigcup_{K\in\mathcal{T}} K = \overline{\Omega}$,
- two regions $K_1, K_2 \in \mathcal{T}_h, K_1 \neq K_2$ are either disjoint or $K_1 \cap K_2$ is formed by a common vertex of K_1 and K_2 or by a common face of K_1 and K_2.

(we shall use a triangulation $\mathcal{T}_h$ in the discretized problem). We apply the stabilizations introduced in Chapter 2 and we get

$$\begin{aligned} a_\Omega(\boldsymbol{u},\boldsymbol{v}) + b_\Omega(\boldsymbol{b},\boldsymbol{u},\boldsymbol{v}) - c_\Omega(\boldsymbol{v},p) + c_\Omega(\boldsymbol{u},q) + \gamma(\nabla\cdot\boldsymbol{u},\nabla\cdot\boldsymbol{v})_\Omega \\ + \sum_{K\in\mathcal{T}} \left(-\nu\Delta\boldsymbol{u} + (\boldsymbol{b}\cdot\nabla)\boldsymbol{u} + \nabla p, \kappa_K(\boldsymbol{b}\cdot\nabla\boldsymbol{v}) + \tau_K\nabla q\right)_K = 0 \\ \forall\, \boldsymbol{v} \in \boldsymbol{H}^1_0(\Omega), q \in L^2_0(\Omega). \end{aligned}$$

We use the finite element method to discretize this problem. Description of the procedure will be presented in the next chapter. We study a continuous formulation here. But we employ the fact that we shall use P1/P1 elements during the discretization (and therefore we can eliminate the term $\Delta\boldsymbol{u} = 0$).

We introduce a notation (summation convention is employed):

$$\begin{aligned} d_K(\boldsymbol{b}^1,\boldsymbol{b}^2,\boldsymbol{u},\boldsymbol{v}) &:= \left(\boldsymbol{b}^1\cdot\nabla\boldsymbol{u}, \boldsymbol{b}^2\cdot\nabla\boldsymbol{v}\right)_K = \int_K b^1_i \frac{\partial u_k}{\partial x_i} b^2_j \frac{\partial v_k}{\partial x_j}\, d\boldsymbol{x}, \\ g_K(\boldsymbol{b},\boldsymbol{u},p) &:= (\nabla p, \boldsymbol{b}\cdot\nabla\boldsymbol{u})_K = \int_K \frac{\partial p}{\partial x_i} b_j \frac{\partial u_i}{\partial x_j}\, d\boldsymbol{x}, \\ r_K(p,q) &:= (\nabla p, \nabla q)_K = \int_K \frac{\partial p}{\partial x_i}\frac{\partial q}{\partial x_i}\, d\boldsymbol{x}. \end{aligned}$$

After the convergence of the Oseen iteration process the final problem reads:

$$\begin{aligned} &a_\Omega(\boldsymbol{u},\boldsymbol{v}) + b_\Omega(\boldsymbol{u},\boldsymbol{u},\boldsymbol{v}) - c_\Omega(\boldsymbol{v},p) + \gamma(\nabla\cdot\boldsymbol{u},\nabla\cdot\boldsymbol{v})_\Omega \\ &\quad + \sum_{K\in\mathcal{T}} \kappa_K[d_K(\boldsymbol{u},\boldsymbol{u},\boldsymbol{u},\boldsymbol{v}) + g_K(\boldsymbol{u},\boldsymbol{v},p)] = 0 \qquad \forall\, \boldsymbol{v} \in \boldsymbol{H}^1_0(\Omega), \\ &c_\Omega(\boldsymbol{u},q) + \sum_{K\in\mathcal{T}} \tau_K[g_K(\boldsymbol{u},\boldsymbol{u},q) + r_K(p,q)] = 0 \qquad \forall\, q \in L^2_0(\Omega). \end{aligned} \tag{4.3}$$

4.2 Objective function

We consider the same types of domains as in the previous chapter, see Figures 3.1 and 3.2 for the domain description. $\Omega_C \subseteq \Omega$ is the criterion domain where the objective function is computed and $\Omega_D \subset \Omega$ is the design domain which can be modified by moving $\Gamma_D \subset \partial\Omega$.

We consider the shape optimization problem:

$$\min_\Omega \Psi(\Omega,\boldsymbol{u}), \tag{4.4}$$

$$\text{subject to: } (\boldsymbol{u},p) \text{ satisfy (4.3)},$$

$$\Omega \text{ in } \mathcal{O},$$

$$\text{where } \Psi(\Omega,\boldsymbol{u}) = \tfrac{\nu}{2}\int_{\Omega_C} |\nabla\boldsymbol{u}|^2\, d\boldsymbol{x} = \tfrac{1}{2} a_{\Omega_C}(\boldsymbol{u},\boldsymbol{u}). \tag{4.5}$$

The condition $(4.4)_2$ imposes the admissibility of the state, while the condition $(4.4)_3$ restricts the shape variation of Ω.

4.3 Sensitivity analysis

The goal of this section is to introduce the sensitivity formula which describes how the quantities of interest change when the design domain is being modified. More precisely, we follow the approach of the material derivative associated with the so-called design velocity field $\vec{\mathcal{V}} : \overline{\Omega}_D \to I\!R^3$ representing the deformation of the domain. Thereby for any infinitesimal design change in the direction of the velocity field $\vec{\mathcal{V}}$ we shall be able to predict the associated sensitivity as the directional domain derivative. The approach presented in this section is based on articles [8, 25].

Let $u : \Omega \to I\!R$ be a real valued function and $f_\Omega(u)$ a real valued functional depending on the domain Ω. In what follows, we refer by $\delta f_\Omega(u)|_{\vec{\mathcal{V}}}$ to the total (directional) derivative of a functional $f_\Omega(u)$, whereas the notation $\delta_D f_\Omega(u)|_{\vec{\mathcal{V}}}$ denotes the *partial derivative with respect to the domain perturbation* (infinitesimal) in the direction $\vec{\mathcal{V}}$. We shall use a simplified notation, $\delta f_\Omega(u) := \delta f_\Omega(u)|_{\vec{\mathcal{V}}}$ etc., for simplicity.

The total sensitivity of $f_\Omega(u)$ is given by

$$\delta f_\Omega(u) = \delta_D f_\Omega(u) + \delta_u f_\Omega(u) \circ \delta u, \tag{4.6}$$

where $\delta_u f_\Omega(u) \circ v$ means the Gateaux differential of $f_\Omega(u)$ with respect to u in the direction v. In the shape optimization problems, quantity u is typically the solution of a considered state problem. That means, u depends on the design of Ω, so that δu is the material derivative of u with respect to the domain perturbation.

We have to introduce the *feasible design velocity fields* in the context of problem (4.4): $\vec{\mathcal{V}}$ is feasible with respect to Ω, iff

$$\begin{aligned} &\operatorname{supp} \vec{\mathcal{V}} \subset \overline{\Omega}_D \quad \text{and} \quad \vec{\mathcal{V}} = 0 \text{ on } \Gamma_{in-out} \cup \Gamma_F, \\ &\vec{\mathcal{V}} \text{ is differentiable in } \Omega. \end{aligned} \tag{4.7}$$

4.3.1 Sensitivity formula

In this section we derive the sensitivity formula of $\Psi(\boldsymbol{u})$ in the sense of relation (4.6). We consider the Lagrangian associated with (4.4):

$$\begin{aligned} \mathcal{L}(\Omega, \boldsymbol{u}, p; \boldsymbol{w}, q) &= \Psi(\Omega, \boldsymbol{u}) \\ &+ a_\Omega(\boldsymbol{u}, \boldsymbol{w}) + b_\Omega(\boldsymbol{u}, \boldsymbol{u}, \boldsymbol{w}) - c_\Omega(\boldsymbol{w}, p) \\ &+ \gamma(\nabla \cdot \boldsymbol{u}, \nabla \cdot \boldsymbol{w})_\Omega + \sum_{K \in \mathcal{T}} \kappa_K \left[d_K(\boldsymbol{u}, \boldsymbol{u}, \boldsymbol{u}, \boldsymbol{w}) + g_K(\boldsymbol{u}, \boldsymbol{w}, p) \right] \\ &+ c_\Omega(\boldsymbol{u}, q) + \sum_{K \in \mathcal{T}} \tau_K \left[g_K(\boldsymbol{u}, \boldsymbol{u}, q) + r_K(p, q) \right], \end{aligned} \tag{4.8}$$

where $\boldsymbol{w} \in \boldsymbol{H}^1_0(\Omega)$ and $q \in L^2_0(\Omega)$ are the Lagrange multipliers associated with state problem constraints from (4.4).

The desired sensitivity formula can be derived with aid of the "inf-sup" problem

$$\inf_{\Omega,\boldsymbol{u},p} \sup_{\boldsymbol{w},q} \mathcal{L}(\Omega,\boldsymbol{u},p;\boldsymbol{w},q).$$

This approach permits us to consider only such triplets of primary-variables states $(\Omega,\boldsymbol{u},p)$, that for each design Ω we find the associated admissible state $(\boldsymbol{u},p)$. Further we shall consider only such paths in the set of all $(\Omega,\boldsymbol{u},p)$. With this restriction we can derive the sensitivity of $\mathcal{L}$:

$$\begin{aligned}
&\delta\mathcal{L}(\Omega,\boldsymbol{u},p;\boldsymbol{w},q)\circ(\vec{\mathcal{V}},\delta\boldsymbol{u},\delta p) \qquad (4.9)\\
&\quad= \delta_D\Psi(\Omega,\boldsymbol{u}) + \delta_D a_\Omega(\boldsymbol{u},\boldsymbol{w}) + \delta_D b_\Omega(\boldsymbol{u},\boldsymbol{u},\boldsymbol{w}) - \delta_D c_\Omega(\boldsymbol{w},p)\\
&\qquad+\gamma\,\delta_D(\nabla\cdot\boldsymbol{u},\nabla\cdot\boldsymbol{w})_\Omega\\
&\qquad+\sum_{K\in\mathcal{T}}\kappa_K\left[\delta_D d_K(\boldsymbol{u},\boldsymbol{u},\boldsymbol{u},\boldsymbol{w}) + \delta_D g_K(\boldsymbol{u},\boldsymbol{w},p)\right]\\
&\qquad+\delta_D c_\Omega(\boldsymbol{u},q) + \sum_{K\in\mathcal{T}}\tau_K\left[\delta_D g_K(\boldsymbol{u},\boldsymbol{u},q) + \delta_D r_K(p,q)\right]\\
&\qquad+a_\Omega(\delta\boldsymbol{u},\boldsymbol{w}) + b_\Omega(\delta\boldsymbol{u},\boldsymbol{u},\boldsymbol{w}) + b_\Omega(\boldsymbol{u},\delta\boldsymbol{u},\boldsymbol{w}) - c_\Omega(\boldsymbol{w},\delta p)\\
&\qquad+\gamma(\nabla\cdot\delta\boldsymbol{u},\nabla\cdot\boldsymbol{w})_\Omega\\
&\qquad+\sum_{K\in\mathcal{T}}\kappa_K\left[d_K(\delta\boldsymbol{u},\boldsymbol{u},\boldsymbol{u},\boldsymbol{w}) + d_K(\boldsymbol{u},\delta\boldsymbol{u},\boldsymbol{u},\boldsymbol{w}) + d_K(\boldsymbol{u},\boldsymbol{u},\delta\boldsymbol{u},\boldsymbol{w})\right]\\
&\qquad+\sum_{K\in\mathcal{T}}\kappa_K\left[g_K(\delta\boldsymbol{u},\boldsymbol{w},p) + g_K(\boldsymbol{u},\boldsymbol{w},\delta p)\right] + c_\Omega(\delta\boldsymbol{u},q)\\
&\qquad+\sum_{K\in\mathcal{T}}\tau_K\left[g_K(\delta\boldsymbol{u},\boldsymbol{u},q) + g_K(\boldsymbol{u},\delta\boldsymbol{u},q) + r_K(\delta p,q)\right]\\
&\qquad+\delta_{\boldsymbol{u}}\Psi(\Omega,\boldsymbol{u})\circ\delta\boldsymbol{u}\\
&\quad= \delta\Psi(\Omega,\boldsymbol{u}),
\end{aligned}$$

where the last equality follows from the state admissibility - for a given design Ω, the state admissibility condition (4.3) holds and all terms in (4.8) vanish except of $\Psi(\Omega,\boldsymbol{u})$.

The term $\delta_D\Psi(\Omega,\boldsymbol{u})$ depends on the choice of the criterion domain Ω_C. If we have $\Omega_C \subseteq \Omega_F$ (Ω_F is the fixed part of domain) we get $\delta_D\Psi(\Omega,\boldsymbol{u}) = 0$ because the criterion domain is independent of the shape changes. For $\Omega_C \cap \Omega_D =: \Omega_I \neq \emptyset$ it holds $\delta_D\Psi(\Omega,\boldsymbol{u}) = \frac{1}{2}\delta_D a_{\Omega_I}(\boldsymbol{u},\boldsymbol{u})$ because of the definition of $\Psi(\Omega,\boldsymbol{u})$. We shall further use the general relationship

$$\delta_D\Psi(\Omega,\boldsymbol{u}) = \frac{1}{2}\delta_D a_{\Omega_C}(\boldsymbol{u},\boldsymbol{u}). \qquad (4.10)$$

Expressing the KKT optimality conditions for the Lagrangian (4.8), $\delta_{\boldsymbol{u}}\mathcal{L}(\Omega,\boldsymbol{u},p;\boldsymbol{w},q)=0, \delta_p\mathcal{L}(\Omega,\boldsymbol{u},p;\boldsymbol{w},q)=0$, we obtain

$$\begin{aligned}
-\delta_{\boldsymbol{u}}\Psi(\Omega,\boldsymbol{u})\circ\boldsymbol{v} &= a_\Omega(\boldsymbol{v},\boldsymbol{w})+b_\Omega(\boldsymbol{v},\boldsymbol{u},\boldsymbol{w})+b_\Omega(\boldsymbol{u},\boldsymbol{v},\boldsymbol{w}) \\
&\quad+\gamma(\nabla\cdot\boldsymbol{v},\nabla\cdot\boldsymbol{w})_\Omega \\
&\quad+\sum_{K\in\mathcal{T}}\kappa_K\left[d_K(\boldsymbol{v},\boldsymbol{u},\boldsymbol{u},\boldsymbol{w})+d_K(\boldsymbol{u},\boldsymbol{v},\boldsymbol{u},\boldsymbol{w})+d_K(\boldsymbol{u},\boldsymbol{u},\boldsymbol{v},\boldsymbol{w})\right] \\
&\quad+\sum_{K\in\mathcal{T}}\kappa_K\left[g_K(\boldsymbol{v},\boldsymbol{w},p)\right]+c_\Omega(\boldsymbol{v},q) \\
&\quad+\sum_{K\in\mathcal{T}}\tau_K\left[g_K(\boldsymbol{v},\boldsymbol{u},q)+g_K(\boldsymbol{u},\boldsymbol{v},q)\right], \\
0 &= -c_\Omega(\boldsymbol{w},\eta)+\sum_{K\in\mathcal{T}}\kappa_K\left[g_K(\boldsymbol{u},\boldsymbol{w},\eta)\right]+\sum_{K\in\mathcal{T}}\tau_K\left[r_K(\eta,q)\right],
\end{aligned} \tag{4.11}$$

for all $\boldsymbol{v}\in\boldsymbol{H}^1_0(\Omega)$ and for all $\eta\in l^2_0(\Omega)$. Problem (4.11) is called the *adjoint state problem* and allows us to eliminate the total derivatives $\delta\boldsymbol{u}$ and δp from the sensitivity formula (4.9): by substituting the test functions $\boldsymbol{v}=\delta\boldsymbol{u},\eta=\delta p$ in (4.11), we cancel all terms in (4.9) except the partial design sensitivities. Therefore, the sensitivity analysis with a restriction to the admissible states is performed as follows:
Given a design Γ_D, adjust the domain Ω and

- compute the admissible state $(\boldsymbol{u},p)$ by solving (4.3),
- compute the adjoint state $(\boldsymbol{w},q)$ by solving (4.11),
- compute the sensitivity with respect to a given design velocity field $\vec{\mathcal{V}}$ by using

$$\begin{aligned}
\delta\Psi(\Omega,\boldsymbol{u}) &= \frac{1}{2}\delta_D a_{\Omega_C}(\boldsymbol{u},\boldsymbol{u})+\delta_D a_\Omega(\boldsymbol{u},\boldsymbol{w})+\delta_D b_\Omega(\boldsymbol{u},\boldsymbol{u},\boldsymbol{w}) \\
&\quad-\delta_D c_\Omega(\boldsymbol{w},p)+\gamma\,\delta_D(\nabla\cdot\boldsymbol{u},\nabla\cdot\boldsymbol{w})_\Omega \\
&\quad+\sum_{K\in\mathcal{T}}\kappa_K\left[\delta_D d_K(\boldsymbol{u},\boldsymbol{u},\boldsymbol{u},\boldsymbol{w})+\delta_D g_K(\boldsymbol{u},\boldsymbol{w},p)\right] \\
&\quad+\delta_D c_\Omega(\boldsymbol{u},q)+\sum_{K\in\mathcal{T}}\tau_K\left[\delta_D g_K(\boldsymbol{u},\boldsymbol{u},q)+\delta_D r_K(p,q)\right],
\end{aligned} \tag{4.12}$$

  where the first term raises from (4.10).

In the next part we shall derive the particular partial design sensitivities employed in (4.12) which depend on $\vec{\mathcal{V}}$.

4.3.2 Partial shape derivatives

Once the design velocity field is defined in the sense of conditions (4.7), the domain can be parametrized by means of a scalar parameter t:
Let $\vec{\mathcal{V}}$ satisfy (4.7). We introduce the parametrization

$$\overline{\Omega}(t)=\{\boldsymbol{x}_t\},\quad \text{where}\quad \boldsymbol{x}_t=\mathcal{F}_t(\boldsymbol{x})=\boldsymbol{x}+t\cdot\vec{\mathcal{V}}(\boldsymbol{x}),\qquad \boldsymbol{x}\in\overline{\Omega},t\geq 0,$$

where we denote by Ω the initial domain, whereas $\Omega(t)$ is the perturbed one.

Recalling the general sensitivity relation (4.6), we define the *partial shape derivative* of the functional $f_\Omega(u)$:

$$\delta_D f_\Omega(u^t) = \frac{d}{dt}\left(f_{\Omega(t)}(u_t)\right)\Big|_{t=0}, \tag{4.13}$$

where the notation u^t, u_t will be described below.

By $\mathbb{D}\mathcal{F}_t$ we denote the Jacobian matrix of the mapping $\mathcal{F}_t$. If we denote $\mathbb{D}\vec{\mathcal{V}} = \left(\frac{\partial \mathcal{V}_i}{\partial x_j}\right)_{i,j=1}^n$ and by $\mathbb{I}$ the unit matrix we get

$$\mathbb{D}\mathcal{F}_t = \mathbb{I} + t\cdot\mathbb{D}\vec{\mathcal{V}} = \begin{pmatrix} 1+t\cdot\frac{\partial \mathcal{V}_1}{\partial x_1}, & t\cdot\frac{\partial \mathcal{V}_1}{\partial x_2}, & \dots, & t\cdot\frac{\partial \mathcal{V}_1}{\partial x_n} \\ t\cdot\frac{\partial \mathcal{V}_2}{\partial x_1}, & 1+t\cdot\frac{\partial \mathcal{V}_2}{\partial x_2}, & \dots, & t\cdot\frac{\partial \mathcal{V}_2}{\partial x_n} \\ \vdots & & & \vdots \\ t\cdot\frac{\partial \mathcal{V}_n}{\partial x_1}, & t\cdot\frac{\partial \mathcal{V}_n}{\partial x_2}, & \dots, & 1+t\cdot\frac{\partial \mathcal{V}_n}{\partial x_n} \end{pmatrix}.$$

and

$$J_t = \det \mathbb{D}\mathcal{F}_t.$$

We shall need some relations which are easy to prove:

1. $J_t = \det\, \mathbb{D}\mathcal{F}_t = 1 + t\cdot \operatorname{div}\vec{\mathcal{V}} + t^2\cdot R(t,\boldsymbol{x})$,
   $|R(t,\boldsymbol{x})| \le K$, $\forall\, t\in[0,\delta]$ and for almost all $\boldsymbol{x}\in\Omega$ where $K = \text{const} > 0$,
2. $\left(\frac{\partial (x_t)_i}{\partial x_j}\right)\Big|_{t=0} = \delta_{ij}$,
3. $\left(\frac{\partial x_j}{\partial (x_t)_i}\right)\Big|_{t=0} = \delta_{ij}$,
4. $\frac{d}{dt}\left(\frac{\partial (x_t)_i}{\partial x_j}\right)\Big|_{t=0} = \frac{\partial \mathcal{V}_i(x)}{\partial x_j}$,
5. $\frac{d}{dt}\left(\frac{\partial x_j}{\partial (x_t)_i}\right)\Big|_{t=0} = -\frac{\partial \mathcal{V}_j(x)}{\partial x_i}$,

Before we can derive the partial shape derivatives of terms in (4.12) we have to introduce the concept of solutions $\boldsymbol{u}_t$ and $\boldsymbol{u}^t$ in domains $\Omega(t)$ and Ω, respectively.

We consider $\boldsymbol{u}_t$ be a solution of the state problem (4.3) in the perturbed domain $\Omega(t)$ at the time point t. We define $\boldsymbol{u}^t \in \boldsymbol{H}^1(\Omega)$ by prescribing $\boldsymbol{u}^t = \boldsymbol{u}_t \circ \mathcal{F}_t$. Then $\boldsymbol{u}_t$ is a solution of the same problem (4.3) at the same time point t but mapped into the initial domain Ω. It means $\boldsymbol{u}^t(x) = \boldsymbol{u}_t(\mathcal{F}_t(\boldsymbol{x}))$.

From the definition $\boldsymbol{u}^t = \boldsymbol{u}_t \circ \mathcal{F}_t$ we get the formula for computing $\frac{\partial (u_t)_i}{\partial x_k}$ where $(u_t)_i$ is the $i-$th component of vector $\boldsymbol{u}_t$:

$$\frac{\partial u_i^t}{\partial x_j} = \frac{\partial (u_t)_i}{\partial x_k}\frac{\partial (x_t)_k}{\partial x_j} \quad\Rightarrow\quad \frac{\partial (u_t)_i}{\partial x_k} = \frac{\partial u_i^t}{\partial x_j}\frac{\partial x_j}{\partial (x_t)_k}.$$

The same relation holds for all functions $\boldsymbol{v}_t \in \boldsymbol{H}^1(\Omega(t))$.

Now we are ready to apply (4.13) to evaluate the variation of $a_\Omega(\boldsymbol{u}, \boldsymbol{w})$. For this, we map the form $a_{\Omega(t)}(\boldsymbol{u}_t, \boldsymbol{w}_t)$ defined in the perturbed domain $\Omega(t)$ into the initial domain Ω:

$$\begin{aligned} a_{\Omega(t)}(\boldsymbol{u}_t, \boldsymbol{w}_t) &= \nu \int_{\Omega(t)} \frac{\partial (u_t)_i}{\partial (x_t)_k} \frac{\partial (w_t)_i}{\partial (x_t)_k} \, d\boldsymbol{x}_t \\ &= \nu \int_\Omega \frac{\partial u_i^t}{\partial x_j} \frac{\partial x_j}{\partial (x_t)_k} \frac{\partial w_i^t}{\partial x_l} \frac{\partial x_l}{\partial (x_t)_k} J_t \, d\boldsymbol{x}. \end{aligned}$$

Then we obtain

$$\begin{aligned} \delta_D a_\Omega(\boldsymbol{u}^t, \boldsymbol{w}^t) &= \frac{d}{dt} \left(a_{\Omega(t)}(\boldsymbol{u}_t, \boldsymbol{w}_t) \right) \Big|_{t=0} \\ &= \nu \int_\Omega \left[\frac{\partial u_i^t}{\partial x_j} \frac{\partial w_i^t}{\partial x_j} \operatorname{div} \vec{\mathcal{V}} - \frac{\partial \mathcal{V}_j}{\partial x_l} \frac{\partial u_i^t}{\partial x_j} \frac{\partial w_i^t}{\partial x_l} - \frac{\partial u_i^t}{\partial x_j} \frac{\partial \mathcal{V}_l}{\partial x_j} \frac{\partial w_i^t}{\partial x_l} \right] d\boldsymbol{x} \\ &= \nu \int_\Omega \left[\frac{\partial u_i^t}{\partial x_j} \frac{\partial w_k^t}{\partial x_l} \left(\delta_{ik} \delta_{jl} \operatorname{div} \vec{\mathcal{V}} - \delta_{ik} \frac{\partial \mathcal{V}_j}{\partial x_l} - \delta_{ik} \frac{\partial \mathcal{V}_l}{\partial x_j} \right) \right] d\boldsymbol{x}. \end{aligned} \tag{4.14}$$

We can use the analogous procedure for forms $b_\Omega(\boldsymbol{u}, \boldsymbol{u}, \boldsymbol{w})$ and $c_\Omega(\boldsymbol{u}, q)$:

$$\begin{aligned} b_{\Omega(t)}(\boldsymbol{u}_t, \boldsymbol{u}_t, \boldsymbol{w}_t) &= \int_{\Omega(t)} (u_t)_k \frac{\partial (u_t)_i}{\partial (x_t)_k} (w_t)_i \, d\boldsymbol{x}_t \\ &= \int_\Omega u_k^t \frac{\partial u_i^t}{\partial x_j} \frac{\partial x_j}{\partial (x_t)_k} w_i^t \, J_t \, d\boldsymbol{x} \end{aligned}$$

$$\begin{aligned} \delta_D b_\Omega(\boldsymbol{u}^t, \boldsymbol{u}^t, \boldsymbol{w}^t) &= \frac{d}{dt} \left(b_{\Omega(t)}(\boldsymbol{u}_t, \boldsymbol{u}_t, \boldsymbol{w}_t) \right) \Big|_{t=0} \\ &= \int_\Omega \left[u_k^t \frac{\partial u_i^t}{\partial x_k} w_i^t \operatorname{div} \vec{\mathcal{V}} - u_k^t \frac{\partial \mathcal{V}_j}{\partial x_k} \frac{\partial u_i^t}{\partial x_j} w_i^t \right] d\boldsymbol{x} \\ &= \int_\Omega \left[u_k^t \frac{\partial u_i^t}{\partial x_j} w_l^t \left(\delta_{jk} \delta_{il} \operatorname{div} \vec{\mathcal{V}} - \delta_{il} \frac{\partial V_j}{\partial x_k} \right) \right] d\boldsymbol{x} \end{aligned} \tag{4.15}$$

$$\begin{aligned} c_{\Omega(t)}(\boldsymbol{u}_t, q_t) &= \int_{\Omega(t)} q_t \operatorname{div} \boldsymbol{u}_t \, d\boldsymbol{x}_t = \int_{\Omega(t)} q_t \, \frac{\partial (u_t)_i}{\partial (x_t)_i} \, d\boldsymbol{x}_t \\ &= \int_\Omega q^t \frac{\partial u_i^t}{\partial x_k} \frac{\partial x_k}{\partial (x_t)_i} \, J_t \, d\boldsymbol{x}. \end{aligned}$$

$$\begin{aligned} \delta_D c_\Omega(\boldsymbol{u}^t, q^t) &= \frac{d}{dt} \left(c_{\Omega(t)}(\boldsymbol{u}_t, q_t) \right) \Big|_{t=0} \\ &= \int_\Omega q^t \left[\operatorname{div} \boldsymbol{u}^t \operatorname{div} \vec{\mathcal{V}} - \frac{\partial \mathcal{V}_j}{\partial x_i} \frac{\partial u_i^t}{\partial x_j} \right] d\boldsymbol{x} \\ &= \int_\Omega \left[q^t \frac{\partial u_i^t}{\partial x_j} \left(\delta_{ij} \operatorname{div} \vec{\mathcal{V}} - \frac{\partial \mathcal{V}_j}{\partial x_i} \right) \right] d\boldsymbol{x} \end{aligned} \tag{4.16}$$

Then we have to employ the same approach for the partial shape derivatives of terms arising from stabilizations, $\delta_D(\nabla\cdot\boldsymbol{u},\nabla\cdot\boldsymbol{w})_\Omega, \delta_D d_K(\boldsymbol{b}^1,\boldsymbol{b}^2,\boldsymbol{u},\boldsymbol{w}), \delta_D g_K(\boldsymbol{u},\boldsymbol{w},p)$, $\delta_D r_K(p,q)$. Last three terms are defined in elements $K\in\mathcal{T}$. Therefore, we shall denote by $K(t)$ elements of the perturbed domain $\Omega(t)$ and by K elements of the initial domain Ω. Now we can repeat the same procedure as before for these four terms.

$$
\begin{aligned}
(\nabla\cdot\boldsymbol{u}_t,\nabla\cdot\boldsymbol{w}_t)_{\Omega(t)} &= \int_{\Omega(t)} \operatorname{div}\boldsymbol{u}_t \operatorname{div}\boldsymbol{w}_t \,d\boldsymbol{x}_t = \int_{\Omega(t)} \frac{\partial (u_t)_i}{\partial (x_t)_i}\frac{\partial (w_t)_j}{\partial (x_t)_j}\,d\boldsymbol{x}_t \\
&= \int_\Omega \frac{\partial u_i^t}{\partial x_k}\frac{\partial x_k}{\partial (x_t)_i}\frac{\partial w_j^t}{\partial x_l}\frac{\partial x_l}{\partial (x_t)_j}\,J_t\,d\boldsymbol{x}
\end{aligned}
$$

$$
\begin{aligned}
\delta_D(\nabla\cdot\boldsymbol{u}^t,\nabla\cdot\boldsymbol{w}^t)_\Omega &= \frac{d}{dt}\left((\nabla\cdot\boldsymbol{u}_t,\nabla\cdot\boldsymbol{w}_t)_{\Omega(t)}\right)\Big|_{t=0} \qquad (4.17)\\
&= \int_\Omega \left[\operatorname{div}\boldsymbol{u}^t \operatorname{div}\boldsymbol{w}^t \operatorname{div}\vec{\mathcal{V}} - \frac{\partial u_i^t}{\partial x_j}\frac{\partial \mathcal{V}_j}{\partial x_i}\operatorname{div}\boldsymbol{w}^t - \operatorname{div}\boldsymbol{u}^t \frac{\partial w_k^t}{\partial x_l}\frac{\partial \mathcal{V}_l}{\partial x_k}\right] d\boldsymbol{x} \\
&= \int_\Omega \left[\frac{\partial u_i^t}{\partial x_j}\frac{\partial w_k^t}{\partial x_l}\left(\delta_{ij}\delta_{kl}\operatorname{div}\vec{\mathcal{V}} - \delta_{kl}\frac{\partial \mathcal{V}_j}{\partial x_i} - \delta_{ij}\frac{\partial \mathcal{V}_l}{\partial x_k}\right)\right] d\boldsymbol{x}
\end{aligned}
$$

$$
\begin{aligned}
d_{K(t)}(\boldsymbol{b}_t^1,\boldsymbol{b}_t^2,\boldsymbol{u}_t,\boldsymbol{w}_t) &= \int_{K(t)} (b_t^1)_i \frac{\partial (u_t)_k}{\partial (x_t)_i}(b_t^2)_j \frac{\partial (v_t)_k}{\partial (x_t)_j}\,d\boldsymbol{x}_t \\
&= \int_K b_i^{1,t}\frac{\partial u_k^t}{\partial x_l}\frac{\partial x_l}{\partial (x_t)_i} b_j^{2,t}\frac{\partial v_k^t}{\partial x_m}\frac{\partial x_m}{\partial (x_t)_j}\,J_t\,d\boldsymbol{x}
\end{aligned}
$$

$$
\begin{aligned}
\delta_D d_K(\boldsymbol{b}^{1,t},\boldsymbol{b}^{2,t},\boldsymbol{u}^t,\boldsymbol{w}^t) &= \frac{d}{dt}\left(h_{K(t)}(\boldsymbol{b}_t^1,\boldsymbol{b}_t^2,\boldsymbol{u}_t,\boldsymbol{w}_t)\right)\Big|_{t=0} \qquad (4.18)\\
&= \int_K \Big[(\boldsymbol{b}^{1,t}\cdot\nabla)u_k^t(\boldsymbol{b}^{2,t}\cdot\nabla)w_k^t \operatorname{div}\vec{\mathcal{V}} - (\boldsymbol{b}^{1,t}\cdot\nabla)\mathcal{V}_i\frac{\partial u_k^t}{\partial x_i}(\boldsymbol{b}^{2,t}\cdot\nabla)w_k^t \\
&\qquad -(\boldsymbol{b}^{1,t}\cdot\nabla)u_k^t(\boldsymbol{b}^{2,t}\cdot\nabla)\mathcal{V}_l\frac{\partial w_k^t}{\partial x_l}\Big] d\boldsymbol{x} \\
&= \int_K \Big[b_m^{1,t}\frac{\partial u_i^t}{\partial x_j} b_n^{2,t}\frac{\partial w_k^t}{\partial x_l}\Big(\delta_{mj}\delta_{nl}\delta_{ik}\operatorname{div}\vec{\mathcal{V}} - \delta_{ik}\delta_{nl}\frac{\partial \mathcal{V}_j}{\partial x_m} \\
&\qquad +\delta_{jm}\delta_{ik}\frac{\partial \mathcal{V}_l}{\partial x_n}\Big)\Big] d\boldsymbol{x}
\end{aligned}
$$

$$
\begin{aligned}
g_{K(t)}(\boldsymbol{u}_t,\boldsymbol{w}_t,p_t) &= \int_{K(t)} \frac{\partial p_t}{\partial (x_t)_i}(u_t)_j\frac{\partial (w_t)_i}{\partial (x_t)_j}\,d\boldsymbol{x}_t \\
&= \int_K \frac{\partial p^t}{\partial x_k}\frac{\partial x_k}{\partial (x_t)_i}u_j^t\frac{\partial w_i^t}{\partial x_l}\frac{\partial x_l}{\partial (x_t)_j}\,J_t\,d\boldsymbol{x}
\end{aligned}
$$

$$\begin{aligned}\delta_D g_K(\boldsymbol{u}^t, \boldsymbol{w}^t, p^t) &= \frac{d}{dt}\left(g_{K(t)}(\boldsymbol{u}_t, \boldsymbol{w}_t, p_t)\right)\Big|_{t=0} \\ &= \int_K \left[\frac{\partial p^t}{\partial x_i}(\boldsymbol{u}^t \cdot \nabla) w_i^t \operatorname{div} \vec{\mathcal{V}} - \frac{\partial p^t}{\partial x_l}\frac{\partial \mathcal{V}_l}{\partial x_i}(\boldsymbol{u}^t \cdot \nabla) w_i^t \right. \\ &\qquad \left. - \frac{\partial p^t}{\partial x_j}(\boldsymbol{u}^t \cdot \nabla)\mathcal{V}_j \frac{\partial w_i^t}{\partial x_j}\right] d\boldsymbol{x} \\ &= \int_K \left[\frac{\partial p^t}{\partial x_l} u_k^t \frac{\partial w_i^t}{\partial x_j}\left(\delta_{jk}\delta_{il} \operatorname{div} \vec{\mathcal{V}} - \delta_{jk}\frac{\partial \mathcal{V}_l}{\partial x_i} - \delta_{jl}\frac{\partial \mathcal{V}_j}{\partial x_k}\right)\right] d\boldsymbol{x}\end{aligned} \tag{4.19}$$

$$\begin{aligned} r_{K(t)}(p_t, q_t) &= \int_{K(t)} \frac{\partial p_t}{\partial (x_t)_i}\frac{\partial q_t}{\partial (x_t)_i}\, d\boldsymbol{x}_t \\ &= \int_K \frac{\partial p^t}{\partial x_k}\frac{\partial x_k}{\partial (x_t)_i}\frac{\partial q^t}{\partial x_l}\frac{\partial x_l}{\partial (x_t)_i}\, J_t\, d\boldsymbol{x}\end{aligned}$$

$$\begin{aligned}\delta_D r_K(p^t, q^t) &= \frac{d}{dt}\left(r_{K(t)}(p_t, q_t)\right)\Big|_{t=0} \\ &= \int_K \left[(\nabla p^t \cdot \nabla q^t) \operatorname{div} \vec{\mathcal{V}} - \frac{\partial p^t}{\partial x_k}(\nabla \mathcal{V}_k \cdot \nabla q^t) - (\nabla p^t \cdot \nabla \mathcal{V}_k)\frac{\partial q^t}{\partial x_k}\right] d\boldsymbol{x} \\ &= \int_K \left[\frac{\partial p^t}{\partial x_i}\frac{\partial q^t}{\partial x_j}\left(\delta_{ij} \operatorname{div} \vec{\mathcal{V}} - \frac{\partial \mathcal{V}_i}{\partial x_j} - \frac{\partial \mathcal{V}_j}{\partial x_i}\right)\right] d\boldsymbol{x}\end{aligned} \tag{4.20}$$

We can rewrite the sensitivity of $\Psi(\boldsymbol{u})$ given by (4.12) using the field $\vec{\mathcal{V}}$: the total shape derivative can be recovered for any feasible $\vec{\mathcal{V}}$ by applying (4.14)-(4.20) in (4.12):

$$
\begin{aligned}
\delta\Psi(\boldsymbol{u}) = \frac{\nu}{2}\int_{\Omega_C}\left[\frac{\partial u_i^t}{\partial x_j}\frac{\partial u_k^t}{\partial x_l}\left(\delta_{ik}\delta_{jl}\operatorname{div}\vec{\mathcal{V}} - \delta_{ik}\frac{\partial \mathcal{V}_j}{\partial x_l} - \delta_{ik}\frac{\partial \mathcal{V}_l}{\partial x_j}\right)\right]d\boldsymbol{x} \qquad (4.21)\\
+\nu\int_{\Omega}\left[\frac{\partial u_i^t}{\partial x_j}\frac{\partial w_k^t}{\partial x_l}\left(\delta_{ik}\delta_{jl}\operatorname{div}\vec{\mathcal{V}} - \delta_{ik}\frac{\partial \mathcal{V}_j}{\partial x_l} - \delta_{ik}\frac{\partial \mathcal{V}_l}{\partial x_j}\right)\right]d\boldsymbol{x}\\
+\int_{\Omega}\left[u_k^t\frac{\partial u_i^t}{\partial x_j}w_l^t\left(\delta_{jk}\delta_{il}\operatorname{div}\vec{\mathcal{V}} - \delta_{il}\frac{\partial V_j^t}{\partial x_k}\right)\right]d\boldsymbol{x}\\
-\int_{\Omega}\left[p^t\frac{\partial w_i^t}{\partial x_j}\left(\delta_{ij}\operatorname{div}\vec{\mathcal{V}} - \frac{\partial \mathcal{V}_j}{\partial x_i}\right)\right]d\boldsymbol{x}\\
+\gamma\int_{\Omega}\left[\frac{\partial u_i^t}{\partial x_j}\frac{\partial w_k^t}{\partial x_l}\left(\delta_{ij}\delta_{kl}\operatorname{div}\vec{\mathcal{V}} - \delta_{kl}\frac{\partial \mathcal{V}_j}{\partial x_i} - \delta_{ij}\frac{\partial \mathcal{V}_l}{\partial x_k}\right)\right]d\boldsymbol{x}\\
+\sum_{K\in\mathcal{T}}\kappa_K\int_K\left[u_m^t\frac{\partial u_i^t}{\partial x_j}u_n^t\frac{\partial w_k^t}{\partial x_l}\left(\delta_{mj}\delta_{nl}\delta_{ik}\operatorname{div}\vec{\mathcal{V}} - \delta_{ik}\delta_{nl}\frac{\partial \mathcal{V}_j}{\partial x_m} - \delta_{jm}\delta_{ik}\frac{\partial \mathcal{V}_l}{\partial x_n}\right)\right]d\boldsymbol{x}\\
+\sum_{K\in\mathcal{T}}\kappa_K\int_K\left[\frac{\partial p^t}{\partial x_l}u_k^t\frac{\partial w_i^t}{\partial x_j}\left(\delta_{jk}\delta_{il}\operatorname{div}\vec{\mathcal{V}} - \delta_{jk}\frac{\partial \mathcal{V}_l}{\partial x_i} - \delta_{jl}\frac{\partial \mathcal{V}_j}{\partial x_k}\right)\right]d\boldsymbol{x}\\
+\int_{\Omega}\left[q^t\frac{\partial u_i^t}{\partial x_j}\left(\delta_{ij}\operatorname{div}\vec{\mathcal{V}} - \frac{\partial \mathcal{V}_j}{\partial x_i}\right)\right]d\boldsymbol{x}\\
+\sum_{K\in\mathcal{T}}\tau_K\int_K\left[\frac{\partial q^t}{\partial x_l}u_k^t\frac{\partial u_i^t}{\partial x_j}\left(\delta_{jk}\delta_{il}\operatorname{div}\vec{\mathcal{V}} - \delta_{jk}\frac{\partial \mathcal{V}_l}{\partial x_i} - \delta_{jl}\frac{\partial \mathcal{V}_j}{\partial x_k}\right)\right]d\boldsymbol{x}\\
+\sum_{K\in\mathcal{T}}\tau_K\int_K\left[\frac{\partial p^t}{\partial x_i}\frac{\partial q^t}{\partial x_j}\left(\delta_{ij}\operatorname{div}\vec{\mathcal{V}} - \frac{\partial \mathcal{V}_i}{\partial x_j} - \frac{\partial \mathcal{V}_j}{\partial x_i}\right)\right]d\boldsymbol{x},
\end{aligned}
$$

where the first term is obtained from (4.10).

4.3.3 State problem without stabilization

For the stabilized Navier-Stokes equations, the sensitivity formula is prescribed by (4.21). If we consider the Navier-Stokes equations without stabilization, the sensitivity formula is simpler - we omit terms arisen from stabilizations.

The weak formulation of this problem reads: find $\boldsymbol{u} \in \boldsymbol{H}_0^1(\Omega)$ and $p \in L_0^2(\Omega)$ such that

$$
\begin{aligned}
a_\Omega(\boldsymbol{u},\boldsymbol{v}) + b_\Omega(\boldsymbol{u},\boldsymbol{u},\boldsymbol{v}) - c_\Omega(\boldsymbol{v},p) &= 0 \qquad \forall\, \boldsymbol{v} \in \boldsymbol{H}_0^1(\Omega),\\
c_\Omega(\boldsymbol{u},q) &= 0 \qquad \forall\, q \in L_0^2(\Omega).
\end{aligned}
$$

Then we consider only sensitivities for these terms and we get the formula

$$\begin{aligned}
\delta\Psi(\boldsymbol{u}) = \frac{\nu}{2}\int_{\Omega_C}\left[\frac{\partial u_i^t}{\partial x_j}\frac{\partial u_k^t}{\partial x_l}\left(\delta_{ik}\delta_{jl}\operatorname{div}\vec{\mathcal{V}} - \delta_{ik}\frac{\partial \mathcal{V}_j}{\partial x_l} - \delta_{ik}\frac{\partial \mathcal{V}_l}{\partial x_j}\right)\right]d\boldsymbol{x} \qquad (4.22)\\
+\nu\int_{\Omega}\left[\frac{\partial u_i^t}{\partial x_j}\frac{\partial w_k^t}{\partial x_l}\left(\delta_{ik}\delta_{jl}\operatorname{div}\vec{\mathcal{V}} - \delta_{ik}\frac{\partial \mathcal{V}_j}{\partial x_l} - \delta_{ik}\frac{\partial \mathcal{V}_l}{\partial x_j}\right)\right]d\boldsymbol{x}\\
+\int_{\Omega}\left[u_k^t\frac{\partial u_i^t}{\partial x_j}w_l^t\left(\delta_{jk}\delta_{il}\operatorname{div}\vec{\mathcal{V}} - \delta_{il}\frac{\partial V_j^t}{\partial x_k}\right)\right]d\boldsymbol{x}\\
-\int_{\Omega}\left[p^t\frac{\partial w_i^t}{\partial x_j}\left(\delta_{ij}\operatorname{div}\vec{\mathcal{V}} - \frac{\partial \mathcal{V}_j}{\partial x_i}\right)\right]d\boldsymbol{x}\\
+\int_{\Omega}\left[q^t\frac{\partial u_i^t}{\partial x_j}\left(\delta_{ij}\operatorname{div}\vec{\mathcal{V}} - \frac{\partial \mathcal{V}_j}{\partial x_i}\right)\right]d\boldsymbol{x}.
\end{aligned}$$

Chapter 5

Discretization of the state problems

In previous chapters we investigated the Navier-Stokes equations with homogeneous boundary conditions for simplicity. We shall consider a different state problem for simulations - we shall use the Navier-Stokes equations but with other boundary conditions. We used a simplified problem in the theoretical part because we are not able to prove the existence and the uniqueness of the weak solution of the state problem which will be introduced below.

5.1 The state problem

Let $\Omega \subset I\!R^3$ be an open bounded domain defined as

$$\overline{\Omega}_D = \overline{\Omega_D \cup \Omega_F},$$

where Ω_F is the fixed domain and Ω_D is the design domain. We denote by Γ_{in} the inlet boundary of the channel and by Γ_{out} the outlet boundary (see Figure 3.1 where the computational domain is displayed). We use the notation $\Gamma_{in-out} = \Gamma_{in} \cup \Gamma_{out}$. The shape of Ω is modified through the design boundary $\Gamma_D \subset \partial\Omega \setminus \Gamma_{in-out}$.

We solve the incompressible Navier-Stokes equations in Ω: find $\boldsymbol{u}$ and p such that

$$\begin{aligned} -\nu\Delta\boldsymbol{u} + (\boldsymbol{u}\cdot\nabla)\boldsymbol{u} + \nabla p &= 0 \quad && \text{in } \Omega, \\ \operatorname{div}\boldsymbol{u} &= 0 && \text{in } \Omega, \\ \boldsymbol{u} &= 0 && \text{on } \partial\Omega \setminus \Gamma_{in-out}, \\ \boldsymbol{u} &= \boldsymbol{u}_{in} && \text{on } \Gamma_{in}, \\ -p\boldsymbol{n} + \nu\frac{\partial \boldsymbol{u}}{\partial n} &= 0 && \text{on } \Gamma_{out}, \end{aligned} \tag{5.1}$$

where $\boldsymbol{n}$ is the unit outward normal vector on Γ_{out}, $\frac{\partial}{\partial n} = \boldsymbol{n}\cdot\nabla$ and $\boldsymbol{u}_{in}$ is a given velocity profile.

We use the notation presented in previous chapters (summation convection is employed):

$$a_\Omega(\boldsymbol{u},\boldsymbol{v}) = \nu(\nabla\boldsymbol{u},\nabla\boldsymbol{v})_\Omega = \nu\int_\Omega \frac{\partial u_i}{\partial x_j}\frac{\partial v_i}{\partial x_j}\,d\boldsymbol{x},$$

$$b_\Omega(\boldsymbol{u},\boldsymbol{v},\boldsymbol{w}) = ((\boldsymbol{u}\cdot\nabla)\boldsymbol{v},\boldsymbol{w})_\Omega = \int_\Omega u_j\frac{\partial v_i}{\partial x_j}w_i\,d\boldsymbol{x},$$

$$c_\Omega(\boldsymbol{u},p) = (p,\nabla\cdot\boldsymbol{u})_\Omega = \int_\Omega p\frac{\partial u_i}{\partial x_i}\,d\boldsymbol{x}.$$

Then we denote the space of admissible velocities

$$\boldsymbol{W} = \{\boldsymbol{v} \in \boldsymbol{H}^1(\Omega); \boldsymbol{v} = 0 \text{ on } \partial\Omega \setminus \Gamma_{out}\}.$$

The weak formulation of (5.1) is: find $\boldsymbol{u} \in \boldsymbol{H}^1(\Omega)$ and $p \in L^2_0(\Omega)$ such that $\boldsymbol{u} - \boldsymbol{u}_{in} \in \boldsymbol{W}$,

$$\begin{aligned} a_\Omega(\boldsymbol{u}, \boldsymbol{v}) + b_\Omega(\boldsymbol{u}, \boldsymbol{u}, \boldsymbol{v}) - c_\Omega(\boldsymbol{v}, p) &= 0 \qquad \forall\, \boldsymbol{v} \in \boldsymbol{W}, \\ c_\Omega(\boldsymbol{u}, q) &= 0 \qquad \forall\, L^2_0(\Omega). \end{aligned} \tag{5.2}$$

In previous chapters we considered the Navier-Stokes equations with homogeneous Dirichlet conditions (and partly nonhomogeneous Dirichlet conditions), because we are not able to prove the existence and uniqueness of the weak solution of problem (5.1). But terms in (5.2) are the same as in the weak formulation of the Navier-Stokes equations with homogeneous boundary conditions and the sensitivity analysis derived in Chapter 4 is valid also for the problem (5.1). It is due to the homogeneous Neumann boundary condition $(5.1)_5$.

5.2 Finite element discretization

We use the finite element method for the discretization of (5.2).

We construct a polyhedral approximation Ω_h of the domain Ω. We denote by $\mathcal{T}_h$ a triangulation of Ω_h:

- $K \in \mathcal{T}_h$ are closed polyhedra,
- $\bigcup_{K \in \mathcal{T}_h} K = \overline{\Omega}_h$,
- two elements $K_1, K_2 \in \mathcal{T}_h, K_1 \neq K_2$ are either disjoint or $K_1 \cap K_2$ is formed by a common vertex of K_1 and K_2 or by their common face.

Over $\mathcal{T}_h$ we construct finite dimensional spaces and we consider approximations

$$\begin{aligned} &\boldsymbol{X}_h \approx \boldsymbol{H}^1(\Omega_h),\ \boldsymbol{W}_h \approx \boldsymbol{W},\ M_h \approx L^2(\Omega_h),\ M_{h0} \approx L^2_0(\Omega_h), \\ &a_h(\cdot,\cdot) \approx a_{\Omega h}(\cdot,\cdot),\ b_h(\cdot,\cdot,\cdot) \approx b_{\Omega h}(\cdot,\cdot,\cdot),\ c_h(\cdot,\cdot) \approx c_{\Omega h}(\cdot,\cdot), \\ &\boldsymbol{u}_{in_h} \approx \boldsymbol{u}_{in}. \end{aligned}$$

The concrete choice of spaces $\boldsymbol{X}_h$ and M_h depends on the problem which we solve. We consider two problems, the Navier-Stokes equations with and without stabilizations.

5.3 The stabilized Navier-Stokes equations

Because of stabilizations, we can use the P1/P1 approximation to discretize the stabilized system. We define following the finite dimensional spaces:

$$\begin{aligned} &M_h = \{q_h \in C(\overline{\Omega}_h); q_h|_K \in P^1(K)\ \forall\, K \in \mathcal{T}_h\}, \\ &M_{h0} = \{q_h \in M_h; \int_{\Omega_h} q_h \, d\boldsymbol{x} = 0\}, \\ &\boldsymbol{X}_h = [M_h]^3, \quad \boldsymbol{W}_h = \{\boldsymbol{v}_h \in \boldsymbol{X}_h; \boldsymbol{v}_h = 0 \text{ on } \partial\Omega_h \setminus \Gamma_{out}\}. \end{aligned}$$

We use the notation presented in Chapter 4 (summation convection is employed), $K \in \mathcal{T}_h$:

$$\begin{aligned} d_K(\boldsymbol{b}^1, \boldsymbol{b}^2, \boldsymbol{u}, \boldsymbol{v}) &:= \left(\boldsymbol{b}^1 \cdot \nabla \boldsymbol{u}, \boldsymbol{b}^2 \cdot \nabla \boldsymbol{v}\right)_K = \int_K b_i^1 \frac{\partial u_k}{\partial x_i} b_j^2 \frac{\partial v_k}{\partial x_j}\, d\boldsymbol{x}, \\ g_K(\boldsymbol{b}, \boldsymbol{u}, p) &:= (\nabla p, \boldsymbol{b} \cdot \nabla \boldsymbol{u})_K = \int_K \frac{\partial p}{\partial x_i} b_j \frac{\partial u_i}{\partial x_j}\, d\boldsymbol{x}, \\ r_K(p, q) &:= (\nabla p, \nabla q)_K = \int_K \frac{\partial p}{\partial x_i} \frac{\partial q}{\partial x_i}\, d\boldsymbol{x}. \end{aligned}$$

Then the discretized stabilized problem reads: find $\boldsymbol{u}_h, p_h$ such that $\boldsymbol{u}_h - \boldsymbol{u}_{in_h} \in \boldsymbol{X}_{h0}$,

$$\begin{aligned} &a_h(\boldsymbol{u}_h, \boldsymbol{v}_h) + b_h(\boldsymbol{u}_h, \boldsymbol{u}_h, \boldsymbol{v}_h) - c_h(\boldsymbol{v}_h, p_h) + \gamma(\nabla \cdot \boldsymbol{u}_h, \nabla \cdot \boldsymbol{v}_h)_{\Omega_h} \\ &\qquad + \sum_{K \in \mathcal{T}_h} \kappa_K [d_K(\boldsymbol{u}_h, \boldsymbol{u}_h, \boldsymbol{u}_h, \boldsymbol{v}_h) + g_K(\boldsymbol{u}_h, \boldsymbol{v}_h, p_h)] = 0 \qquad \forall\, \boldsymbol{v}_h \in \boldsymbol{W}_h, \\ &c_h(\boldsymbol{u}_h, q_h) + \sum_{K \in \mathcal{T}_h} \tau_K [g_K(\boldsymbol{u}_h, \boldsymbol{u}_h, q_h) + r_K(p_h, q_h)] = 0 \qquad \forall\, q_h \in M_{h0}. \end{aligned} \tag{5.3}$$

5.4 The Navier-Stokes problem without stabilizations

We cannot use the P1/P1 approximation for the Navier-Stokes equations without stabilizations because this pair violates the inf-sup condition (2.3). Therefore, we use the P1-bubble/P1 finite element discretization where the velocity field is discretized by the piecewise linear functions enriched by bubble functions and the pressure by the piecewise linear functions. This pair of spaces was introduced in [2].

We consider the same finite element spaces M_h, M_{h0} that were defined for the stabilized Navier-Stokes problem. Moreover, we define the P1-bubble space:

$$\begin{aligned} &\boldsymbol{B}_h = \{\boldsymbol{v}_h \in \boldsymbol{C}(\overline{\Omega}_h); \boldsymbol{v}_h|_K \in P^3(K) \cap \boldsymbol{H}_0^1(K)\ \forall\, K \in T_h\}, \\ &\boldsymbol{X}_h = [M_h]^3 \oplus \boldsymbol{B}_h, \quad \boldsymbol{W}_h = \{\boldsymbol{v}_h \in \boldsymbol{X}_h; \boldsymbol{v}_h = 0 \text{ on } \partial\Omega_h \setminus \Gamma_{out}\}. \end{aligned}$$

Then the discretized unstabilized problem reads: find $\boldsymbol{u}_h, p_h$ such that $\boldsymbol{u}_h - \boldsymbol{u}_{in_h} \in \boldsymbol{X}_{h0}$,

$$\begin{aligned} a_h(\boldsymbol{u}_h, \boldsymbol{v}_h) + b_h(\boldsymbol{u}_h, \boldsymbol{u}_h, \boldsymbol{v}_h) - c_h(\boldsymbol{v}_h, p_h) &= 0 \qquad \forall\, \boldsymbol{v}_h \in \boldsymbol{W}_h, \\ c_h(\boldsymbol{u}_h, q_h) &= 0 \qquad \forall\, q_h \in M_{h0}. \end{aligned} \tag{5.4}$$

Chapter 6

Numerical methods

In this chapter, we introduce numerical softwares which will be used for simulations. We introduce software for the geometry parametrization by spline boxes and then the second one for solving partial differential equations by the finite element method.

6.1 SPBOX

The sensitivity analysis developed in Chapter 4 is based on the directional derivatives of the objective function with respect to a given design velocity field $\vec{\mathcal{V}}$. Therefore, we need to parametrize the geometry and define the design variables. Then we compute a sensitivity with respect to these parameters.

We use the software SPBOX to create a parametrization of 3D bodies. Its description can be found in [26]. It is based on the Free-Form-Deformation technology which uses the so-called spline description of 3D volumes. FFD technology is introduced in [27].

The parametrization method in the SPBOX is based on the domain parametrization using B-spline or Bezier volumes. There are implemented cubic B-spline volumes specifically. The software SPBOX extends the FFD technology and allows to treat complex geometries by splitting them into several subdomains where each one is handled by one B-spline volume, see Figure 6.1. Moreover there are implemented restrictions to achieve C^0 continuity of the boundary.

We introduce here some features of the method applied in the software SPBOX. The description is based on [25, 26].

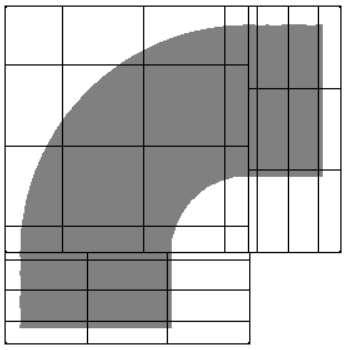

Figure 6.1: Connection of spline boxes

6.1.1 Design variables and gradients

Let Ω_0 be an initial domain embedded in the box $\mathcal{B}_0$ which is decomposed into nonoverlapping sub-boxes $\mathcal{B}_0^I$:

$$\Omega_0 \subset \mathcal{B}_0 = \Pi_{k=1,2,3}(a_k, b_k),$$
$$\mathcal{B}_0 = \sum_{I=1}^{NSB} \mathcal{B}_0^I, \qquad \mathcal{B}_0^I = \Pi_{k=1,2,3}(a_k^I, b_k^I),$$

where NSB is a number of spline boxes.

Each general sub-box $\mathcal{B}^I$ derived from the initial $\mathcal{B}_0^I$ is parametrized by the B-spline volume S^I which is defined in terms of the control vertices and the spline basis functions. If we denote $\overline{\Omega_0^I} = \overline{\Omega_0 \cap \mathcal{B}_0^I}$, we have $\overline{\Omega_0} = \sum_{I=1}^{NSB} \overline{\Omega_0^I}$ and we obtain the derived domain Ω as

$$\overline{\Omega} = \sum_{I=1}^{N} S^I(\{b\}, \{N\}, \overline{\Omega_0^I}),$$

where $\{b\}$ is the control polyhedron and $\{N\}$ is the B-spline basis.

Conditions for the C^0 continuity between attached spline boxes and other user-defined restrictions to positions of $\{b\}$ result in the relation $B(\{b\}) = 0$, where matrix B has not its full rank: $\mathrm{rank}(B) < \dim(\{b\})$.

Then the design variables are introduced as multipliers associated with elements of the kernel of matrix B. We define

$$\{d\}^\alpha \in \mathrm{Ker}\ B \quad \text{for } \alpha = 1, \ldots, \overline{\alpha},\ \overline{\alpha} \leq \mathrm{card}(\mathrm{Ker}\ B),$$

and we consider $\mu_\alpha, \alpha = 1, \ldots, \overline{\alpha}$, to be the multipliers of $\{d\}^\alpha$. Then the control polyhedra are changed according to

$$\{b\} = \{g\} + \sum_{\alpha=1}^{\overline{\alpha}} \mu_\alpha \{d\}^\alpha,$$

where $\{g\}$ are the Greville abscissae, see [16].

The design variables $\mu_\alpha, \alpha = 1, \ldots, \overline{\alpha}$ are defined as multipliers of linear manifolds which control the motion of control points of the B-spline volumes in directions defined by $\{g\}^\alpha, \alpha = 1, \ldots, \overline{\alpha}$. There are included some constraints of the motion of control points (constraints from the continuity of boundary or user defined planar restrictions etc.) and the design variables allow the motion with respect to all given constraints.

Now we can introduce the design velocity field associated with a change in $\mu = (\mu^\alpha)_{\alpha=1,\ldots,\overline{\alpha}}$ denoted by $\delta\mu$:

$$\vec{\mathcal{V}} = \sum_{I=1}^{NSB} S^I \left(\sum_{\alpha=1,\ldots,\overline{\alpha}} \delta\mu^\alpha \{d\}^\alpha, \{N\}, \overline{\Omega_0^I} \right).$$

Then $\vec{\mathcal{V}}$ is admissible by virtue of (4.7), as was shown in [25].

For each variable $\mu^\alpha, \alpha = 1, \ldots, \overline{\alpha}$, we can obtain the α-th basis velocity $\vec{\mathcal{V}}^\alpha$ which we need for computing the design gradients of the objective function $\Psi(\boldsymbol{u})$. We define

$$\vec{\mathcal{V}}^\alpha = \sum_{I=1}^{NSB} S^I(\{d\}^\alpha, \{N\}, \overline{\Omega_0^I})$$

and by evaluating (4.21) (or (4.22) eventually) for $\vec{\mathcal{V}}^\alpha$ we obtain the α-th component of the design gradient,

$$\frac{d}{d\mu^\alpha}\Psi(\Omega, \boldsymbol{u}), \quad \alpha = 1, \ldots, \overline{\alpha}.$$

6.2 SfePy

The software SfePy is being developed at the University of West Bohemia. It is a free software for solving problems described by partial differential equations using the finite element method. Software is written almost entirely in Python, only some routines are written in the C language.

Basic information about the project can be found in [5]. There are introduced some problems which were solved with aid of SfePy - modeling of heterogeneous materials, biomechanics or the shape optimization. The documentation for the software SfePy is in [6]. Sites concerning about the code development are in [7].

SfePy was used for all simulations presented in this thesis. We cooperated with the SfePy-development team from the University of West Bohemia to incorporate the linear geometry constraints in the shape optimization problems into the software. Results will be presented in the next chapter.

6.2.1 Linear and nonlinear solvers

In the shape optimization problems concerning the flow described by the Navier-Stokes equations the nonlinear solver is used for computing both the direct and the adjoint problem. There are two nonlinear solvers implemented in SfePy - the Oseen iterations and the Newton method. We use the Oseen iterations for solving the direct problem of the stabilized Navier-Stokes problem and the Newton method in all other cases.

The Oseen problem was described in Chapter 1. If we use the discretization presented in Chapter 5, we obtain a system of linear equations. By using the Newton method we obtain a system of linear equations too. The system of linear equations is then solved by a linear solver.

We use the software package UMFPACK for solving the linear system. UMFPACK is a set of routines for solving unsymmetric sparse linear systems using the Unsymmetric MultiFrontal method and the direct LU factorization. For the description see [9, 10].

6.2.2 Optimization solver

The steepest descent method is used as the optimization solver. It is a gradient based method. The choice of the step direction is in the opposite direction to the function gradient. The step size is chosen by the line search method complemented by backtracking in each iteration.

The iterative procedure is as follows:

1. Choose a start point x_0 and suitable constants $\tilde{\alpha} > 0, c_f < 1, c_\alpha < 1, c_b < 1$, $c_{min} > 0$; $k = 0$.

2. Let us suppose that at the k-th iteration point x_k, the function value $f(x_k)$ and the gradient of this function $g(x_k) := \nabla f(x_k)$ are given.

3. Let us start with the step size $\alpha_k := \tilde{\alpha}$. Then the line search with backtracking for finding a suitable step size is employed:

   A. put $x_{k+1} := x_k - \alpha_k \cdot g(x_k)$, compute $f(x_{k+1})$;

   B. if $f(x_{k+1})$ does not exist, put $\alpha_k := \alpha_k \cdot c_b$ and go to 3D;

   C. if $f(x_{k+1}) < c_f \cdot f(x_k)$, go to 4,
   else $\alpha_k := \alpha_k \cdot c_\alpha$;

   D. if $\alpha_k < c_{min}$ and $f(x_{k+1})$ exists, go to 4
   if $\alpha_k < c_{min}$ and $f(x_{k+1})$ does not exists, raise error,
   else go to 3A.

4. We have a suitable step size α_k and we compute $x_{k+1} := x_k - \alpha_k \cdot g(x_k)$.

5. Check the convergence and STOP or $k := k + 1$ and go to 3.

In our case, x_k represents the current geometry in which we solve the direct and the adjoint problem. The function f is the objective function and g is its gradient obtained by evaluating the sensitivity.

The whole optimization process works as follows:

1*. In the initial domain Ω solve the direct and the adjoint problem.

2*. Compute the value of the objective function.

3*. Compute the gradient of the objective function derived in the sensitivity analysis in Chapter 4. Gradient is computed with respect to the design variables described in Section 6.1.

4*. Use the steepest descent method and find a new domain $\Omega(t)$.

5*. Solve the direct and the adjoint problem in $\Omega(t)$ and go to 2*.

The solver settings are user-defined. Configuration possibilities are as follows (`eps_rd`, `eps_of` and `eps_ofg` are used for the convergence test):

Option	Description
`i_max`	maximum iterations number
`eps_rd`	relative decrease of the objective function
`eps_of`	absolute value of the objective function
`eps_ofg`	the norm of gradient of the objective function
`ls`	'`True`' or '`False`' for the line search
`ls_method`	'`Backtracking`'
`ls0`	$\tilde{\alpha}$ from the iteration process
`ls_red`	c_α from the iteration process
`ls_red_warp`	c_b from the iteration process
`ls_on`	c_f from the iteration process
`ls_min`	c_{min} from the iteration process
`log`	path to the basic description of computation

Table 6.1: Optimization solver settings

6.2.3 Penalty function method

We implemented the linear geometry constraint to the software SfePy. We employed the penalty function method. The geometry is constrained by a plane specified by one point and the normal vector.

Let us consider a general constrained optimization problem:

$$\begin{aligned} &\text{minimize} && f(\boldsymbol{x}), \\ &\text{subject to} && g_j(\boldsymbol{x}) \leq 0, j = 1, \ldots, p, \end{aligned}$$

where $f(\boldsymbol{x})$ is the objective function to be minimized and $g_j(\boldsymbol{x}), j = 1, \ldots, p$ are inequality constraints. The penalty function method applies an unconstrained optimization algorithm to a penalty function formulation of a constrained problem. We used the penalty method described in [28]:

$$\begin{aligned} &\text{minimize} && P(\boldsymbol{x}), \\ &\text{where} && P(\boldsymbol{x}, \beta) = f(\boldsymbol{x}) + \sum_{j=1}^{p} \beta_j g_j^2(\boldsymbol{x}), \end{aligned}$$

where $\beta = (\beta, \ldots, \beta_p)$ and penalty parameters $\beta_j, j = 1, \ldots, p$ are given by

$$\beta_j \begin{cases} = 0 & \text{if } g_j(\boldsymbol{x}) \leq 0, \\ > 0 & \text{if } g_j(\boldsymbol{x}) > 0. \end{cases}$$

In our case, we consider $f(\boldsymbol{x})$ to be the objective function. Then $\boldsymbol{x}$ is the computational domain and $|g_j(\boldsymbol{x})|$ is the distance of the j-th mesh node from the given plane, p is the number of mesh nodes. We shall further use the notation $g(\boldsymbol{x}_j)$ instead of $g_j(\boldsymbol{x})$, where $\boldsymbol{x}_j$ is the j-th mesh node. When $\boldsymbol{x}_j$ crosses the given plane, the function $g(\boldsymbol{x}_j)$ is positive (see Figure 6.2) and the corresponding penalty parameter $\beta_j > 0$. We choose all parameters fixed during the computation, i.e. $\beta_j := \beta_0 > 0$ if they are not zero.

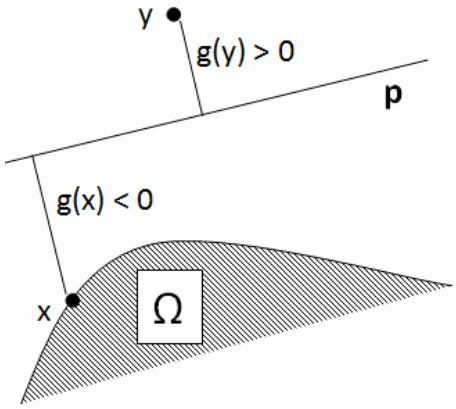

Figure 6.2: Function g with respect to the plane p and the domain Ω

The function $g(\boldsymbol{x}_j)$ could be derived easily. If we denote by $\boldsymbol{n}$ the plane normal vector, by $\boldsymbol{x}_0$ the point defining the plane and by Ω the domain, then the function reads

$$g(\boldsymbol{x}_j) = \frac{\boldsymbol{x}_0 \cdot \boldsymbol{n} - \boldsymbol{x}_j \cdot \boldsymbol{n}}{\|\boldsymbol{n}\|_2} \quad \forall\, \boldsymbol{x}_j \in \Omega. \tag{6.1}$$

We shall need the sensitivity of $g(\boldsymbol{x}_j)$ with respect to the design velocity field $\vec{\mathcal{V}}$ too. We shall add this term to the sensitivity of the objective function during the optimization. We get

$$g(\boldsymbol{x}_j) = -\frac{\vec{\mathcal{V}}(\boldsymbol{x}_j) \cdot \boldsymbol{n}}{\|\boldsymbol{n}\|_2} = -\vec{\mathcal{V}}(\boldsymbol{x}_j) \cdot \boldsymbol{n} \quad \forall\, \boldsymbol{x}_j \in \Omega,$$

if we consider $\|\boldsymbol{n}\|_2 = \sqrt{\sum_{i=1}^{3} n_i^2} = 1$.

The penalty function method was implemented into the steepest descent method. The procedure is as follows:

1) Choose an appropriate penalty constant $\beta_0 > 0, k := 0$.

2) Let us suppose that we have the k-th iteration of the steepest descent method, the domain $\Omega(t_k)$ and the plane defined by the point $\boldsymbol{x}_0$ and by the normal vector $\boldsymbol{n}$, $\|\boldsymbol{n}\|_2 = 1$.

3) We compute functions $g(\boldsymbol{x}_j), j = 1, \ldots, p$ using (6.1), where p is number of mesh nodes of $\Omega(t_k)$.

4) For $j = 1, \ldots, p$: if $g(\boldsymbol{x}_j) > 0$, then $\beta_j := \beta_0$, else $\beta_j := 0$.

5) When evaluating the objective function in the domain $\Omega(t_k)$, add the term $\sum_{j=1}^{p} \beta_j g^2(\boldsymbol{x}_j)$ to its value.
When evaluating the gradient of the objective function in $\Omega(t_k)$, add the term $-2\sum_{j=1}^{p} \beta_j g(\boldsymbol{x}_j)\vec{\mathcal{V}}(\boldsymbol{x}_j) \cdot \boldsymbol{n}$ to the sensitivity formula (4.21) (or to (4.22) when considering state problem without stabilizations).

6) We obtained a new domain $\Omega(t_{k+1})$ by the steepest descent method. Set $k := k+1$ and go to 1).

6.2.4 Input data

When solving the optimization problem, configurations and data necessary for iterations are downloaded from a data file. We present here the basic description of the data file. More details can be found in [6].

Input data are sorted as described bellow. User can modify all of them. It is also possible to incorporate new features (i.e. a new objective function) into the data file and then simply switch between them with the aid of the `options` table as will be mentioned in point 8 below.

1. A geometry which will be used for the simulation is chosen.

2. Regions like a criterion domain, inlet, outlet and walls are defined. The design domain is created automatically.

3. Boundary conditions are described. We have prescribed the inlet velocity, no-slip condition on the wall and a zero pressure on the outlet in our test cases.

4. Then a material is defined - we enter the domain where the particular material occurs. Then its qualities like viscosity and density values follow.

5. Further, fields of variables (the velocity field and the pressure) with appropriate finite element types are defined.

6. Equations to solve are written. We need to enter the direct and the adjoint problem and the formula of the objective function and its sensitivity.

7. The solvers configurations follow. We described the configuration of the optimization solver. There are analogous possibilities by configuration the nonlinear solvers. The linear solver UMFPACK is predefined in Python.

8. At the end, there is the `options` table which manages the computation. We specify the linear and nonlinear solver which will be used. We could also switch between several objective functions which are set on.

Chapter 7

Numerical results

In this chapter we shall present results obtained by methods described in the thesis. We use spline boxes made by the software SPBOX for the geometry parametrization and the software SfePy to solve the shape optimization problem using the adjoint method.

We consider the laminar, incompressible flow described by the Navier-Stokes equations. We present results for both the stabilized and the unstabilized formulations. We shall describe some aspects of the problem setup which affect the optimized design. Problem of the shape optimization with linear design constraints will be presented too.

Computations were performed on the computer Intel(R) Core(TM)2 Duo CPU, 2.00 GHz with 3GB RAM.

7.1 State problem, objective functions and geometries

We use the presented state problem (5.1) for simulations. The discretized stabilized formulation is described by (5.3), while the discretized formulation without stabilizations by (5.4). If we do not use the stabilized formulation, we could consider only limited values of viscosity in order $10^{-3}\, m/s^2$. The solution is unstable for smaller magnitude. We tested the stabilized formulation for a lower viscosity value.

We used two types of objective functions for computations. We consider the objective function introduced in Chapter 4, but the difference is in the criterion domain Ω_C. The first choice is to consider $\Omega_C \subset \Omega_F$ where Ω_F is the fixed part of the domain (see Figures 3.1, 3.2). We denote

$$\Psi_1(\boldsymbol{u}) = \frac{\nu}{2} \int_{\Omega_C} |\nabla \boldsymbol{u}|^2 \, d\boldsymbol{x} = \frac{1}{2} a_{\Omega_C}(\boldsymbol{u}, \boldsymbol{u}). \tag{7.1}$$

Then it holds $\delta_D \Psi_1(\boldsymbol{u}) = 0$, because Ω_C does not change during iterations.

The second possibility which we shall use for simulations is the objective function defined in the whole computational domain, i.e. $\Omega_C = \Omega$. The appropriated objective function is defined as

$$\Psi_2(\boldsymbol{u}) = \frac{\nu}{2} \int_{\Omega} |\nabla \boldsymbol{u}|^2 \, d\boldsymbol{x} = \frac{1}{2} a_{\Omega}(\boldsymbol{u}, \boldsymbol{u}). \tag{7.2}$$

Then we obtain $\delta_D \Psi_2(\boldsymbol{u}) = \delta_D a_\Omega(\boldsymbol{u}, \boldsymbol{u})$.

The sensitivity analysis is derived in Chapter 4.

We shall test both objective functions and we shall show the influence of our choice on the final shape of channel. We shall use the notation Ψ_1 and Ψ_2 in the whole chapter.

We consider three types of geometries for computations. We present them now and we shall be referencing on this description in the following text:

Geometry name	Geometry description	Computational mesh
Geometry 1	twisted tube, diameter 1 cm	6316 tetrahedral elements with 1575 vertices
Geometry 2	bended pipe, diameter 10 cm	15086 tetrahedral elements with 3134 vertices
Geometry 3	half tyre-like, diameter 6 cm	8161 tetrahedral elements with 1823 vertices

Table 7.1: Description of geometries used for optimization

7.2 Stabilization parameters

In this section we present results obtained for the stabilized formulation of the Navier-Stokes equations described in Chapter 2. Assuming scaling the Oseen problem such that $b_\infty := \|\boldsymbol{b}\|_\infty \sim 1$, denoting $c_F \sim \operatorname{diam}\Omega$ the Friedrichs constant for Ω, stabilization parameters were designed in [18] as follows:

$$\gamma = \nu + b_\infty c_F,$$

τ_K and κ_K satisfying the following constraint where C is a suitable constant:

$$0 \le \tau_K \le \kappa_K \le C \frac{\min(1; \frac{1}{\sigma}) h_K^2}{\nu + b_\infty c_F + \sigma c_F^2 + b_\infty^2 \min(\frac{c_F^2}{\nu}; \frac{1}{\sigma})},$$

where σ arises from the time discretization of the nonstationary problem and it holds $\sigma = 0$ in our case. We select stabilization parameters in the following form:

$$\begin{aligned} \gamma &= c_\gamma(\nu + b_\infty c_F), \\ \tau_K &= c_\tau \frac{\nu\, h_K^2}{\nu^2 + \nu\, b_\infty c_F + b_\infty^2 c_F^2}, \\ \kappa_K &= c_\kappa \frac{\nu\, h_K^2}{\nu^2 + \nu\, b_\infty c_F + b_\infty^2 c_F^2}, \end{aligned} \tag{7.3}$$

where $1 \le c_\gamma, 0 \le c_\tau \le c_\kappa$ are user-defined constants.

We use Geometry 1 for simulations presented in this section. We shall test the stabilized solution of the Navier-Stokes equations for two viscosity values. Then solving the shape optimization problem for the stabilized state problem will be reported.

7.2.1 Direct problem for different viscosity values

We show solutions of the stabilized Navier-Stokes equations for two viscosity values below. We can compare results with the unstabilized solution in the case of a higher viscosity flow. We shall test the stabilized formulation for two different stabilization parameter values.

In the first test case we consider the flow properties $\nu = 1.25 \cdot 10^{-3}\, m/s^2$, $\rho = 1\, kg/m^3$ and the inlet velocity $\boldsymbol{u}_{in} = 1\, cm/s$. The solution of the unstabilized formulation is displayed in Figure 7.1. The solution of the stabilized Navier-Stokes equations with stabilization parameter values $c_\gamma = 1, c_\tau = c_\kappa = 0.1$ is presented in Figure 7.2. The solution of the stabilized state problem with stabilization parameters chosen as $c_\gamma = 10$, $c_\tau = c_\kappa = 1$ is shown in Figure 7.3.

The second test case is a low viscosity flow. We consider a liquid characterized by $\nu = 1.25 \cdot 10^{-5}\, m/s^2$, $\rho = 1\, kg/m^3$ and $\boldsymbol{u}_{in} = 1\, cm/s$. Solution of this problem is displayed in Figure 7.4.

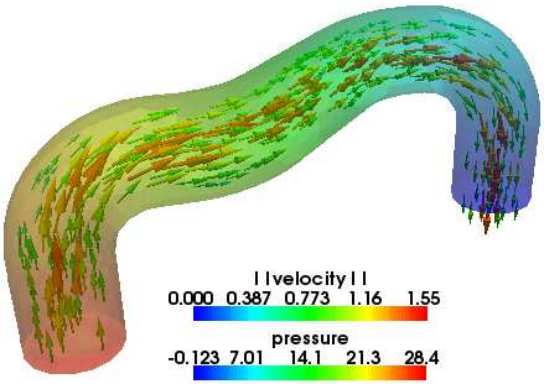

Figure 7.1: The unstabilized formulation, $\nu = 1.25 \cdot 10^{-3}\ m/s^2$

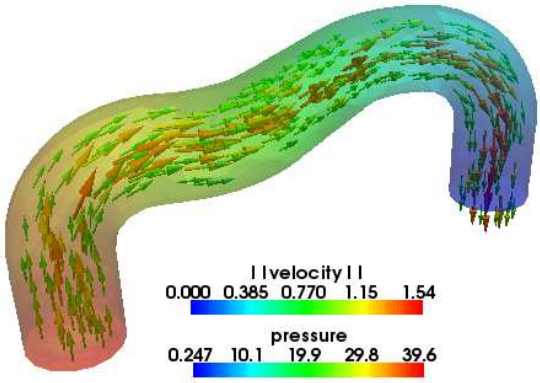

Figure 7.2: The stabilized formulation, $\nu = 1.25 \cdot 10^{-3}\ m/s^2$, we choose $c_\gamma = 1$, $c_\tau = c_\kappa = 0.1$

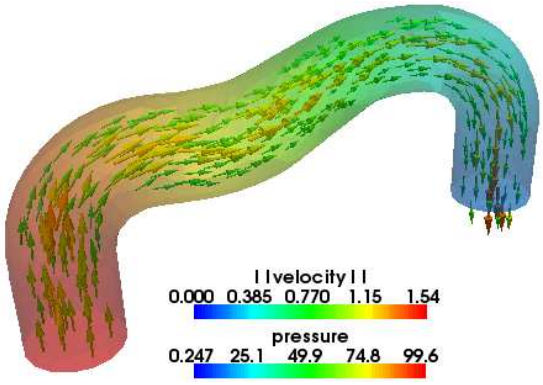

Figure 7.3: The stabilized formulation, $\nu = 1.25 \cdot 10^{-3}\ m/s^2$, we choose $c_\gamma = 10$, $c_\tau = c_\kappa = 1$

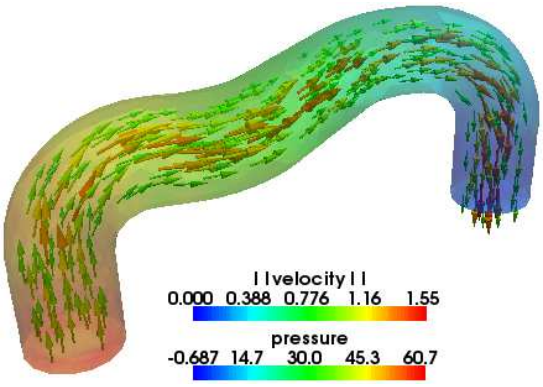

Figure 7.4: The stabilized formulation, $\nu = 1.25 \cdot 10^{-5}\ m/s^2$, we choose $c_\gamma = 5.5$, $c_\tau = c_\kappa = 4$

By comparing solutions of the stabilized formulation for the liquid described by the viscosity value $\nu = 1.25 \cdot 10^{-3}\, m/s^2$ we can see that the choice of stabilization parameters influence the final solution. The solution with lower stabilization parameters values (Figure 7.2) is closer to the solution of the unstabilized problem than the solution with higher stabilization parameters (Figure 7.3).

Case of the low viscosity flow was tested too. It is not possible to solve this problem without stabilizations. We can see that it is necessary to use higher stabilization parameters values to obtain a solution.

It is clear that the choice of stabilization parameters influence the final result and the crucial question is an appropriate selection of them. We need to stabilize the solution enough and at the same time not to spoil the solution by an over-stabilization.

7.2.2 Optimization problem for both the stabilized and the unstabilized formulations

We shall present the solution of the shape optimization problem for the stabilized Navier-Stokes equations in this section. Because we consider the viscosity of the flow in order $10^{-3}\, m/s^2$, we could compare the result with the solution of the shape optimization algorithm for the unstabilized state problem.

We use Geometry 1 for simulations presented in this section and the fluid properties are $\nu = 1.25 \cdot 10^{-3}\, m/s^2, \rho = 1\, kg/m^3$, the inlet velocity is $\boldsymbol{u}_{in} = 1\, m/s$. We consider Ψ_1 to be the objective function. The criterion domain Ω_C is depicted by two grey planes in figures.

In the stabilized formulation of the Navier-Stokes equations we used stabilization parameters values $c_\gamma = 1, c_\tau = c_\kappa = 0.1$. The initial design is shown in Figure 7.5, the optimized design in Figure 7.6. Graphs of the steepest descent algorithm convergence for this test case are displayed in Figure 7.9.

In all graphs in this chapter we shall use the following notation: `of` means the objective function, we denote by `||ofg||` the Eucleidian norm of the objective function gradient and `alpha` is the length of the line-search step.

Results of the shape optimization for the unstabilized state problem follow. The initial shape of channel is displayed in Figure 7.7 and the optimized geometry in Figure 7.8. Graphs of the convergence of the optimization algorithm are shown in Figure 7.10.

Statistics of both computations are introduced in Table 7.2.

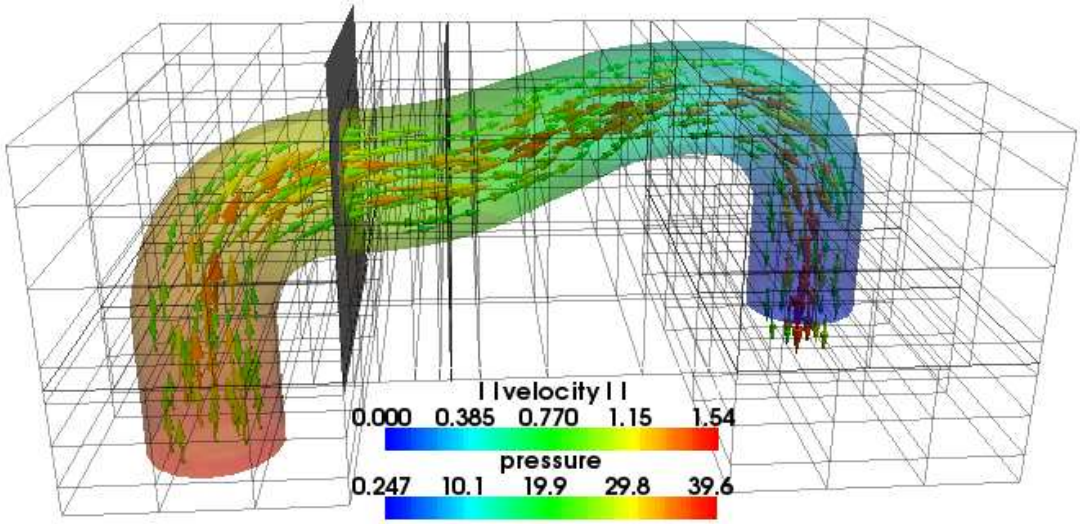

Figure 7.5: Initial design for the stabilized state problem

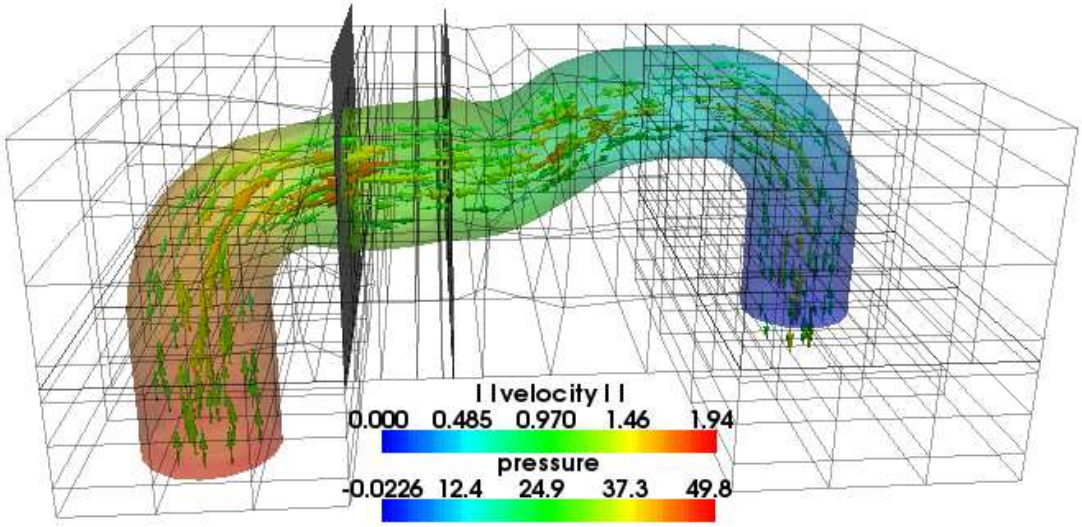

Figure 7.6: Optimized design for the stabilized state problem

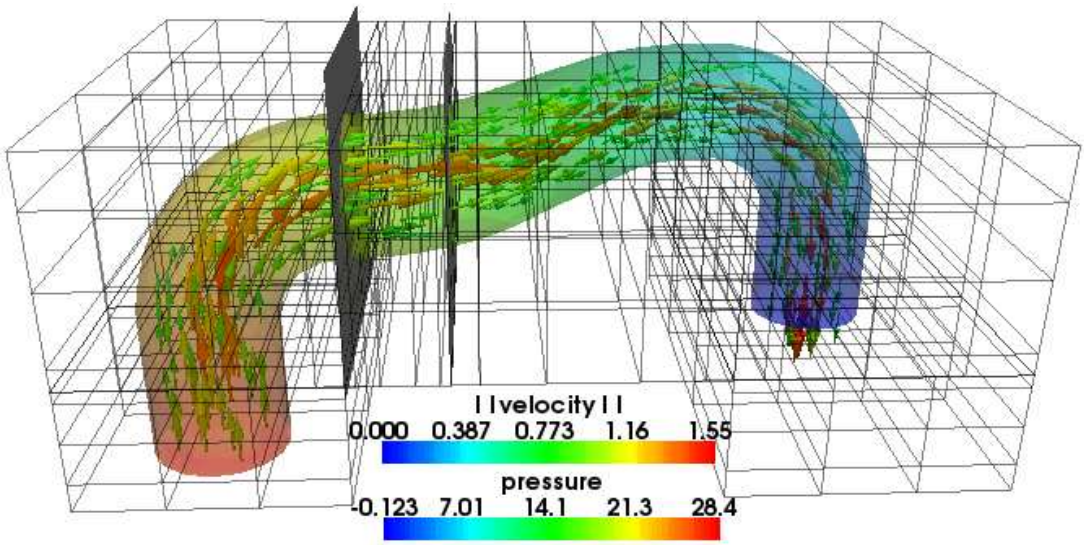

Figure 7.7: Initial design for the unstabilized state problem

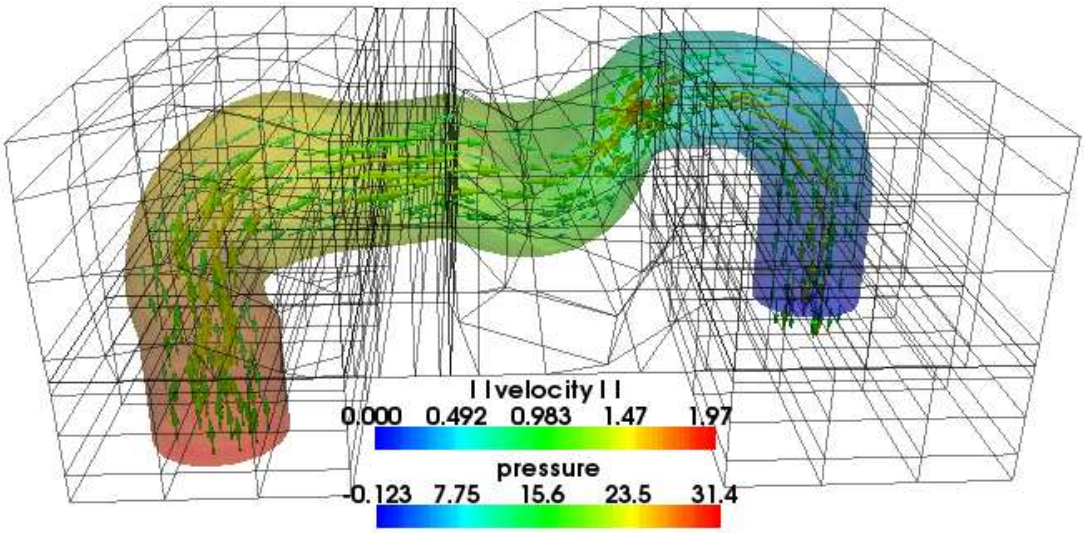

Figure 7.8: Optimized design for the unstabilized state problem

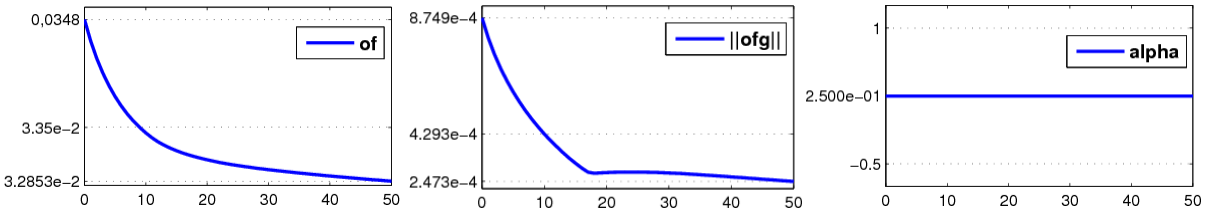

Figure 7.9: Convergence of the steepest descent optimization algorithm for the stabilized formulation

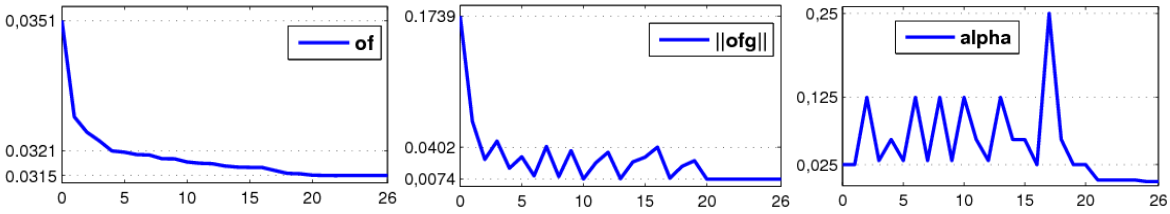

Figure 7.10: Convergence of the steepest descent optimization algorithm for the unstabilized formulation

Computation parameter	Unstabilized formulation	Stabilized formulation
Optimization iterations	26	50
OF in the initial domain	0.0350778166384	0.0348008357787
OF in the final domain	0.0314980960976	0.0328527465888
Reduction of OF	10.2%	5.6%
OF evaluations	103 (226 s)	101 (278 s)
OF gradient evaluations	27 (895 s)	51 (3256 s)
Initial domain volume	6.99241805354e-06	6.99241805354e-06
Final domain volume	7.51361346725e-06	6.85564040442e-06
Relative volume increase	7.5%	-2%

Table 7.2: The stabilized and the unstabilized formulations - statistics

By comparing optimized domains for both problems we can see that the final shape of channel changed less for the stabilized formulation. Also the relative decrease of the objective function value is lower in the stabilized case. We can see that the stabilization of the state problem affects the solution of the shape optimization process. We shall consider only the unstabilized formulation of the shape problem for the rest of simulations presented in this chapter. An appropriate choice of stabilization parameters values could be a topic of the future research.

7.3 Influence of the geometry parametrization

In this section we show how different geometry parametrizations influence the result of the shape optimization problem. We use Geometry 1 for testing. The following flow quantities are considered: $\nu = 1.25 \cdot 10^{-3}\, m/s^2, \rho = 1\, kg/m^3, \boldsymbol{u}_{in} = 1\, m/s$. We employ the objective

function Ψ_2. We consider two types of spline boxes for the geometry parametrization. Restrictions considered for spline boxes define the fixed part of the computational domain, Ω_F (see Figure 3.1).

In the first choice of parametrization there are implemented some extra constraints in spline boxes and the domain stays unchanged in a quite large part. In the second case we did not define additional constraints and only small parts of the domain lying near the inlet and the outlet boundary parts do not change during iterations. We can see the difference by comparing the optimized designs for both cases.

The initial design related to the first type of parametrization is presented in Figure 7.11. The optimized channel is shown in Figure 7.12. Graphs of the optimization algorithm convergence are displayed in Figure 7.15.

Results for the second type of parametrization follow. The initial domain is depicted in Figure 7.13, while the optimized design is in Figure 7.14. Graphs of the convergence are shown in Figure 7.16.

Computations statistics are displayed in Table 7.3.

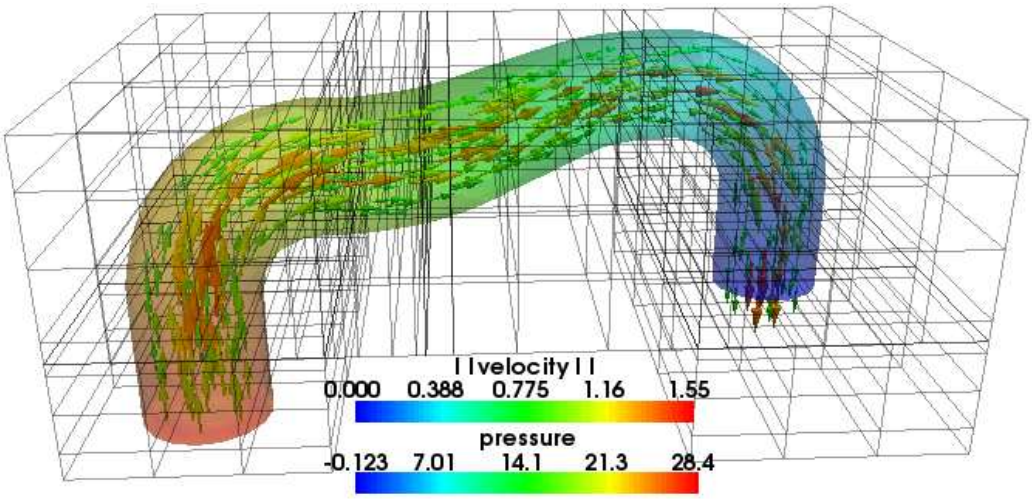

Figure 7.11: Initial design for the first type of parametrization

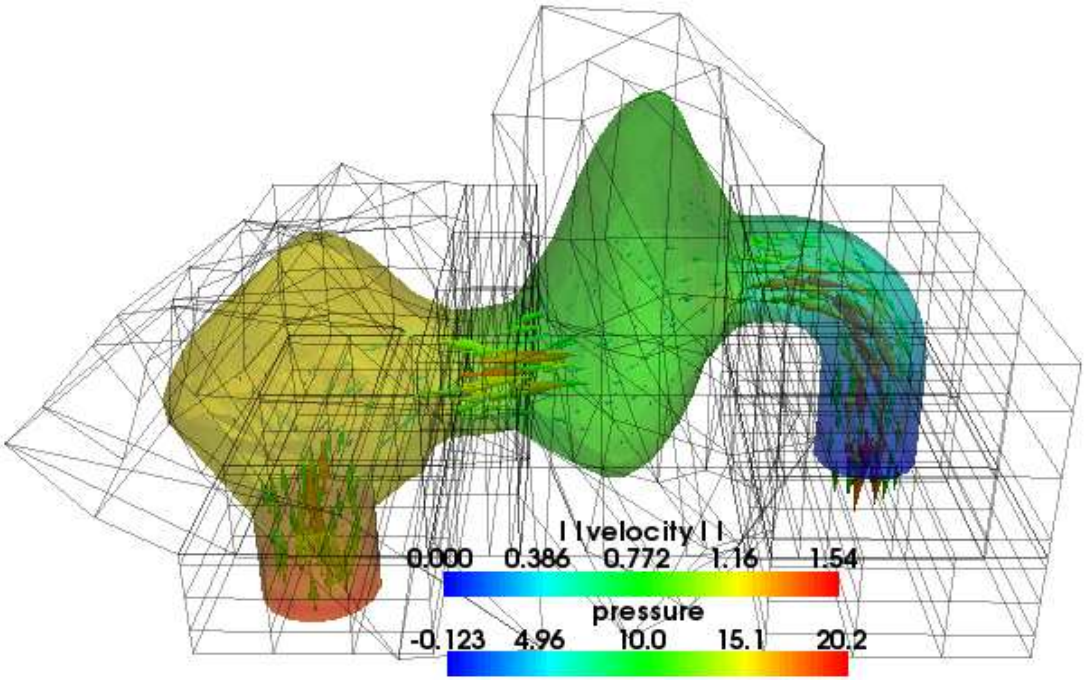

Figure 7.12: Optimized design for the first type of parametrization

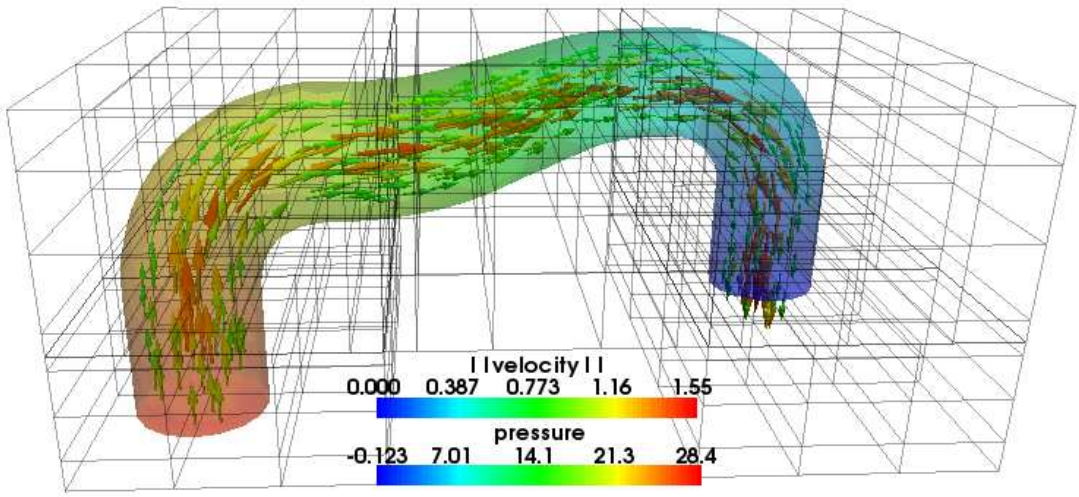

Figure 7.13: Initial design for the second type of parametrization

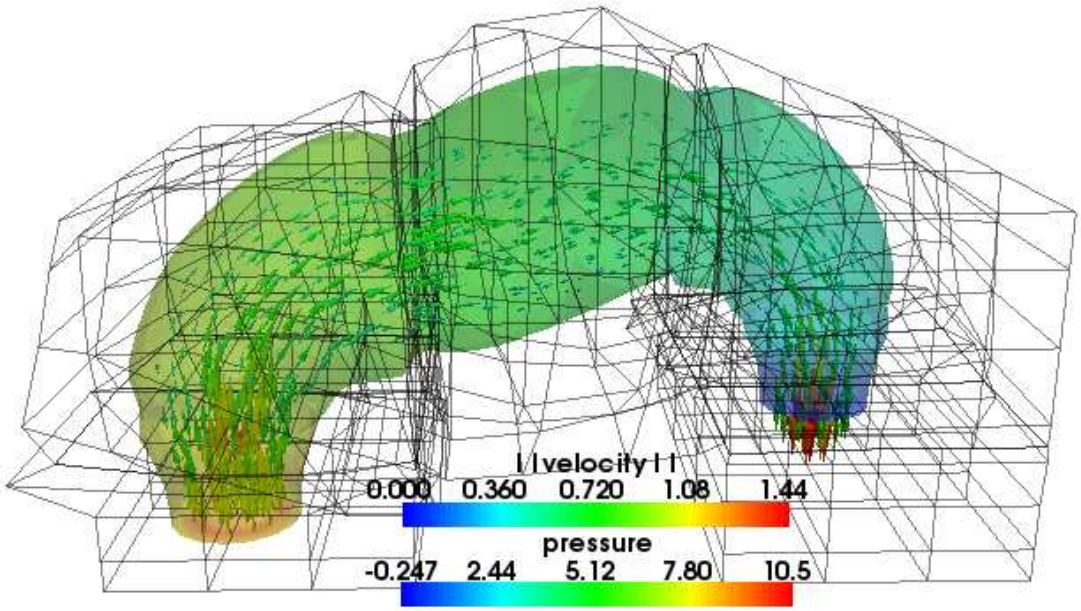

Figure 7.14: Optimized design for the second type of parametrization

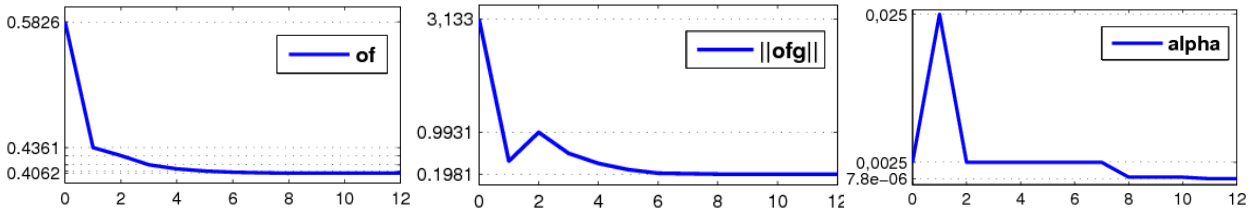

Figure 7.15: Convergence of the steepest descent optimization algorithm for the first type of parametrization

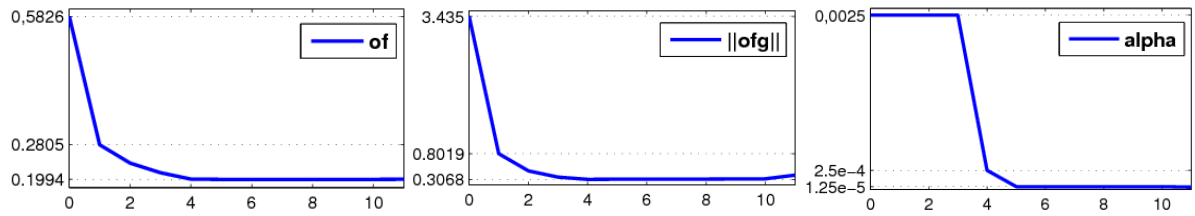

Figure 7.16: Convergence of the steepest descent optimization algorithm for the second type of parametrization

Computation parameter	First type	Second type
Optimization iterations	12	11
OF in the initial domain	0.582643421222	0.582643425555
OF in the final domain	0.406167958808	0.199383710828
Reduction of OF	30.29%	65.78%
OF evaluations	56 (67 s)	64 (81 s)
OF gradient evaluations	13 (554 s)	12 (1558 s)
Initial domain volume	6.99241805354e-06	6.99241805354e-06
Final domain volume	1.6359636265e-05	1.4290440995e-05
Relative volume increase	134%	104.4%

Table 7.3: Comparison of two parametrization types - statistics

We could see that results for two geometry parametrizations are very different. In the first case there are implemented some extra constraints of the shape variation. Therefore, some parts of the channel stay unchanged during the iteration steps while other go through large deformations.

In our second choice, spline boxes are more free and only the inlet and the outlet boundary parts stay unchanged. Consequently the whole domain deforms. Quite interesting fact is that despite it the volume of the final geometry is bigger in the first case (see Table 7.3). In my opinion, it is harder for the domain in the first case to achieve the flow uniformity in the whole domain because of the spline box restrictions. Therefore, the free part of domain becomes very large to reach the uniform velocity at least in this part.

We can also note that we achieve only the C^0 continuity of the final boundary - see Figure 7.14 and parts of the geometry occurring near boundaries between two adjacent spline boxes. It would be useful for the future to implement more constraints in the SPBOX to enforce a higher degree of the boundary smoothness.

7.4 Influence of the criterion domain

Here we compare results of the shape optimization process concerning two objective functions, Ψ_1 and Ψ_2, in this part. The difference is in the definition of the criterion domain; Ω_C is fixed for Ψ_1, while Ω_C is the whole computational domain for Ψ_2 and is free to change.

We use Geometry 2 for computations and the fluid properties are the following:
$\nu = 1.25 \cdot 10^{-3}\, m/s^2, \rho = 1\, kg/m^3, \boldsymbol{u}_{in} = 3\, m/s$.

At first we compute the shape optimization problem for the objective function Ψ_1. The initial domain is shown in Figure 7.17. The optimized channel is depicted in Figure 7.18. Graphs of the convergence of the optimization solver are displayed in Figure 7.21.

Then figures related to the optimization with Ψ_2 follow. The initial shape is displayed in Figure 7.19 and the optimized design in Figure 7.20. Graphs illustrating the optimization algorithm convergence are shown in Figure 7.22.

Statistics are written in Table 7.4.

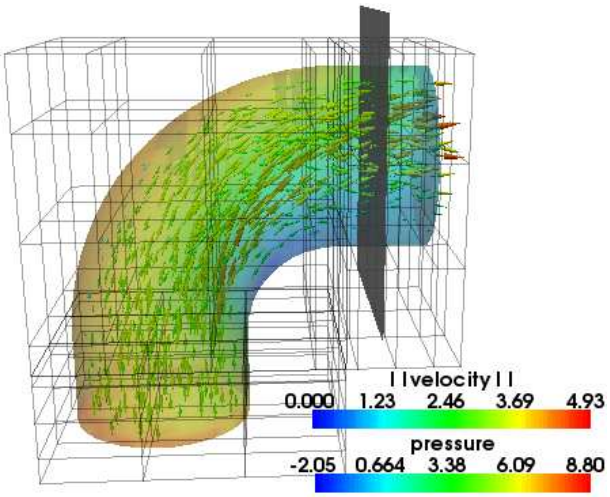

Figure 7.17: Initial design for the objective function Ψ_1

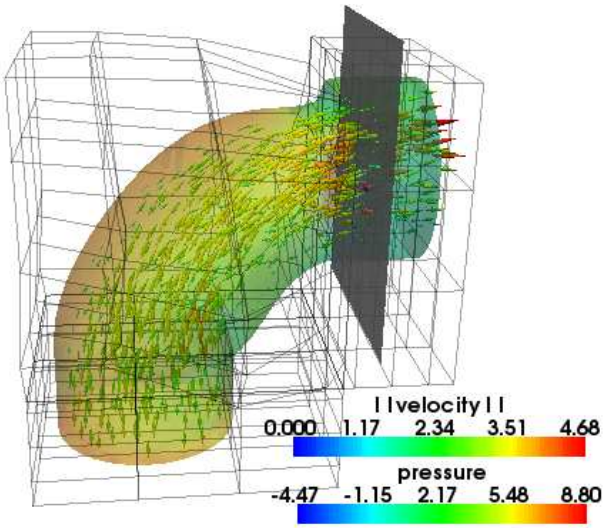

Figure 7.18: Optimized design for the objective function Ψ_1

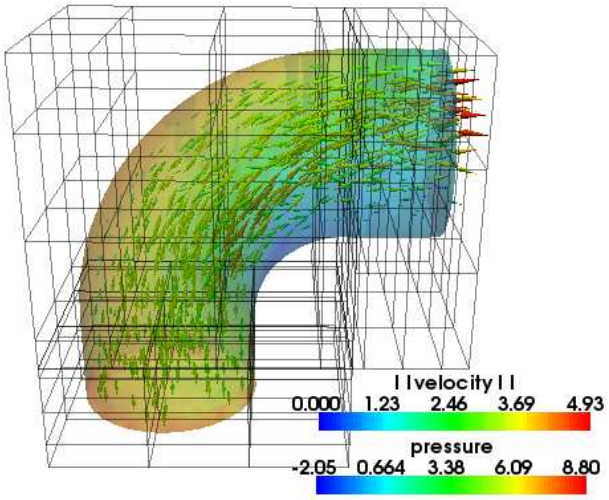

Figure 7.19: Initial design for the objective function Ψ_2

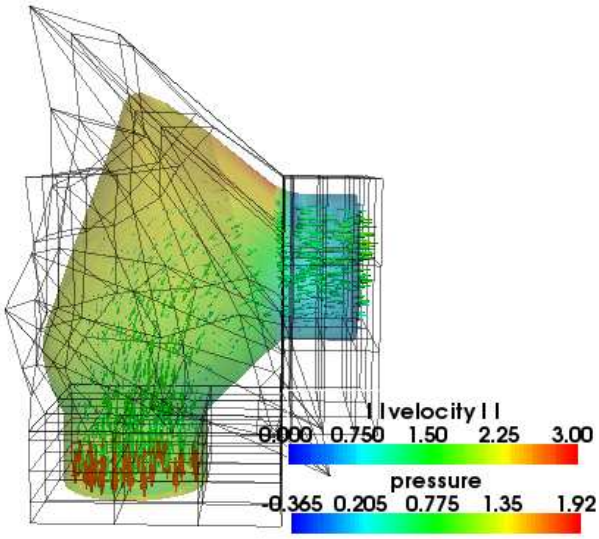

Figure 7.20: Optimized design for the objective function Ψ_2

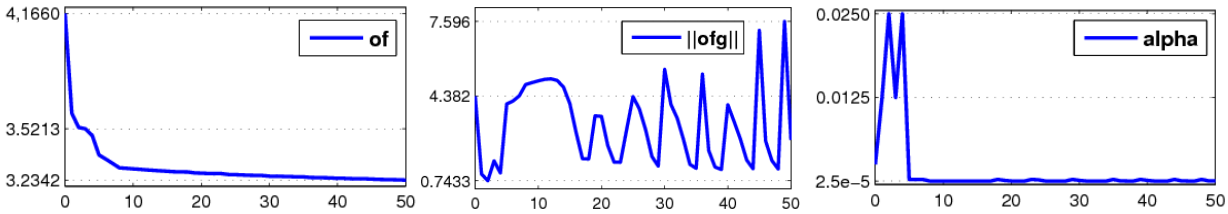

Figure 7.21: Convergence of the steepest descent optimization algorithm for the objective function Ψ_1

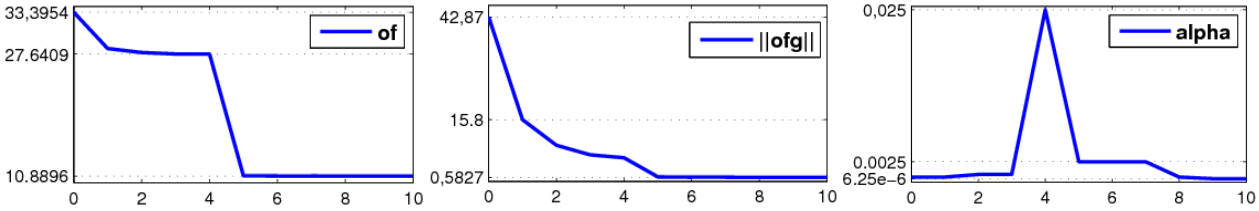

Figure 7.22: Convergence of the steepest descent optimization algorithm for the objective function Ψ_2

Computation parameter	Objective function Ψ_1	Objective function Ψ_2
Optimization iterations	50	10
OF in the initial domain	4.16602030311	33.3954199821
OF in the final domain	3.23422439108	10.8896289924
Reduction of OF	22.37%	67.39%
OF evaluations	316 (7725 s)	50 (1171 s)
OF gradient evaluations	51 (1993 s)	11 (531 s)
Initial domain volume	0.00200929204593	0.00200929204593
Final domain volume	0.00210390000565	0.00332361172006
Relative volume increase	4.7%	65.4%

Table 7.4: Comparison of two objective functions, Ψ_1 and Ψ_2 - statistics

It is obvious that considering the objective function Ψ_2 shape changes are larger. If we study Table 7.4 we can see that considering the objective function Ψ_2 the optimization algorithm needed only 10 iterations to achieve an optimal form while for Ψ_1 it needed 50 iterations. Also the reduction of the objective function value is much better for Ψ_2.

In my opinion, it is because a large part of the criterion domain for Ψ_2 is the object of optimization (only small boundary parts near the inlet and the outlet are fixed) and we can influence the objective function by changing the shape of the domain where the objective function Ψ_2 is computed. On the contrary, in the case of Ψ_1 the criterion domain does not change during the shape optimization process and the objective function value is influenced only by changing of the shape of the domain part where the objective function is not considered. Because we use the no-slip condition describing the viscous flow, the viscosity value leads to a lower effect of the domain changes, it inhibits the flow influence to the domain.

7.5 Influence of the penalty parameter value

In the following computation we employ the linear inequality geometry constraint introduced in Chapter 6. The constraint is given by the defined plane which is displayed in figures. We shall test solutions of the optimization process for different penalty constant values. Geometry 1 will be used for computing and the flow properties are $\nu = 1.25 \cdot 10^{-3}\, m/s^2$, $\rho = 1\, kg/m^3, \boldsymbol{u}_{in} = 1\, m/s$. We use the objective function Ψ_2.

We shall test the shape optimization problem including the linear geometry constraint for penalty values $\beta_0 = 10$ and $\beta_0 = 100$. We compare these results with the solution obtained without any restriction. We can note that the problem without penalization is the same as presented in Section 7.3 in Figures 7.11 and 7.12.

All presented optimization problems begin with the same initial design which is displayed in Figure 7.23. The final design for the optimization without any penalization is presented in Figure 7.24. The convergence graphs are shown in Figure 7.27.

The optimized design for the problem involving the geometry constraint with the penalty value $\beta_0 = 10$ is displayed in Figure 7.25. Graphs of the convergence of the optimization solver are presented in Figure 7.28.

When we solve the optimization problem including the linear geometry constraint with the penalty value $\beta_0 = 100$, we obtain the optimized design shown in Figure 7.26. The algorithm convergence graphs are displayed in Figure 7.29.

Statistics are introduced in Table 7.5.

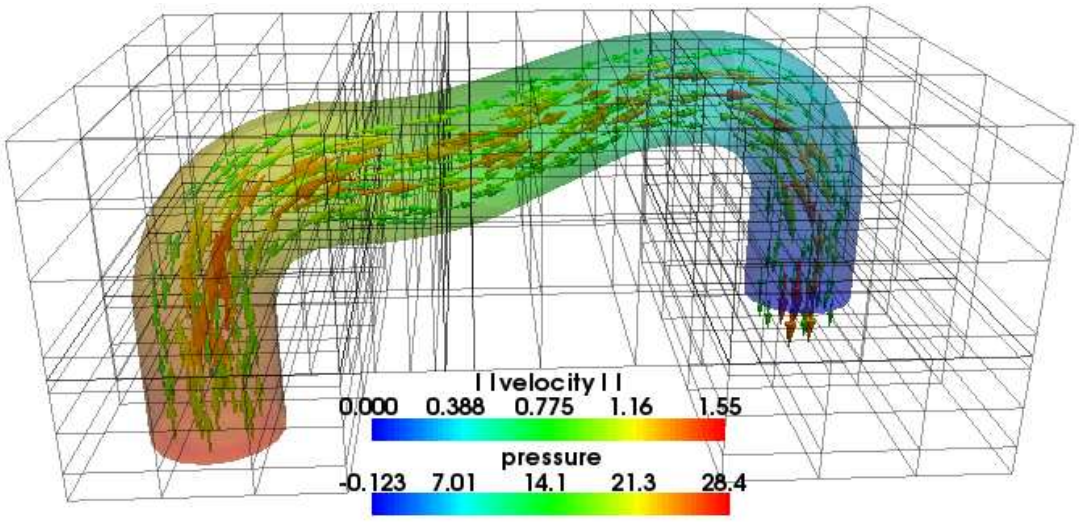

Figure 7.23: Initial design for all penalty values

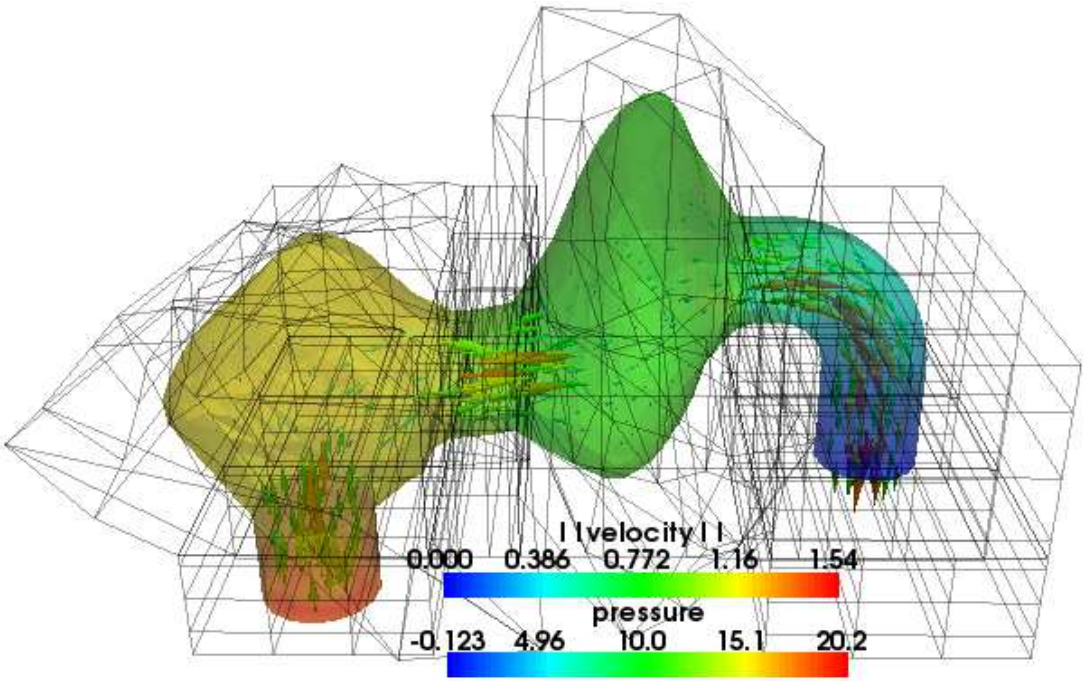

Figure 7.24: Optimized design for the penalty value $\beta_0 = 0$

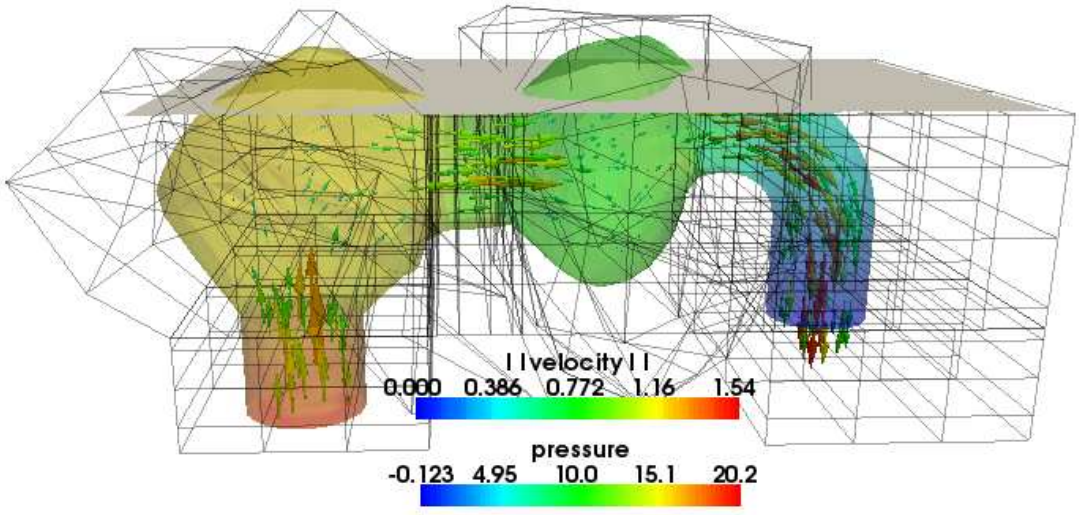

Figure 7.25: Optimized design for the penalty value $\beta_0 = 10$

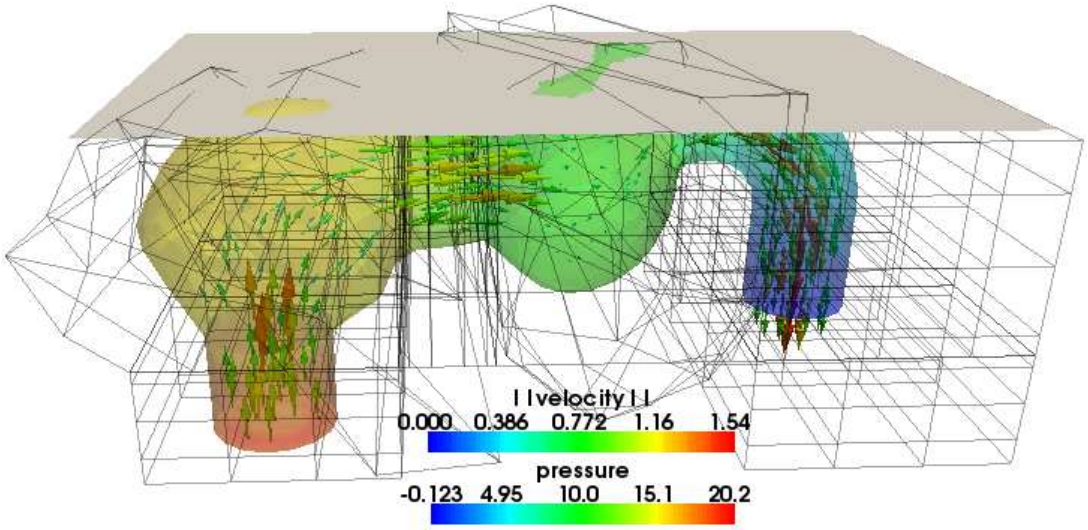

Figure 7.26: Optimized design for the penalty value $\beta_0 = 100$

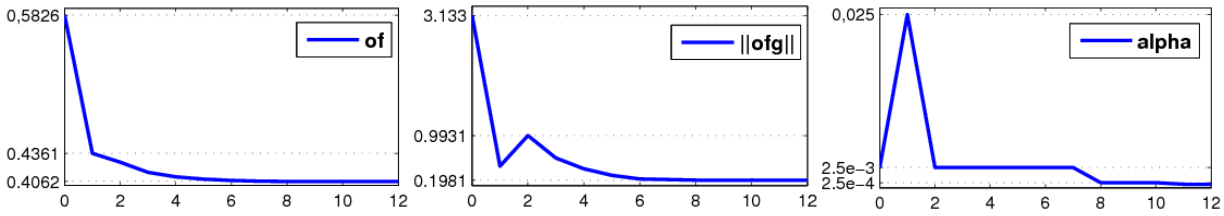

Figure 7.27: Convergence of the steepest descent optimization algorithm for the case without penalization, i.e. $\beta_0 = 0$

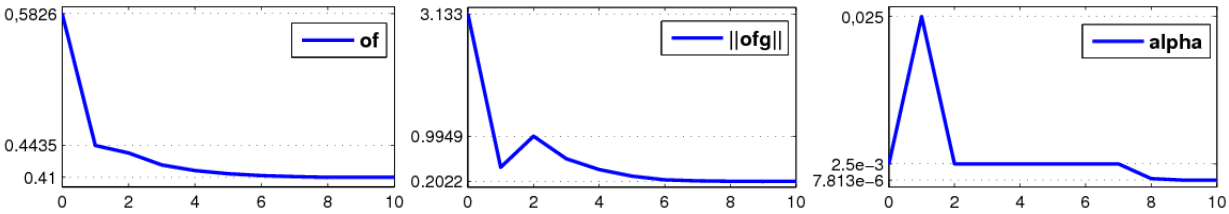

Figure 7.28: Convergence of the steepest descent optimization algorithm for the penalty value $\beta_0 = 10$

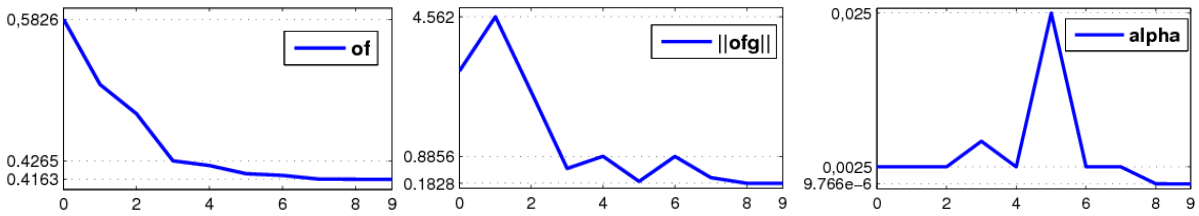

Figure 7.29: Convergence of the steepest descent optimization algorithm for the penalty value $\beta_0 = 100$

Computation parameter	Penalty $\beta_0 = 0$	Penalty $\beta_0 = 10$	Penalty $\beta_0 = 100$
Optimization iterations	12	10	9
OF in the initial domain	0,582643421222	0.582643421222	0.582643421222
OF in the final domain	0.406167958808	0.410014103339	0,416265529432
Reduction of OF	30.3%	29.6%	28.6%
OF evaluations	56 (67 s)	46 (59 s)	44 (71 s)
OF gradient evaluations	13 (554 s)	11 (484 s)	10 (424 s)
Initial domain volume	6.99241805354e-06	6.99241805354e-06	6.99241805354e-06
Final domain volume	1.6359636265e-05	1.41809481285e-05	1.26302478688e-05
Relative volume increase	134%	102.8%	80.6%

Table 7.5: Comparison of three penalty values $\beta_0 = 0, 10, 100$ - statistics

By comparing Figures 7.24, 7.25 and 7.26 it is obvious that the resulting geometry changes for different penalty values - the geometry tries to reach an optimal shape so that the channel does not exceed the defined plane. For a bigger penalty value the geometry becomes flatter on the upper side where the restrictive plane occurs. Despite we can see that the geometry crosses the plane for both penalty values - but for $\beta_0 = 100$ the part which crosses the plane is smaller.

In Table 7.5 we can read that the volume of the optimized design is smaller for a higher penalty value. It is because the geometry becomes more flatter on the upper side than it grows downside. Also the final value of the objective function is better for a smaller penalty, even if reductions of the objective function values are very similar in all tested cases. It corresponds to the fact that the local minimum of the objective function matches the geometry which crosses the plane - and when we restrict the geometry changes in this direction, the final geometry shape is farther from the solution obtained without any restriction.

7.6 Problem with three planar restrictions of the design

As the last study we shall present the computation considering three linear geometry constraints. We consider Geometry 3 and the objective function Ψ_2. Restricting planes are located around the geometry, see Figure 7.33. Only one restrictive plane is shown in Figures 7.31 and 7.32. That is because of a better view. We shall compare the result of the problem involving three planar restrictions with the solution obtained without any restriction.

The flow is described by $\nu = 1.25 \cdot 10^{-3}\, m/s^2, \rho = 1\, kg/m^3, \boldsymbol{u}_{in} = 1\, m/s$ and the objective function Ψ_2 is used. The penalty value is $\beta_0 = 100$ for all three planes.

Both shape optimizations start with the same initial design. It is shown in Figure 7.30. The optimized design for the problem without any restriction is displayed in Figure 7.31. There is depicted one planar restriction considered in the following optimization process because we can then better compare results. Convergence graphs are shown in Figure 7.34.

The optimized shape of channel for the problem involving three planar restrictions is presented in Figures 7.32 and 7.33. We could compare Figure 7.32 with the solution of the previous test case. In Figure 7.33 there are depicted all restriction planes used during the iteration process. Graphs of the solver convergence are in Figure 7.35.

Statistics are written in Table 7.6.

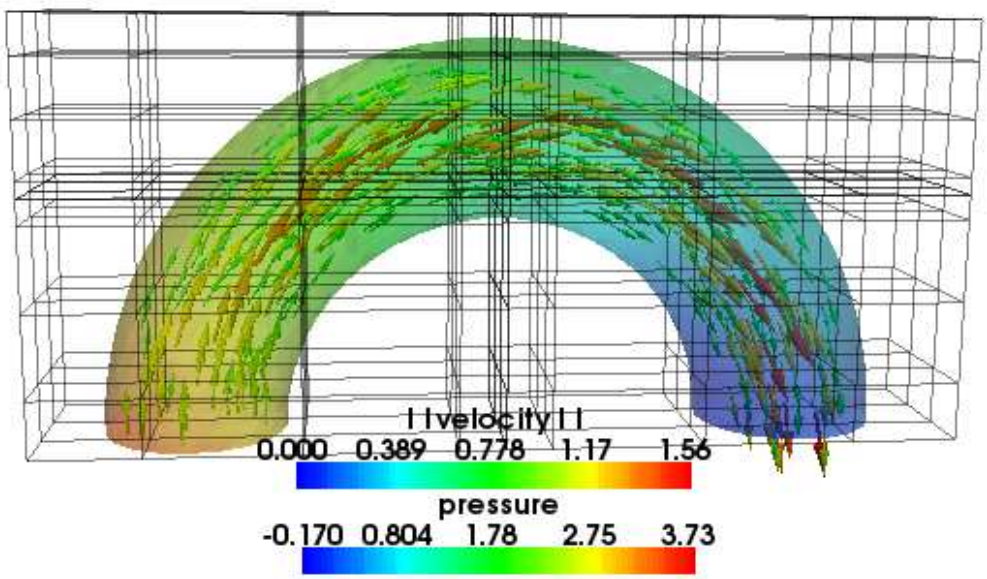

Figure 7.30: Initial design

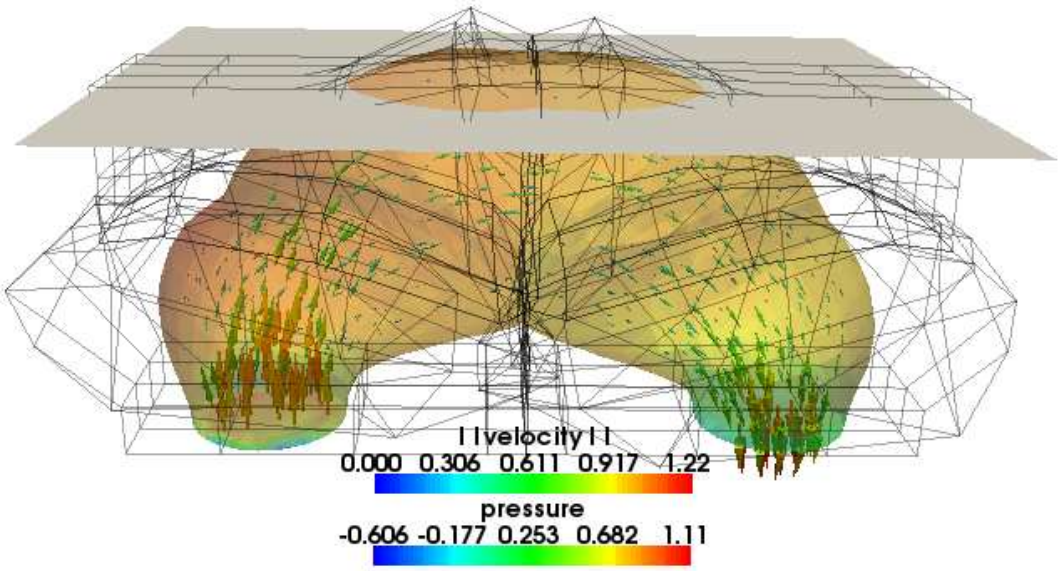

Figure 7.31: Optimized design without any restriction

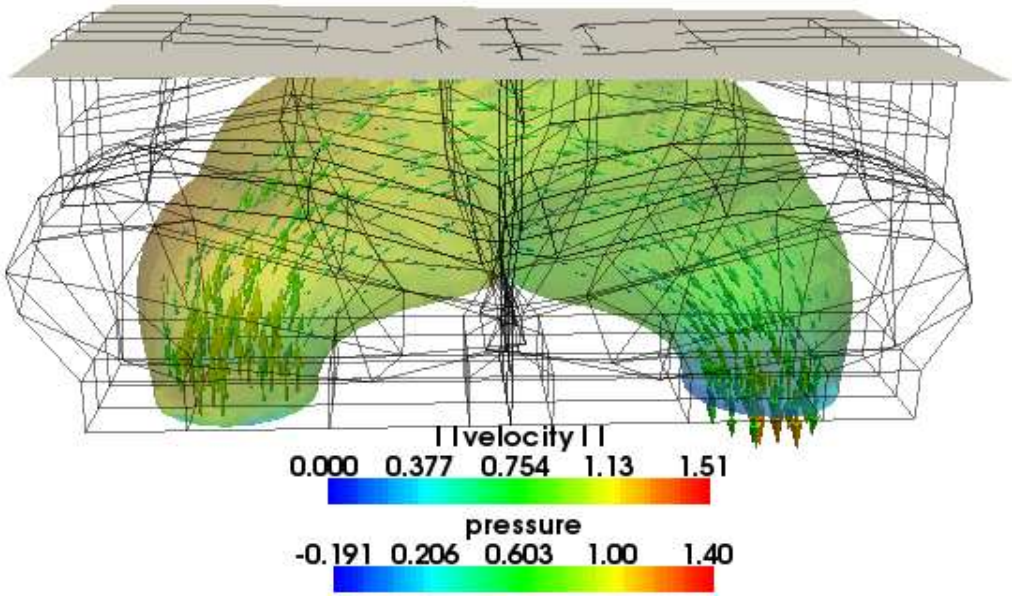

Figure 7.32: Optimized design considering three constraining planes

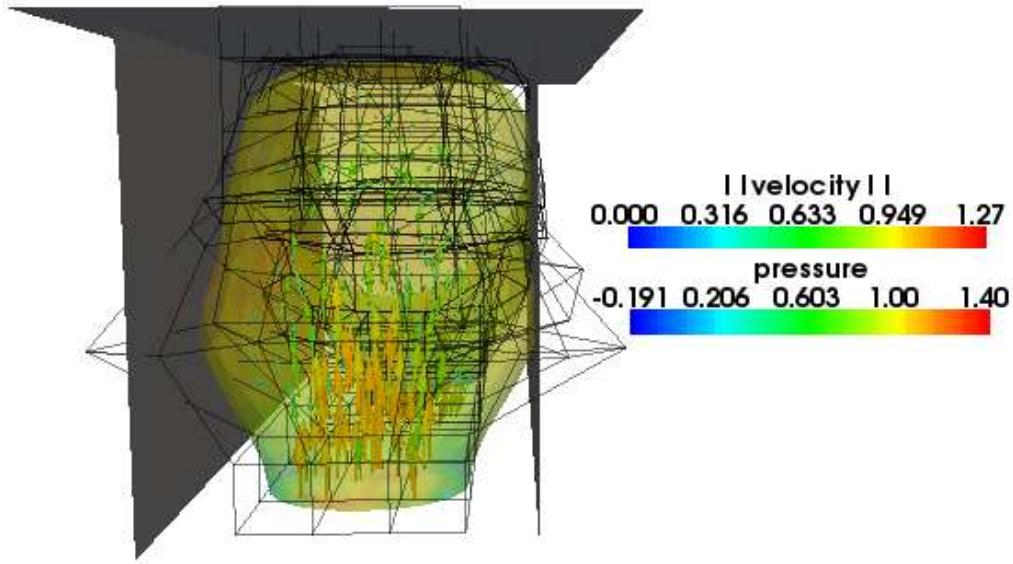

Figure 7.33: Optimized design considering three constraining planes, second view

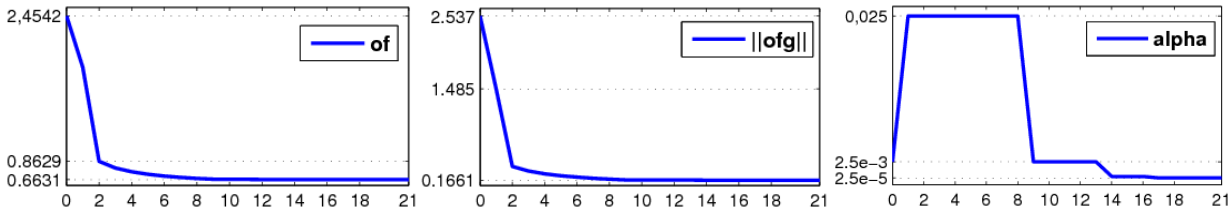

Figure 7.34: Convergence of the steepest descent optimization algorithm without any restriction

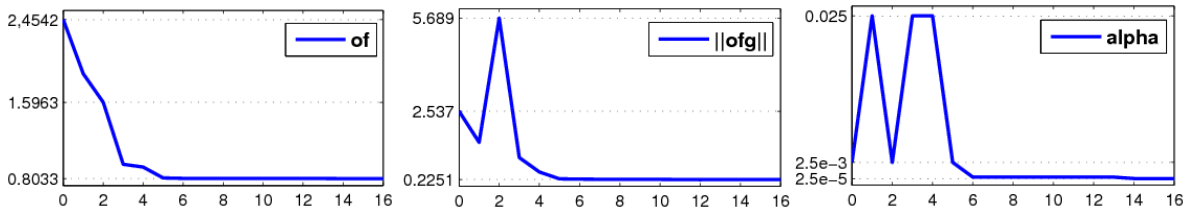

Figure 7.35: Convergence of the steepest descent optimization algorithm for three constraining planes

Computation parameter	Without restriction	Three constraining planes
Optimization iterations	21	16
OF in the initial domain	2,45416923116	2.45416923116
OF in the final domain	0.663079126709	0,803302108967
Reduction of OF	73%	67.3%
OF evaluations	88 (163 s)	74 (125 s)
OF gradient evaluations	22 (2803 s)	17 (2127 s)
Initial domain volume	0.00087736231121	0,00087736231121
Final domain volume	0.00283407316522	0,00191787060777
Relative volume increase	223%	118.6%

Table 7.6: Comparison of the optimization process with and without linear geometry restrictions - statistics

We can see that all restrictive planes influence the optimized design - the shape is less inflated in all three constrained directions. Also the optimized domain volume is smaller for the restricted shape.

By comparing the objective function values for the optimized domains we could see an analogous result as in the previous section. The reduction of the objective function value is similar for both optimization problems but the decrease is higher for the problem without any linear geometry restriction.

Conclusion

Summary of derivations

At this place we would like to summarize the main goals of the thesis.

We introduced the theoretical results concerning the Navier-Stokes equations in Chapters 1 and 2. We described the stabilization technique which is necessary for computing low viscosity flows. Due to the stabilized formulation of the Navier-Stokes equations we were able to use the P1/P1 discretization of the state problem. Theory of the shape optimization problem in fluid dynamics was introduced in Chapter 3 and then the derivation of the sensitivity analysis for the stabilized formulation followed in Chapter 4.

We studied softwares SPBOX and SfePy which were used for computations. We extended the shape optimization problem for the linear inequality constraint of the domain shape. We implemented the penalty method into the software SfePy. The shape constraint is important for practical applications of the shape optimization method.

There are more possibilities how to improve the presented penalty method. Firstly, the penalty parameter value could be chosen more adequately, and its value could change during the computation. We used a fixed parameter value during the optimization process. Secondly, the future work could also include an expansion of the penalty method, for example by using a more complex augmented Lagrangian method which combines the classical Lagrange method with the penalty function method.

Characterization of results and possibilities of the future research

In Chapter 7 we introduced results of selected model tasks. We optimized the shape of channel for the stabilized formulation of the Navier-Stokes equations. We obtained results for the viscosity value $\nu = 1.25 \cdot 10^{-3}\ m/s^2$ which we could compare with the solution of the Navier-Stokes equations without stabilizations. It is possible to find such values of stabilization parameters for which the computation with choice of an unstable finite element pair runs. We obtained the result of the Navier-Stokes equations for a low viscosity value ($\nu = 1.25 \cdot 10^{-5}\ m/s^2$) too. But we can see that the solution is very sensitive to the selection of stabilization parameters. It is necessary to find appropriate stabilization parameter values for which the solution is stable enough and at the same time not to spoil the solution by an over-stabilization. This task will remain the core focus of the future work. We used only the unstabilized formulation of the Navier-Stokes equations for further simulations, because the shape optimization process is very inhibited by effects of stabilization parameters.

We showed the influence of different choices of spline boxes used for the domain parametrization on the result of the optimization process. We can see that difference in the domain parametrization leading to different optimized design. Therefore, the creation of an appropriate domain parametrization is an important step in the shape optimization. It could be useful to implement a higher continuity constraints into the software SPBOX in the future. There is currently C^0 continuity implemented.

Also the choice of the objective function, or of the criterion domain in our examples, is an important step in the optimization process. We considered two types of criterion domains. At first we consider a fixed criterion domain. The second choice was to consider the criterion domain being the whole body. Therefore, in the second approach the criterion domain was changed during the optimization. In the second choice, the optimized domain changed more significantly. The reason for that is, considering the viscous flow, that the viscosity damps the influence of the flow in the criterion domain if the criterion domain is not changed during the computational process.

Then the influence of the chosen penalty parameter value was tested. It is obvious that the optimized design depends on the selection of the penalty parameter value. When we constraint the geometry by one plane, the channel tries to satisfy the constraint and simultaneously to reach an optimized design which is better than the initial one in the sense of the objective function value. As expected, the objective function decreased less in case where a higher penalty was used.

In the other example we showed that we can consider more linear geometry constraints in the shape optimization problem. We introduced the result considering three constraining planes. The penalty method could be further improved as we mentioned previously.

Another possible way how to improve the computational procedure described in the thesis is to implement higher order method for the optimization process, i.e. the quasi-Newton methods or methods of the sequential quadratic programming. Also the extension of the software SfePy for solving external flows could be an interesting and beneficial step. The expansion of considered objective functions is connected with this aim. For external flows, the objective functions for minimization of aerodynamic drag or the lift maximization are suggested. And also for internal flows some other interesting objective functions could be implemented. For example the pressure losses minimization or an equal mass objective function to deal with pipeline with more outlet parts which have different cross-sections to ensure the same volume of the outgoing fluid in each of them.

Bibliography

[1] Amstutz S., Andrä H.: *A new algorithm for topology optimization using a level-set method*. Frauenhofer-Institut für Techno- and Wirtschaftsmathematik, 2005.

[2] Arnold D., Brezzi F., Fortin M.: *A stable finite element for the Stokes equations*. Calcolo 21: 337-344, 1984,.

[3] Campobasso M.S., Duta M.C., Giles M.B.: *Adjoint Calculation of Sensitivities of Turbomachinery Objective Functions*. Journal of Propulsion and Power 19 (4), 2003.

[4] Chenais D.: *On the existenece of a solution in a domain identification problem*. J. Math. Anal. Appl., 1975.

[5] Cimrman R. and others: *SfePy: Simple Finite Elements in Python*. SfePy homepage, http://sfepy.kme.zcu.cz

[6] Cimrman R. and others: *SfePy documentation*. http://docs.sfepy.org/doc

[7] Cimrman R. and others: *SfePy, development page*. http://sfepy.org

[8] Cimrman R., Rohan E.: *Shape sensitivity analysis for stabilized Navier-Stokes equations*. In Proceedings of the conference Engineering Mechanics 2008, Svratka.

[9] Davis T.A., Duff, I.S.: *An unsymmetric-pattern multifrontal method for sparse LU factorization*. SIAM J. Matrix Anal. Applic. 18(1): 140-158, 1997.

[10] Davis T.A., Duff, I.S.: *A combined unifrontal/multifrontal method for unsymmetric sparse matrices*. ACM Trans. Math. Softw. 25(1): 1-19, 1999.

[11] Feistauer M.: *Mathematical Methods in Fluid Dynamics*. Longman Scientific & Technical, Harlow, 1993.

[12] Girault V., Raviart P.-A.: *Finite Element Approximation of the Navier-Stokes Equations*. Springer-Verlag, Berlin Heidelberg, 1979.

[13] Girault V., Raviart P.-A.: *Finite Element Methods for Navier-Stokes Equations. Theory and Algorithms*. Springer-Verlag, Berlin, 1986.

[14] Gersborg-Hansen A.: *Topology optimization of flow problems*. Technical University of Denmark, Department of Mathematics, 2007.

[15] Haslinger J., Mäkinen R.A.E.: *Introduction to Shape Optimization*. SIAM, Philadelphia, 2003.

[16] Hoschek J., Lasser D.: *Grundlangen der geometrischen Datenverarbeitung*. Teubner Verlag, Stuttgart, 1989.

[17] Jameson A., Martinelli L. and others: *Aerodynamic Shape Optimization Techniques Based On Control Theory*. Control Theory, CIME (International Mathematical Summer): 21-27, 1998.

[18] Matthies G., Lube G.: *On streamline-diffusion methods for inf-sup stable discretisations of the generalised Oseen problem*. Number 2007-02 in Preprint Series of Institut für Numerische und Andgewandte Matematik, Georg-August-Universität Göttingen.

[19] Menzel S., Olhofer M., Sendhoff B.: *Application of Free Form Deformation Techniques in Evolutionary Design Optimisation*. In Proceedings of 6th World Congress on Structural and Multidisciplinary Optimization, Rio de Janeiro, 2005.

[20] Moigne A.: *A discrete Navier-Stokes adjoint method for aerodynamic optimisation of Blended Wing-Body configurations*. Cranfield University, College of Aeronautics, PhD. thesis, 2002.

[21] Mohammadi B., Pironneau O.: *Applied Shape Optimization for Fluids*. Oxford University Press, Oxford, 2001.

[22] Nadarajah S.K., Jameson A.: *A Comparison of the Continuous and Discrete Adjoint Approach to Automatic Aerodynamic Optimization*. Stanford University, Department of Aeronautics and Astronautics, 2000.

[23] Osher S., Santosa F.: *Level-set methods for optimization problems involving geometry and constraints: frequencies of a two-density inhomogeneous drum*. J. Comp. Physik 171, 2001.

[24] Othmer C., Kaminski T., Giering R.: *Computation of topological sensitivity in fluid dynamics: cost function versatility*. European Conference on Computational Fluid Dynamics, 2006.

[25] Rohan E., Cimrman R.: *Shape sensitivity analysis for flow optimization in closed channels*. In Proceedings of the conference Engineering Mechanics 2006, Svratka.

[26] Rohan E.: *SPBOX, User's guide*. Release 2007.

[27] Samareh J.A.: *Multidisciplinary Aerodynamic-Structural Shape Optimization Using Deformation (MASSOUD)*. 8th AIAA/NASA/USAF/ISSMO Symposium on Multidisciplinary Analysis and Optimization, 2000.

[28] Snyman J.A.: *Practical Mathematical Optimization*. Springer Science + Business Media, Inc. New York, 1999.

[29] Stebel J.: *Shape optimization for Navier–Stokes equations with viscosity*. Charles University in Prague, Faculty of Mathematics and Physics, PhD. thesis, 2007.

[30] Stebel J., Haslinger J., Málek J.: *Shape optimization in problems governed by generalised Navier-Stokes equations: existence analysis*. Control and Cybernetics 34 (1), 2005.

[31] Stebel J., Haslinger J. and others: *Shape Optimization for Navier-Stokes Equations with Algebraic Turbulence Model: Existence Analysis*. Applied Mathematics and Optimization 60 (2): 185-212, 2009.

[32] Temam R.: *Navier-Stokes Equations: Theory and Numerical Analysis*. Studies in Mathematics and Its Applications 2, North-Holland, Amsterdam, New York, Oxford, 1977.

[33] Vassberg J.C., Jameson A.: *Aerodynamic Shape Optimization, Part I: Theoretical Background*. Von Karman Institute, Brussels, Belgium, 2006.

[34] Vassberg J.C., Jameson A.: *Aerodynamic Shape Optimization, Part II: Sample Applications*. Von Karman Institute, Brussels, Belgium, 2006.

[35] Wu H., Yang S. and others: *Comparison of Three Geometric Representations of Airfoils for Aerodynamic Optimization*. 16th AIAA Computational Fluid Dynamics Conference, 2003.